

G-7768

SUMMARY REPORT

on

STUDY OF BALLISTIC PROTECTIVE, CHEMICAL AND  
PHYSICAL PROPERTIES OF 200 M-1 HELMETS  
AND 200 HELMET BLANKS

*k-7768*  
to

*J. A. Geist, Jr. Corp.*  
DEPARTMENT OF THE ARMY

U. S. ARMY NATICK LABORATORIES  
NATICK, MASSACHUSETTS 01760

July 28, 1967

Prepared under Contract No. DA19-129-AMC-1005(N)

by

D. H. Fisher, A. Rudnick, F. C. Holden  
and R. E. Maringer

*[Signature]*

BATTELLE MEMORIAL INSTITUTE  
Columbus Laboratories  
505 King Avenue  
Columbus, Ohio 43201

Report Documentation Page				Form Approved OMB No. 0704-0188	
Public reporting burden for the collection of information is estimated to average 1 hour per response, including the time for reviewing instructions, searching existing data sources, gathering and maintaining the data needed, and completing and reviewing the collection of information. Send comments regarding this burden estimate or any other aspect of this collection of information, including suggestions for reducing this burden, to Washington Headquarters Services, Directorate for Information Operations and Reports, 1215 Jefferson Davis Highway, Suite 1204, Arlington VA 22202-4302. Respondents should be aware that notwithstanding any other provision of law, no person shall be subject to a penalty for failing to comply with a collection of information if it does not display a currently valid OMB control number.					
1. REPORT DATE <b>28 JUL 1967</b>		2. REPORT TYPE		3. DATES COVERED <b>00-00-1967 to 00-00-1967</b>	
4. TITLE AND SUBTITLE <b>Summary Report on Study of Ballistic Protective, Chemical And Physical Properties of 200 M-i Helmets And 200 Helmet Blanks</b>				5a. CONTRACT NUMBER	
				5b. GRANT NUMBER	
				5c. PROGRAM ELEMENT NUMBER	
6. AUTHOR(S)				5d. PROJECT NUMBER	
				5e. TASK NUMBER	
				5f. WORK UNIT NUMBER	
7. PERFORMING ORGANIZATION NAME(S) AND ADDRESS(ES) <b>Battelle Memorial Institute,Columbus Laboratories,505 King Ave,Columbus,OH,43201</b>				8. PERFORMING ORGANIZATION REPORT NUMBER	
9. SPONSORING/MONITORING AGENCY NAME(S) AND ADDRESS(ES)				10. SPONSOR/MONITOR'S ACRONYM(S)	
				11. SPONSOR/MONITOR'S REPORT NUMBER(S)	
12. DISTRIBUTION/AVAILABILITY STATEMENT <b>Approved for public release; distribution unlimited</b>					
13. SUPPLEMENTARY NOTES					
14. ABSTRACT					
15. SUBJECT TERMS					
16. SECURITY CLASSIFICATION OF:			17. LIMITATION OF ABSTRACT <b>Same as Report (SAR)</b>	18. NUMBER OF PAGES <b>132</b>	19a. NAME OF RESPONSIBLE PERSON
a. REPORT <b>unclassified</b>	b. ABSTRACT <b>unclassified</b>	c. THIS PAGE <b>unclassified</b>			

G-7768 (362)

(Approved by R. E. Maringer before typing)

cc: F. Holden/DPPM Files  
F. Wentz  
R. Maringer  
A. Rudnick  
P. Frost  
D. Fisher  
Files

July 31, 1967

Commanding Officer  
U. S. Army Natick Laboratories  
Natick, Massachusetts 01760

Attention Mr. Charles W. Davis  
Mechanical Engineering Division

Dear Sir:

Contract No. DA19-129-ME-1005(W)

Enclosed are three copies of the summary report on "A Study of Ballistic Protective, Chemical, and Physical Properties of 200 M-1 Helmets and 200 Helmet Blanks". This report covers Phases I and II of a three phase program. Recommendations for Phase III are included in the report. A formal proposal for the Phase III effort will be submitted in the near future.

A complete set of the ballistic test data is being forwarded under separate cover. These data were not incorporated into the report because of their voluminous nature.

The results of this study are very gratifying. The major objective of identifying a parameter suitable as a non-destructive index of ballistic performance has been achieved. Measurement of this parameter, thickness, is well-suited to production type quality control, and may permit one hundred percent inspection.

In addition to this, other valuable insights have been gained into the nature of the M-1 helmet. Specifically, these insights indicate that (1) present material specifications are adequate, and may even be relaxed somewhat without affecting ballistic performance (2) the increased understanding gained of the symmetry of the helmet will greatly simplify future testing and (3) relatively minor alterations in processing may result in greatly improved ballistic properties.

The manhours of effort by category expended on Phases I and II of this program will be forwarded as soon as all costs are finalized by our Accounting Department. This information should be available within two weeks.

Commanding Officer

2

July 31, 1967

We will appreciate receiving your comments on the results of this study. If you have any questions, please let us know.

Very truly yours,

Dolbert H. Fisher

DHF:ebm

Enclosures (3)

Air Mail

cc: Purchasing and Contracting Officer  
U. S. Army Natick Laboratories  
Natick, Massachusetts 01760  
Attention Helen L. O'Brien

## TABLE OF CONTENTS

	<u>Page</u>
SUMMARY. . . . .	1
INTRODUCTION . . . . .	2
EXPERIMENTAL PROCEDURE . . . . .	4
Helmets . . . . .	5
Hardness Measurements. . . . .	5
Thickness Measurements . . . . .	8
Metallographic Studies . . . . .	8
Ballistic Tests. . . . .	9
Test Range Set-Up . . . . .	10
Loading Set-Up. . . . .	13
Velocity Control. . . . .	15
Trajectory Control. . . . .	17
Helmet Blanks . . . . .	18
Hardness and Thickness Measurements. . . . .	18
Chemical Analysis. . . . .	19
Tensile Tests. . . . .	19
Ballistic Tests. . . . .	20
EXPERIMENTAL RESULTS . . . . .	20
Hardness and Thickness Characteristics. . . . .	22
Chemical Composition. . . . .	30
Metallographic Observations . . . . .	30
Mechanical Properties of Helmet Blanks. . . . .	32
Ballistic Properties. . . . .	32
CORRELATIONS WITH $V_p$ 50. . . . .	36
Thickness - $V_p$ 50 Correlations. . . . .	38
Hardness - $V_p$ 50 Correlations . . . . .	46
$V_p$ 50 Correlations with other Parameters. . . . .	48
HELMET DEFORMATION STUDIES . . . . .	49
Effect of Rolling Direction on Properties . . . . .	51
Stress-Strain Behavior. . . . .	68
DISCUSSION . . . . .	82
Observations on the Helmet . . . . .	82
Observations on the $V_p$ 50 . . . . .	85
Experimental Problems. . . . .	85
Computations Procedure . . . . .	86

TABLE OF CONTENTS  
(Continued)

	<u>Page</u>
Effects of Parameters Studied on $V_p$ 50. . . . .	88
RECOMMENDATIONS FOR PHASE III. . . . .	90
APPENDIX . . . . .	A1

## LIST OF FIGURES

	<u>Page</u>
FIGURE 1. ZONE LAY-OUT ON HELMETS AND BLANKS. . . . .	6
FIGURE 2. HARDNESS-TESTING EQUIPMENT. . . . .	7
FIGURE 3. TEST-FIRING MEASUREMENT AND FIRING SET-UP . . . . .	11
FIGURE 4. BALLISTIC-TEST VELOCITY MEASUREMENT CONFIGURATION . . .	12
FIGURE 5. M-1 HELMET BALLISTIC-TEST POSITIONING FIXTURE . . . . .	14
FIGURE 6. SHELL-LOADING SET-UP GENERAL VIEW . . . . .	16
FIGURE 7. M-1 HELMET BLANK TEST FIXTURE . . . . .	21
FIGURE 8. THE EFFECT OF THICKNESS ON THE HARDNESS OF A TYPICAL M-1 HELMET. . . . .	23
FIGURE 9. FREQUENCY OF OCCURRENCE OF ZONES BEING THE THICKEST, THINNEST, OR HARDEST IN 200 HELMETS . . . . .	24
FIGURE 10. FIRING ZONE LAYOUT SHOWING MOST FREQUENT HARD, THIN, AND THICK ZONES. . . . .	25
FIGURE 11. THE VARIATION IN HARDNESS AND THICKNESS IN A TYPICAL M-1 HELMET . . . . .	27
FIGURE 12. DISTRIBUTION OF THICKNESS FOR 200 HELMETS AND 200 HELMET BLANKS. . . . .	28
FIGURE 13. DISTRIBUTION OF AVERAGE HARDNESS FOR 200 M-1 HELMETS AND BLANKS . . . . .	29
FIGURE 14. DISTRIBUTION OF SILICON, CARBON, AND MANGANESE FROM 200 HEATS OF HELMET STEEL . . . . .	31
FIGURE 15. DISTRIBUTION OF TENSILE STRESS FOR 200 HEATS OF M-1 HELMET MATERIAL. . . . .	33
FIGURE 16. $V_{50}$ DISTRIBUTION FOR 200 M-1 HELMETS AND HELMET BLANKS. . . . .	35
FIGURE 17. $V_p$ 50 VERSUS ZONE NUMBER FOR 96 ZONES IN M-1 HELMETS .	37
FIGURE 18. THE EFFECT OF AVERAGE THICKNESS ON THE $V_{50}$ FOR 200 M-1 HELMETS. . . . .	39
FIGURE 19. EFFECT OF THICKNESS ON THE $V_{50}$ FOR UPPER SECTION (BANDS A, B, AND C) OF 200 M-1 HELMETS . . . . .	40
FIGURE 20. EFFECT OF THICKNESS ON THE $V_{50}$ FOR LOWER SECTIONS (BANDS D AND E) OF 200 M-1 HELMETS . . . . .	41

LIST OF FIGURES  
(Continued)

	<u>Page</u>
FIGURE 21. EFFECT OF THICKNESS ON $V_{50}$ OF 96 AREAS FROM 200 M-1 HELMETS. . . . . <sup>P</sup>	42
FIGURE 22. THE EFFECT OF THICKNESS ON THE $V_{50}$ OF M1 HELMET BLANKS. . . . . <sup>P</sup>	43
FIGURE 23. COMPARISON OF THICKNESS AND $V_{50}$ FOR HELMETS AND BLANKS . . . . . <sup>P</sup>	45
FIGURE 24. EFFECT OF HARDNESS ON THE $V_{50}$ FOR 96 AREAS IN EACH OF 200 HELMETS. . . . . <sup>P</sup>	47
FIGURE 25. GRIDDED BLANK AND HELMET . . . . .	50
FIGURE 26. HARDNESS AND THICKNESS DATA ON HELMET M 322B . . . . .	52
FIGURE 27. HARDNESS AND THICKNESS DATA ON HELMET M 326A . . . . .	53
FIGURE 28. HARDNESS AND THICKNESS DATA ON HELMET I 334B . . . . .	54
FIGURE 29. HARDNESS AND THICKNESS DATA ON HELMET I 2491 . . . . .	55
FIGURE 30. HARDNESS AND THICKNESS DATA ON HELMET I 2505 . . . . .	56
FIGURE 31. HARDNESS AND THICKNESS DATA ON HELMET I 6674 . . . . .	57
FIGURE 32. HARDNESS AND THICKNESS DATA ON HELMET I 7421 . . . . .	58
FIGURE 33. HARDNESS AND THICKNESS DATA ON HELMET I 9926 . . . . .	59
FIGURE 34. DEFORMATIONS OF 1-INCH GRIDS IN HELMET M 322B. . . . .	60
FIGURE 35. DEFORMATIONS OF 1-INCH GRIDS IN HELMET I 2505. . . . .	61
FIGURE 36. DEFORMATIONS OF 1-INCH GRIDS IN HELMET I 9926. . . . .	62
FIGURE 37. DEFORMATIONS OF 1-INCH GRIDS IN HELMET I 7421. . . . .	63
FIGURE 38. DEFORMATIONS OF 1-INCH GRIDS IN HELMET I 6674. . . . .	64
FIGURE 39. DEFORMATIONS OF 1-INCH GRIDS IN HELMET M 334B. . . . .	65
FIGURE 40. DEFORMATIONS OF 1-INCH GRIDS ON HELMET M 326A. . . . .	66
FIGURE 41. DEFORMATIONS OF 1-INCH GRIDS IN HELMET I 2491. . . . .	67
FIGURE 42. PLOTS OF TRUE STRAINS ON 1-INCH GRIDS FOR HELMET M 322B, COMPARING LEFT (A) TO RIGHT (A) SYMMETRY . . .	69
FIGURE 43. PLOTS OF TRUE STRAINS ON 1-INCH GRIDS FOR HELMET I 9926, COMPARING LEFT-TO-RIGHT SYMMETRY . . . . .	70



LIST OF FIGURES  
(Continued)

	<u>Page</u>
FIGURE 44. PLOTS OF TRUE STRAINS ON 1-INCH GRIDS FOR HELMET M 334B, COMPARING LEFT-TO-RIGHT SYMMETRY . . . . .	71
FIGURE 45. PLOTS OF TRUE STRAINS ON 1-INCH GRIDS FOR HELMET I 7421, COMPARING LEFT-TO-RIGHT SYMMETRY . . . . .	72
FIGURE 46. PLOTS OF TRUE STRAINS ON 1-INCH GRIDS FOR HELMET I 2505, COMPARING LEFT-TO-RIGHT SYMMETRY . . . . .	73
FIGURE 47. PLOTS OF TRUE STRAINS ON 1-INCH GRIDS FOR HELMET I 2491, COMPARING LEFT-TO-RIGHT SYMMETRY . . . . .	74
FIGURE 48. PLOTS OF TRUE STRAINS ON 1-INCH GRIDS FOR HELMET I 6674, COMPARING LEFT-TO-RIGHT SYMMETRY . . . . .	75
FIGURE 49. PLOTS OF TRUE STRAINS ON 1-INCH GRIDS FOR HELMET M 326A, COMPARING LEFT-TO-RIGHT SYMMETRY . . . . .	76
FIGURE 50. EFFECT OF STRAIN ON FLOW STRESS AND HARDNESS OF HELMET STEEL . . . . .	78
FIGURE 51. EFFECT OF STRAIN ON FLOW STRESS AND HARDNESS OF HELMET STEEL . . . . .	80
FIGURE 52. PLOTS OF $R_C$ HARDNESS VS EFFECTIVE TRUE STRAINS FOR HELMET M 322B. . . . .	81
FIGURE 53. PLOTS OF $R_C$ HARDNESS VS $\ln t_o/t$ FOR HELMET M 322B. . .	83
FIGURE A-1. EFFECT OF AVERAGE HARDNESS ON THE COMPOSITE $V_{p50}$ OF M-1 HELMETS . . . . .	A-25
FIGURE A-2. THE EFFECT OF MANGANESE ON THE COMPOSITE $V_{p50}$ OF M-1 HELMETS . . . . .	A-26
FIGURE A-3. EFFECT OF CARBON ON THE COMPOSITE $V_{p50}$ OF M-1 HELMETS. . . . .	A-27
FIGURE A-4. EFFECT OF SILICON ON THE COMPOSITE $V_{p50}$ OF M-1 HELMETS. . . . .	A-28

## FOREWORD

This report was prepared by Battelle Memorial Institute for the United States Army under Contract No. DA-129-AMC-1005(N). The work was administered under the direction of the Army Natick Laboratories, Natick, Massachusetts, with Mr. Charles Davis acting as Project Officer.

This report covers work conducted from June 24, 1966 to July 24, 1967.

The ballistic tests on the M-1 helmets and helmet blanks were conducted by American Machine and Foundry Company, York, Pennsylvania under the supervision of Mr. E. H. Weiss, Program Manager and Mr. R. J. Moure, Project Engineer. A report on this work was submitted to Battelle and is incorporated in appropriate sections of this report.

### ABSTRACT

A study of M-1 helmets was conducted to find an inspection technique to replace the  $V_p$  50 as a quality control index of ballistics performed. The  $V_p$  50 of 200 helmets and 200 helmet blanks representing 200 heats of steel was determined. Other parameters studied were thickness, hardness, chemical composition, microstructure, and tensile stress-strain properties. Of these, only thickness was found to be sufficiently sensitive of  $V_p$  50 to be of value as a quality control criterion. Recommendations are made for a study leading to the implementation of these findings.

Among other observations made in the study was the possibility that significant improvement in ballistic resistance of M-1 helmets might result from annealing the helmets after forming. Recommendations along this line are also made.

SUMMARY REPORT

on

STUDY OF BALLISTIC PROTECTIVE, CHEMICAL AND PHYSICAL PROPERTIES  
OF 200 M-1 HELMETS AND 200 HELMET BLANKS

to

U. S. ARMY NATICK LABORATORIES

DA19-129-AMC-1005(N)

from

BATTELLE MEMORIAL INSTITUTE  
Columbus Laboratories

July 28, 1967

SUMMARY

A study was conducted to find an inspection technique for M-1 helmets to replace the currently used  $V_p$  50. To do this, helmets and helmet blanks made from some 200 heats and heat treatment lots of steel were studied. The ballistic performance of these helmets and helmet blanks was analyzed in terms of chemical composition, microstructure, stress-strain characteristics, hardness, and thickness.  $V_p$  50's were computed for the helmet as a whole and for specific sections of the helmets. Of the parameters studied, only thickness was found to correlate strongly enough with ballistic performance to be of direct value as an inspection technique. For the range of thicknesses studied, the  $V_p$  50 increases about 20 fps per 0.001-inch of thickness.

On the basis of the findings, recommendations are given for a Phase III study\* to explore details of using thickness as an

---

\* The current study consisted of Phases I and II. Phase III, the development of inspection methods, was to be proposed upon conclusion of Phase II.

inspection technique. Questions to be answered are primarily (1) where the thicknesses should be measured, i.e., the most appropriate areas of the helmet from a detection point of view, and (2) how thickness should be measured, i.e., the most appropriate method from a production point of view. After answering these questions, the study would be directed at establishing design details of a production model.

Although the study was aimed principally at finding a new helmet inspection technique, there were some important side benefits. In particular, interesting insights into helmets and into the  $V_p$  50 test were found. As an example, correlations between  $V_p$  50 and hardness were observed. These correlations were not strong enough to be of value as an inspection technique for helmets, but did indicate the possibility of improving the ballistic resistance of helmets by annealing them after forming. Suggestions for a study leading to the implementation of these findings are also made.

### INTRODUCTION

The head has been shown statistically to be one of the most vulnerable parts of a footsoldier's body. The helmet is, therefore, a critically important part of his armor. Relatively little is known about the factors influencing the effectiveness of a helmet. As one result of this, it is not known whether significant improvements in helmet protection might not be attained within the framework of acceptable sizes and weights. Another result of insufficient understanding of helmets is associated with establishing production standards

and quality control tests. It is with this latter problem that this study was mainly concerned.

Present acceptance specifications of finished helmets are based upon arbitrarily established minimum  $V_p$  50 values. Spot checks on each lot of helmets are made to assure that this specification is met. This procedure is costly, time consuming, and of questionable reliability. It was recognized that a much more satisfactory inspection procedure might result if some more fundamental property or combination of properties of the helmet were used as a criterion. The problem, of course, lies in relating the properties to the ballistic protection afforded by the helmet.

In this program, the M-1 helmet was studied to identify some of the properties which affect ballistic performance. The program was divided into two general phases. Phase I was concerned primarily with experimental evaluation of M-1 helmets, and Phase II with analysis of the resulting data. The ultimate objective (Phase III) is to develop an economical method, preferably a nondestructive-testing procedure, to assure that production helmets possess a prescribed minimum ballistic limit.

Phases I and II are summarized in this report and recommendations for Phase III are outlined.

### EXPERIMENTAL PROCEDURE

Two hundred helmets and 200 helmet blanks representing 200 different heats of steel were furnished to Battelle by the U. S. Army Natick Laboratories. These were paired on the basis of heat numbers stamped on the inside front of the helmet and on the blank. In most cases, for each helmet there was a corresponding blank. A total of 196 helmet-blank pairs plus four single helmets and four single blanks was studied.

The helmets were received in the finished form including paint and hardware. Prior to testing, the paint and hardware were removed.\* All blanks were evaluated in the as-received condition.

Thickness and hardness measurements and ballistic tests were conducted on each helmet and blank. In addition, each helmet was examined metallographically and tensile tests and chemical analyses were conducted on specimens taken from each blank. These evaluations were supplemented by forming studies in which grid patterns were placed on blanks prior to forming them into helmets. The distortion of the grid pattern was used to describe the flow of metal during the forming process.

The helmets and blanks were divided into 32 zones as shown in Figure 1. Using as a center the uppermost point of the helmet or the center of the blank, 6 concentric circles were drawn having the following radii measured over the material surface: 1-1/4-inch, 2-1/2-inch, 3-3/4-inch, 5 inches, 6-1/4-inch and 7-1/2-inch. These

---

\* The paint was removed by soaking for 1/2 hour in a commercial paint remover.

were then divided into the 32 zones as shown in the figure. As the studies progressed, considerable variations in hardness and thickness were observed within some zones of the helmets. Therefore, each of the 32 zones was divided into 3 areas, making a total of 96 areas identified in each helmet. Orientation of the zones with respect to the helmet configuration was maintained for all helmets. The location of the stamped heat number served as the reference for the blanks (this number is located at the front of the helmet when formed).

### Helmets

#### Hardness Measurements

Hardness measurements were made using a modified Rockwell Hardness machine shown in Figure 2. Modifications to the hardness machine included a U-shaped anvil support and a spherical shaped anvil to accommodate the various radii of the helmet. In order to assure that all measurements were made normal to the surface, a 2-inch diameter pressure ring was used on the convex side to clamp the helmet. Thus, as the helmet was raised for preloading (minor load 10 K<sub>g</sub>) for hardness measurements, the pressure ring oriented the surface normal to the axis of travel. This procedure also served to stabilize the helmet during the hardness measuring cycle.

Hardness measurements were conducted according to ASTM Standards E-18 using a diamond cone and the Rockwell C scale. Inspection of the anvil side of the impressions indicated that the material was thick enough to use the R<sub>C</sub> scale.\* A calibration test block with a hardness of R<sub>C</sub> 45 was used as the standard for hardness

---

\* With thin materials, the anvil can influence the measured hardness. Such an effect would be indicated by markings on the under side of the specimen.



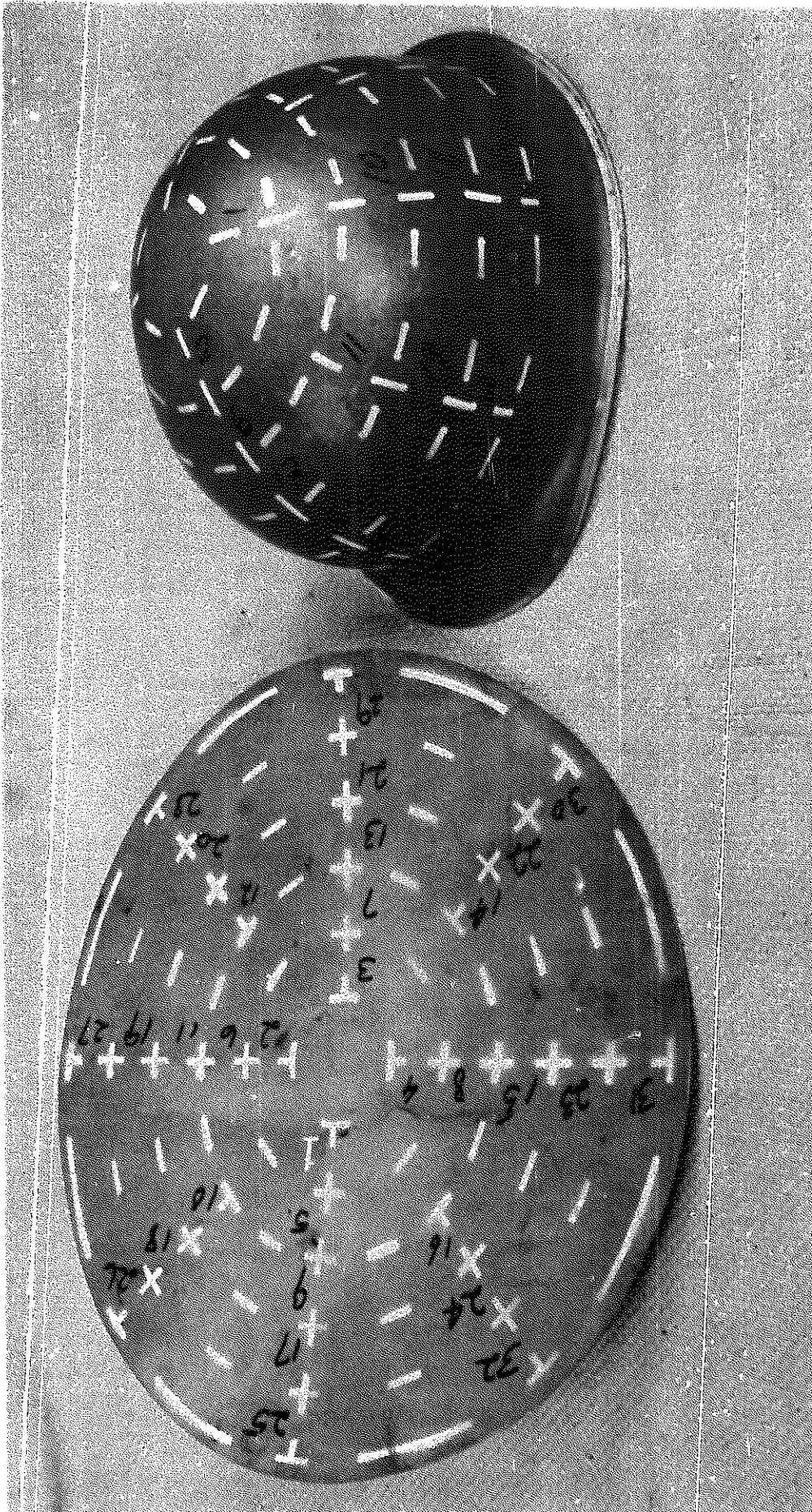


FIGURE 1. ZONE LAYOUT ON HELMETS AND BLANKS

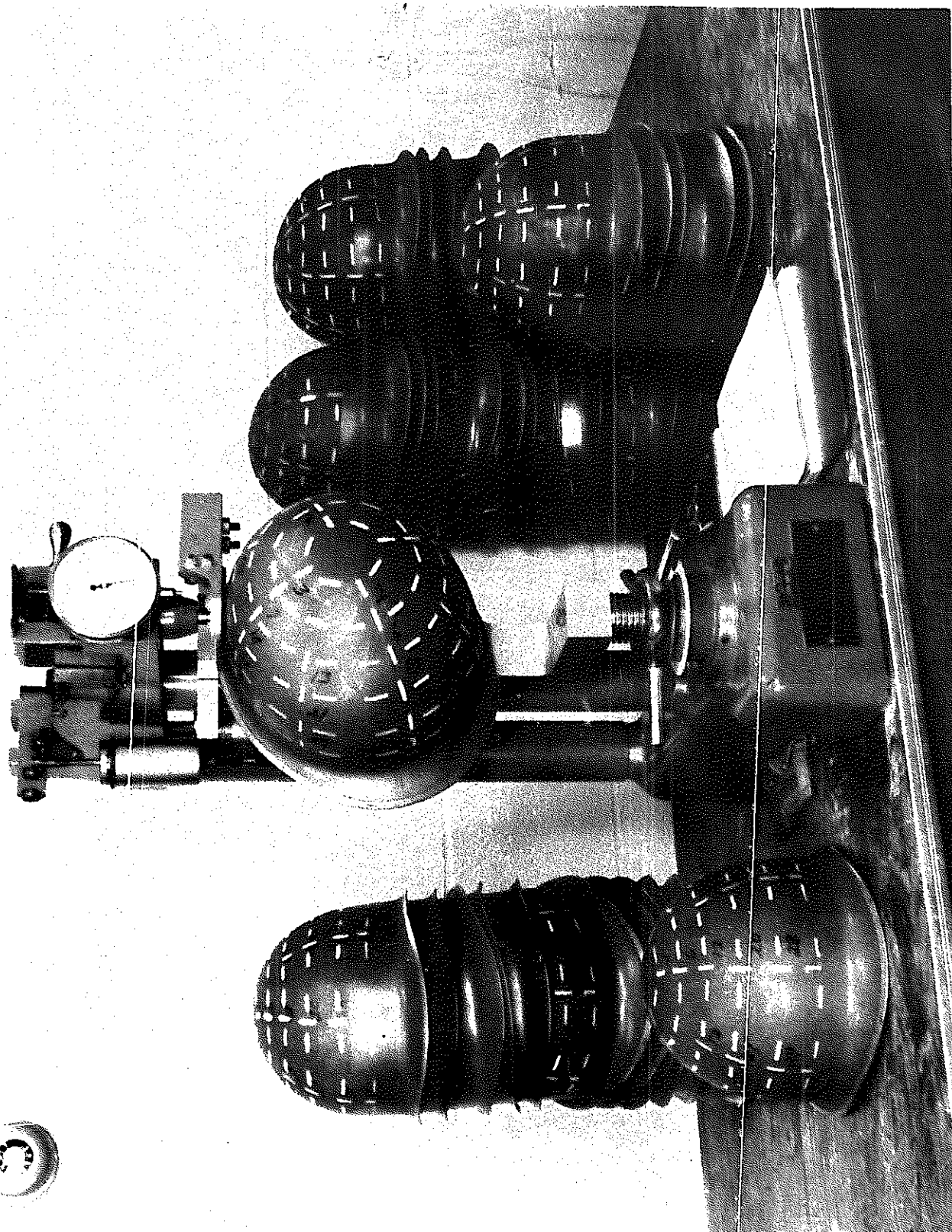


FIGURE 2. HARDNESS-TESTING EQUIPMENT

measurements on the helmets. The hardness measurements are considered accurate to  $\pm 2R_c$  numbers.

Three hardness measurements were taken in each of the 32 zones for a total of 96 readings per helmet. One reading was taken at the center and the other two near the ends of the zone. Initially it was planned to average the three readings to obtain one hardness value for each zone. However, the hardness variations within some zones were sufficiently great (as much as 7  $R_c$  numbers) that the average value could not be considered as representative. It was this and a similar observation for thickness that led to our dividing each zone into 3 areas, giving a total of 96 areas for consideration in the evaluation studies.

#### Thickness Measurements

The Rockwell hardness machine was converted to a thickness measuring device by replacing the indenter-and-dial assembly with a dial indicator graduated to 0.0001-inch. The data were determined to be repeatable to within  $\pm 0.0005$ -inch. Each measurement was taken within about 1/4-inch from the hardness indentation. The hardness and thickness are, therefore, considered to be from the same location. As with hardness, a total of 96 measurements was made on each helmet.

#### Metallographic Studies

Metallographic examinations were made on sections removed from the formed and ballistically tested helmets. The sections were triangular pieces about 1 inch long by 1/4-inch wide at the base and had been removed from the front of the helmet, an area which had not been subjected to extensive forming.

### Ballistic Tests

After the hardness and thickness measurements were completed, the helmets were sent to The American Machine and Foundry Company, York, Pennsylvania for ballistic testing. The hardness and thickness data for the 96 areas, ordered according to increasing thickness, were furnished with each helmet.

The ballistic tests were conducted, utilizing the T-37, .22 Cal. fragment simulator and the following procedure:

- (1) One (1) shot was fired into each of the thirty-two (32) firing zones (Figure 1) starting at the thinnest zone and continuing in the order of progressively increasing material thickness.
- (2) The powder load was corrected according to increased thickness of each succeeding shot fired. The intention was to achieve a nearly equal number of penetrations and non-penetrations within a minimum velocity range.
- (3) Penetration was considered to be complete when the impacting projectile or any fragment thereof, or any fragment of the test panel passed to the rear of the test panel with sufficient energy to pierce the witness plate resulting in a hole that was complete to the light of a 60 watt bulb placed to the rear of this witness plate.
- (4) The helmets were supported by a positioning fixture which provided firm support and which allowed adjusting the location of the helmet to permit each of the firing zones to be placed at an angle of zero degrees obliquity.
- (5) Records were maintained of loads, velocities and impact data for calculation of specific ballistic limits for each helmet.
- (6) Generally, ballistic testing was performed in accordance with MIL-STD-662.

Test Range Set-Up. Figures 3 and 4 show the layout of the equipment in the firing range. The locations of the rifle, triggering devices and target material complied with the requirements of paragraph 5.3 of MIL-STD-662A. The time interval measurement system consisted of redundant sets of two each photo electric screens spaced 5.0 feet  $\pm$  0.02 inches apart. The electronic counter (Electric Counters Incorporated) was started when the projectile passed through the first screen. The counter stopped when the projectile passed through the second screen. The time interval was measured to within  $0.1 \times 10^{-6}$  seconds. The back-up time interval system was superimposed on this range and consisted of the identical type screens (spaced 6 inches from the primary set) and a second ECI counter. This counter was slaved to the master reference oscillator of the primary counter to prevent cross talk. The oscillator maintained an accuracy  $\pm$  3 parts per  $10^{-7}$  per week. These measurements exceeded the requirements specified in paragraph 4.1.3.1 of MIL-STD-662A.

The screens were secured together on both top and bottom to prevent vibration and variation in spacing due to the concussion. Proper shielding prevented spurious transients from giving unwanted responses to the counters. The lamp and photo-cell portions of the screens were shaded to improve their signal to noise ratios. In normal operation the average of the two counter readings was used to compute the velocity. The counter readings did not differ by more than 2  $\mu$ s maximum, the average difference was 1.3  $\mu$ s.



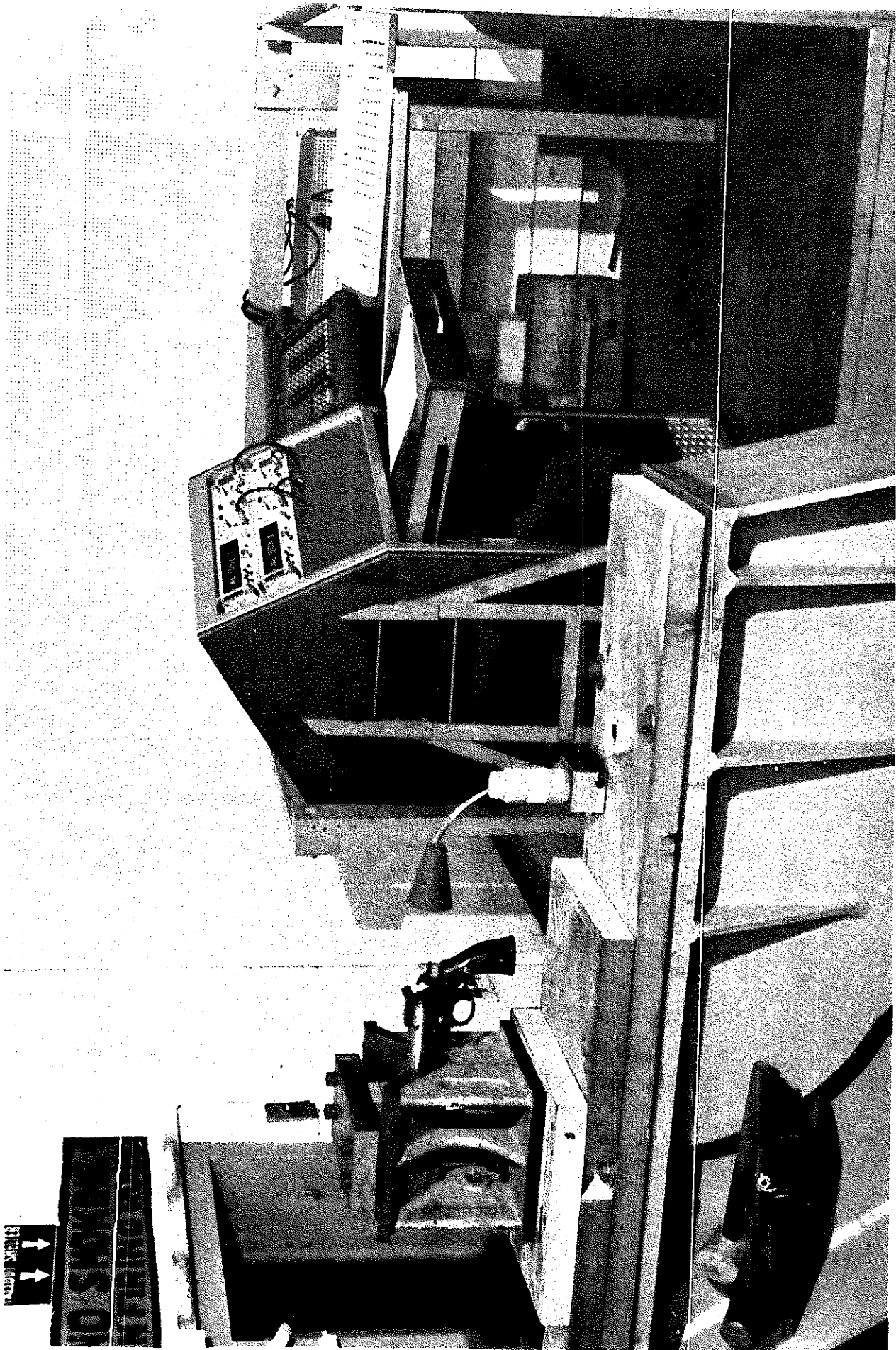


FIGURE 3. TEST-FIRING MEASUREMENT AND FIRING SETUP

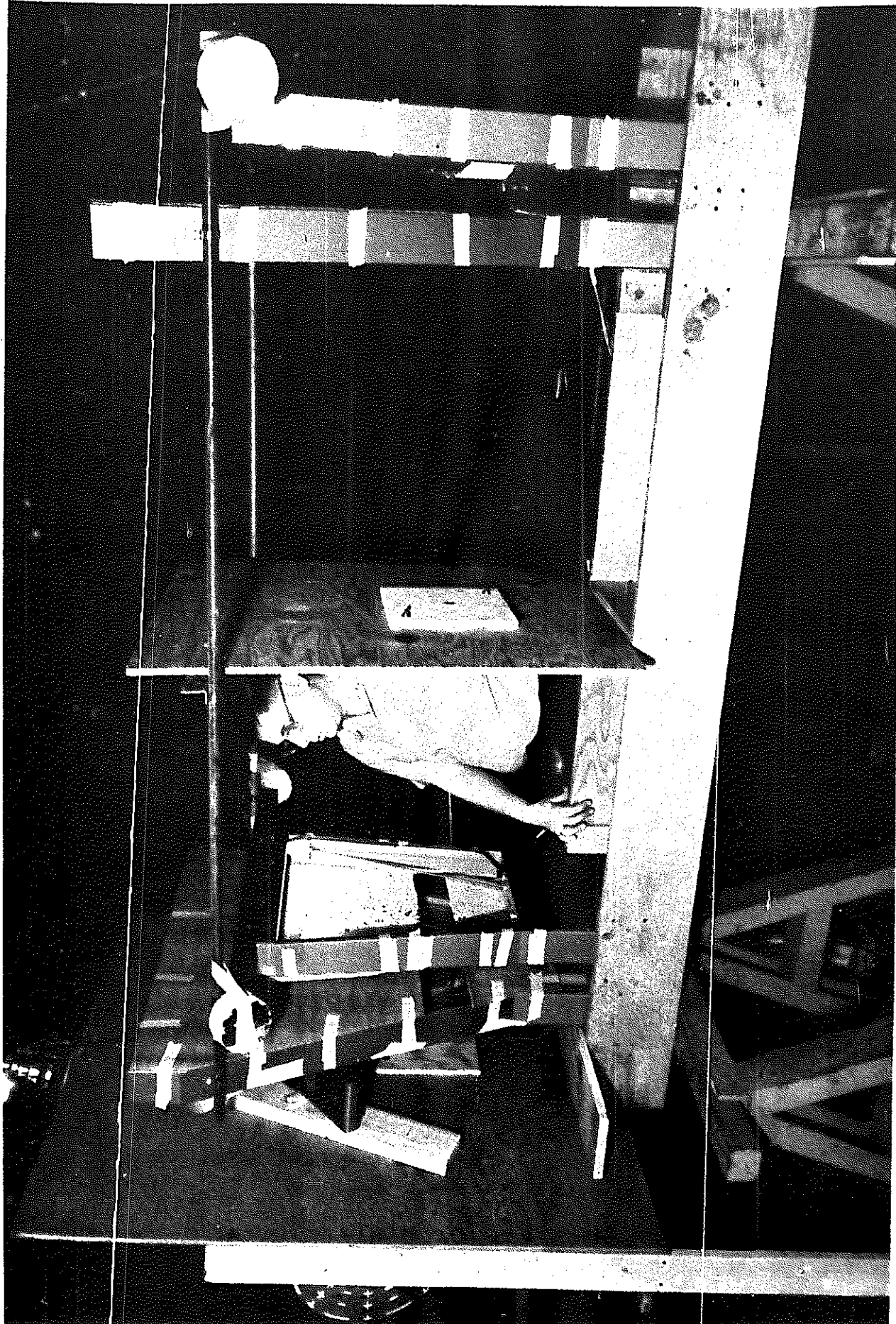


FIGURE 4. BALLISTIC-TEST VELOCITY MEASUREMENT CONFIGURATION

Target alignment was achieved through illumination with a high intensity lamp shining through the gun barrel to the point where the hardness of the helmet was measured in each zone. The perpendicularity of the planned impact point to the trajectory of the projectile was verified by means of a small (2" x 1/4" dia.) squared end magnet placed on this point (a second magnet inside the helmet held it in place). Proper alignment was indicated by the concentricity of the cast shadow to the base of this cylindrical magnet.

The helmet supporting fixture is illustrated in Figure 5. This fixture was designed to permit manual alignment of all zones with respect to the path of the projectile.

The witness plate consisted of a 3" x 3" x 0.02" type 2024 T-3 aluminum sheet. This plate was inserted in a holder that afforded firm peripheral support on all edges. The support was located three inches behind the helmet or helmet blank.

Loading Set-Up. The 12,000 rounds of .22 Cal. T-36 fragment simulators were measured for dimensions and sampled for weight and hardness. Ninety-nine percent of the projectiles met the requirements of MIL-P-46593A with the specified maximum O.D. of  $0.226 \pm 0.002$  inches. However, the projectiles were separated for size so that, on any new gun barrel, the smallest diameter would be shot first and the next larger diameters utilized to compensate for wear of the barrel.

A "powder trickler" was set up so that the powder would load directly on the scale pan of a Mettler Automatic Precision Balance.



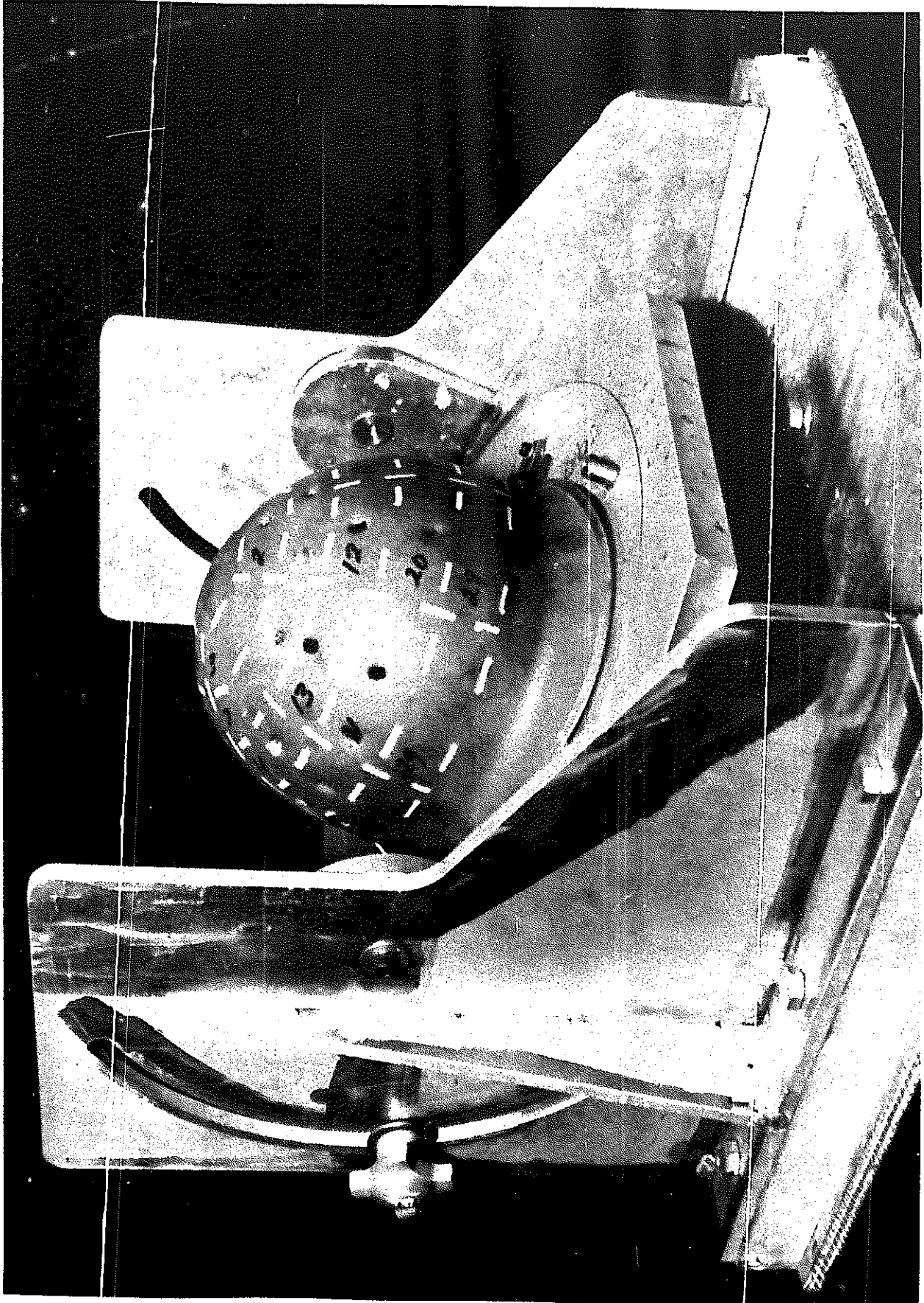


FIGURE 5. M-1 HELMET BALLISTIC-TEST-POSITIONING FIXTURE

The cases were loaded in one mg. increments from 50 to 80 milligrams of powder. Experimentation showed that Bullseye flake powder gave the most consistent velocity.

Paraffin wadding was found to result in better velocity control than paper wads with or without crimping of the case. Solid paraffin, 0.066-inch thick was pressed into the shell and against the powder. To reduce the case volume, this wadding was utilized in powder loads above 58 mgs. A paper wad was added to the wax wad for greater reliability at the lower loads. The remainder of the shell case was then filled with liquid paraffin wax and permitted to solidify.

Various methods of adding the wax to the loaded and plugged shell were tried. A constant-temperature heated receptacle was utilized to keep the melted wax between 180 - 190 degrees F. The loaded shells were mounted in a metal frame that acted as a heat sink. The melted wax was allowed to drip into the shell until the wax was level with the top. After solidification of the paraffin, the loaded cartridges were stored in marked boxes.

Figure 6 illustrates the powder weighing balance and "trickler" and the general set-up for shell loading.

Velocity Control. The objective of the velocity control was to maintain the velocities of any one powder load to within 50 feet per second. This was attempted through the following means:

- (a) Precise weighing of the powder. The weight of the powder load was measured to within  $\pm 0.2$  percent.

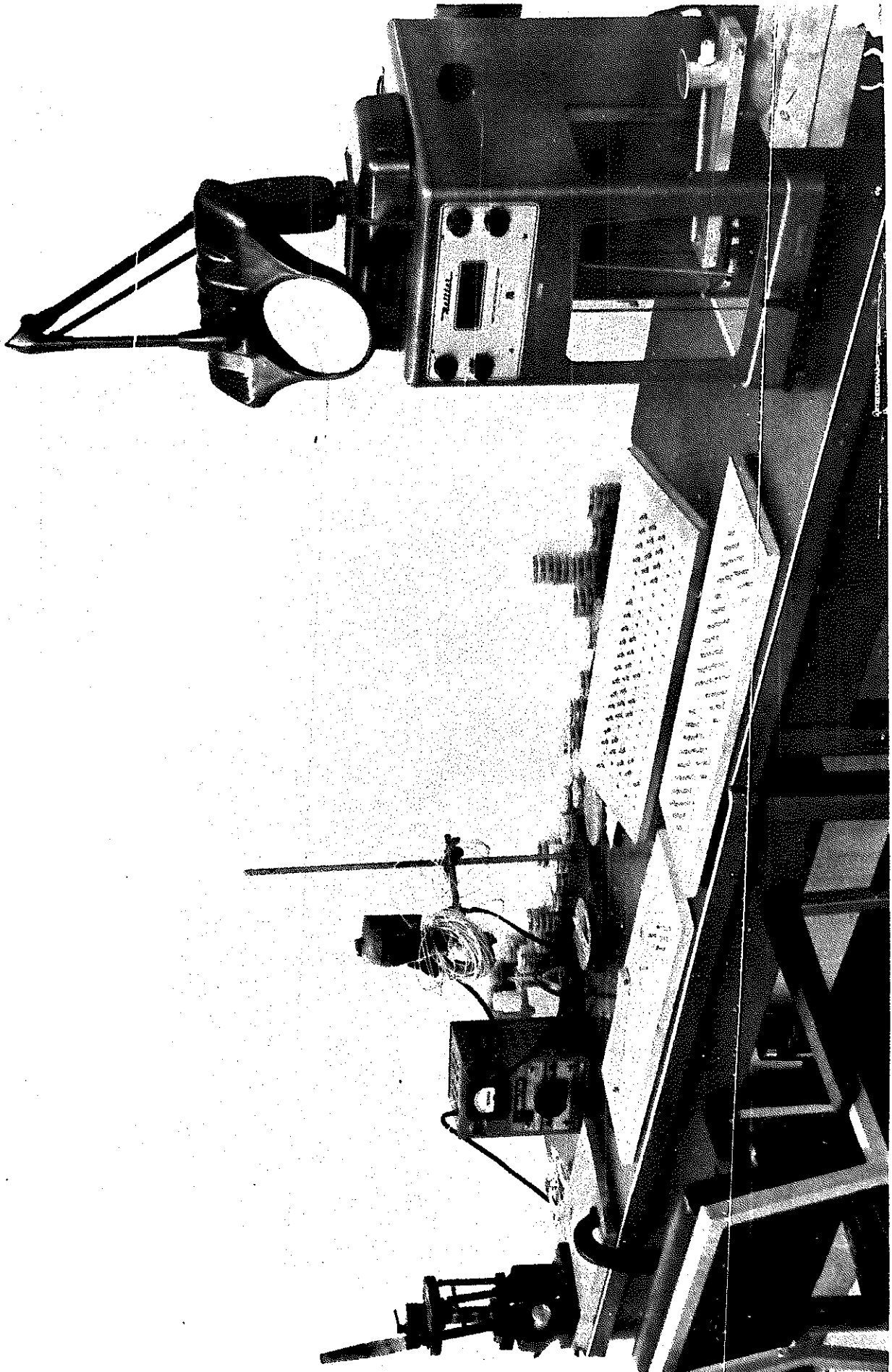


FIGURE 6. SHELL-LOADING SETUP, GENERAL VIEW

- (b) Sealing the wad and powder load into the shell with the wax held at a temperature just above its melting point and providing a heat sink to dissipate the heat. Prior to this control, the wax sometimes melted the wax wad, fused with the powder, and prevented complete powder burn.
- (c) All shells were prepared in a consistent manner to ensure uniformity.
- (d) The projectile was loaded into the firing chamber with the flat point horizontal and the "skirt" portion of the projectile butted against the shell for each firing. It was noted that increasing the gap between the projectile and the shell decreased the velocity of the projectile.
- (e) A twenty-three (23) inch rifle barrel was shortened to eleven and one half (11-1/2) inches, when it was noted that the longer length of the barrel decreased the velocity due to the drag of the rifling on the projectile. No significant loss of accuracy resulted from this shorter barrel.

The Measurement Controls utilized for the tests exceeded the requirements of Paragraph 4.1.3.1, MIL-STD-662A.

Trajectory Control. Through the collimation techniques and orthogonality measurements described earlier, the impact point of the projectile remained very close to the point of hardness and thickness measurement. Analysis of two (2) sampled helmets showed maximum deviations of 1/4-inch for the 78 shots with an average deviation of 3/32 inch.

The orientation of the projectile could be readily determined on the tested material. Unlike heavier armor plate, the approximate 0.04-inch thick steel showed a clear impression of the blunt nose of the projectile on the non-penetrating shots. Excessive pitch or yaw would have left a recognizable impression upon the material. Additional measurements were made of the projectile orientation through impaction

into a homogenous target mass of "Duxseal" which is similar to "Plasticene" modeling clay. The entering hole left by the projectile was round and the projectile, when found, was in the proper orientation.

The use of high quality gun barrels, their frequent replacement (average 2000 shots per barrel) upon significant decrease in velocity due to wear, and close control of the projectile parameters provided good projectile orientation at the point of impact with the helmet. This was verified by frequent inspection of the impressions made by non-penetration shots in the helmets. Attempts to photograph the projectile were abandoned after one week of experimentation, without satisfactory results, due to the requirements of the schedule.

#### Helmet Blanks

The helmet blanks were 15-3/4 inches in diameter with a nominal thickness of 0.045 inch. Most of the blanks were severely wrinkled. In addition, all were dish shaped, some as much as one inch.

#### Hardness and Thickness Measurements

The shape of the helmet blanks posed a difficult problem in obtaining good hardness and thickness measurements. Reliable measurements require that the surface being measured be normal to the line of measurement. A wavy surface, as found on the blanks, can introduce errors in the data.

Hardness and thickness measurements were made on 15 blanks according to the stenciled zone layout shown in Figure 1. For zones located in areas of extreme wrinkling, several readings were required

to arrive at a representative average. However, the results indicated good uniformity of hardness and thickness in each blank. On the basis of these observations, the remainder of the 200 blanks were measured for hardness and thickness in selected flat areas to obtain an average for each blank. A minimum of 10 measurements was used to compute the average for each property.

The areas selected for the hardness and thickness measurements were marked as firing zones for the ballistics tests. In most of the blanks, these areas were randomly spaced across the surface to assure a reasonable average of the hardness and thickness.

#### Chemical Analysis

Each of the 200 blanks was analyzed for carbon, silicon, and manganese content. Carbon was determined by a combustion-gravimetric technique and silicon and manganese by an X-ray fluorescence technique. A Philips vacuum path X-ray spectograph was used for the X-ray fluorescence analysis.

#### Tensile Tests

Two tensile tests were conducted on specimens from each helmet blank to determine the mechanical properties of the as-received material in directions transverse to and longitudinal with the rolling direction. The gage section of the specimens was 1/4-inch by blank thickness by 2 inches long. A dual-range extensometer with sensitivities of 0.001 and 0.01 inch per inch was used to measure strain. The load-strain data were recorded on an X-Y strip chart. Properties obtained

from these tests included the 0.2 percent offset yield stress, maximum stress, and work-hardening characteristics of each heat of material. Total elongation was obtained from small scribe marks placed on the specimens before the test was started. In addition, hardness measurements were made on each specimen after the test was completed.

### Ballistic Tests

The ballistic tests on the blanks were conducted in a manner similar to that of the helmet described previously. Average hardness and thickness data and the corresponding blanks were furnished to The American Machine and Foundry Company for firing. Since each blank exhibited a uniform thickness, the firing sequence was not specified.

The blank supporting fixture is illustrated in Figure 7. Three bolt clamps mounted at 120° on a 5" bolt circle were used to hold the blank in the firing position. These bolts were torqued to 30-inch-pounds  $\pm 2$  to reduce variations in the response of the blank to the projectile impact. Other components of the system were as described for the ballistic tests on the helmet.

### EXPERIMENTAL RESULTS

A major part of the data obtained in Phase I of this study is summarized in Table A1 of the Appendix. Columns 2 through 10 contain data from tests conducted on the helmet blank, while columns 11 through 13 are from tests on the helmet. Column 14 represents the average percent reduction in thickness of the material during forming.



FIGURE 7. M-1 HELMET-BLANK TEST FIXTURE



The data are listed in order of increasing  $V_p$  50 of the blanks. Because of the large amount of data generated in this program, a computer was used for much of the analysis.

### Hardness and Thickness Characteristics

Early in the program, it was noted that the thinnest areas of the helmet were not necessarily the hardest. Thickness measurements indicated variations within the helmets of as much as 0.010 inch and hardness as much as 11 points on the  $R_c$  scale. In a majority of the helmets, the thickest areas were also the hardest areas. Figure 8 is a representative plot of hardness versus thickness for a helmet. This plot suggests that the helmet can be divided into three sections for evaluation. The top section of the helmet, designated as bands A, B, and C, exhibits a reasonable correlation between hardness and thickness. This correlation becomes less obvious in bands D and E, the latter being both hard and thick.

A bar graph representing the distribution of thickness and hardness by zone number for the 200 helmets is shown in Figure 9. From this figure, it can be seen that the lower numbered zones (those toward the crown) are usually the thinnest, whereas the zones near the rim are the thickest and hardest.

A firing-zone layout showing the most frequent hard, thin and thick zones from the 200 helmets is given in Figure 10. As indicated, all of the "extreme" areas are on the back of the helmet. It is of interest to note the symmetry of these extreme areas. The segregations are demonstrated most clearly by plotting hardness and thickness against zone number and considering the relative behavior of these parameters in various circumferential bands. This is done

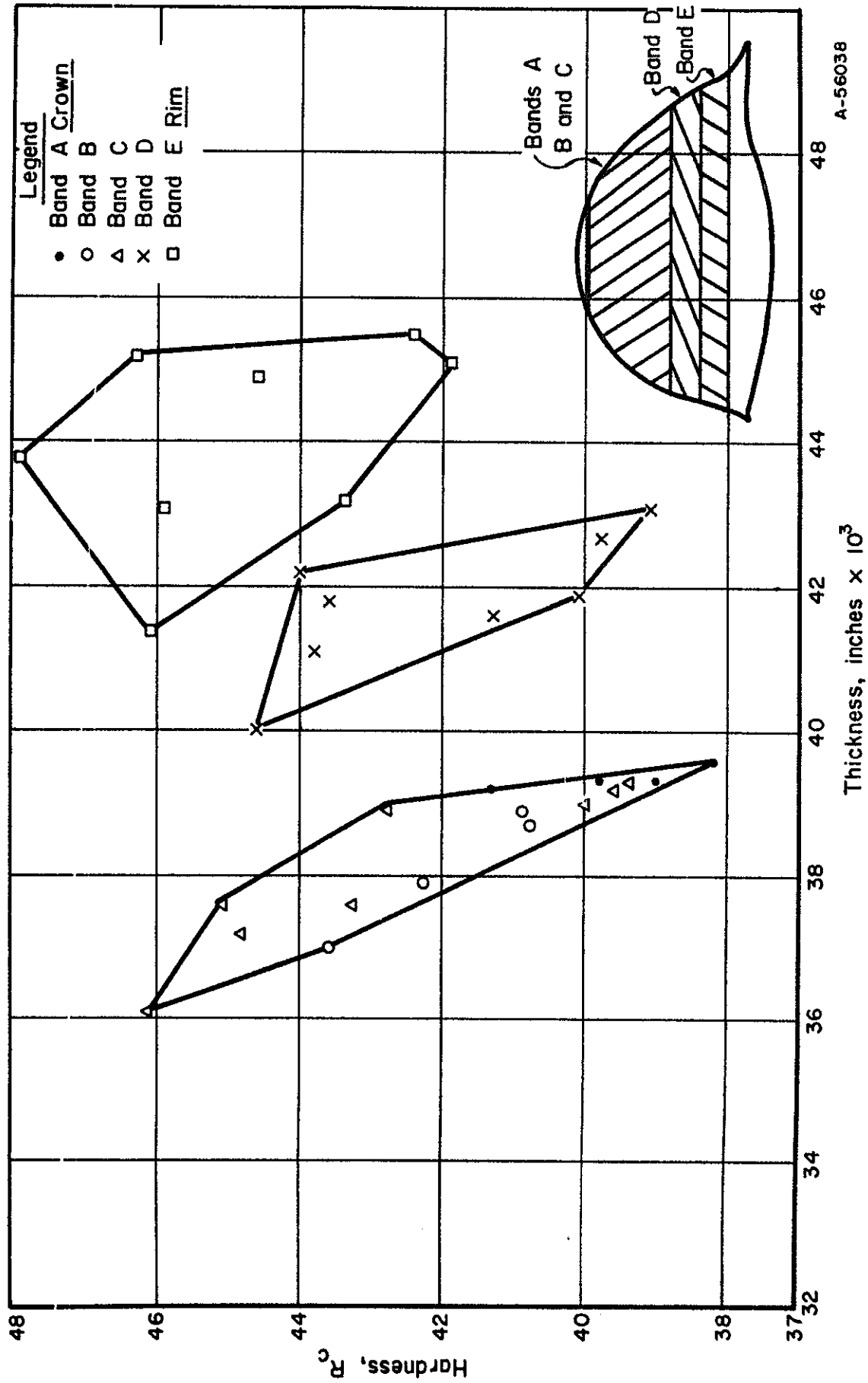


FIGURE 8. THE EFFECT OF THICKNESS ON THE HARDNESS OF A TYPICAL M-1 HELMET

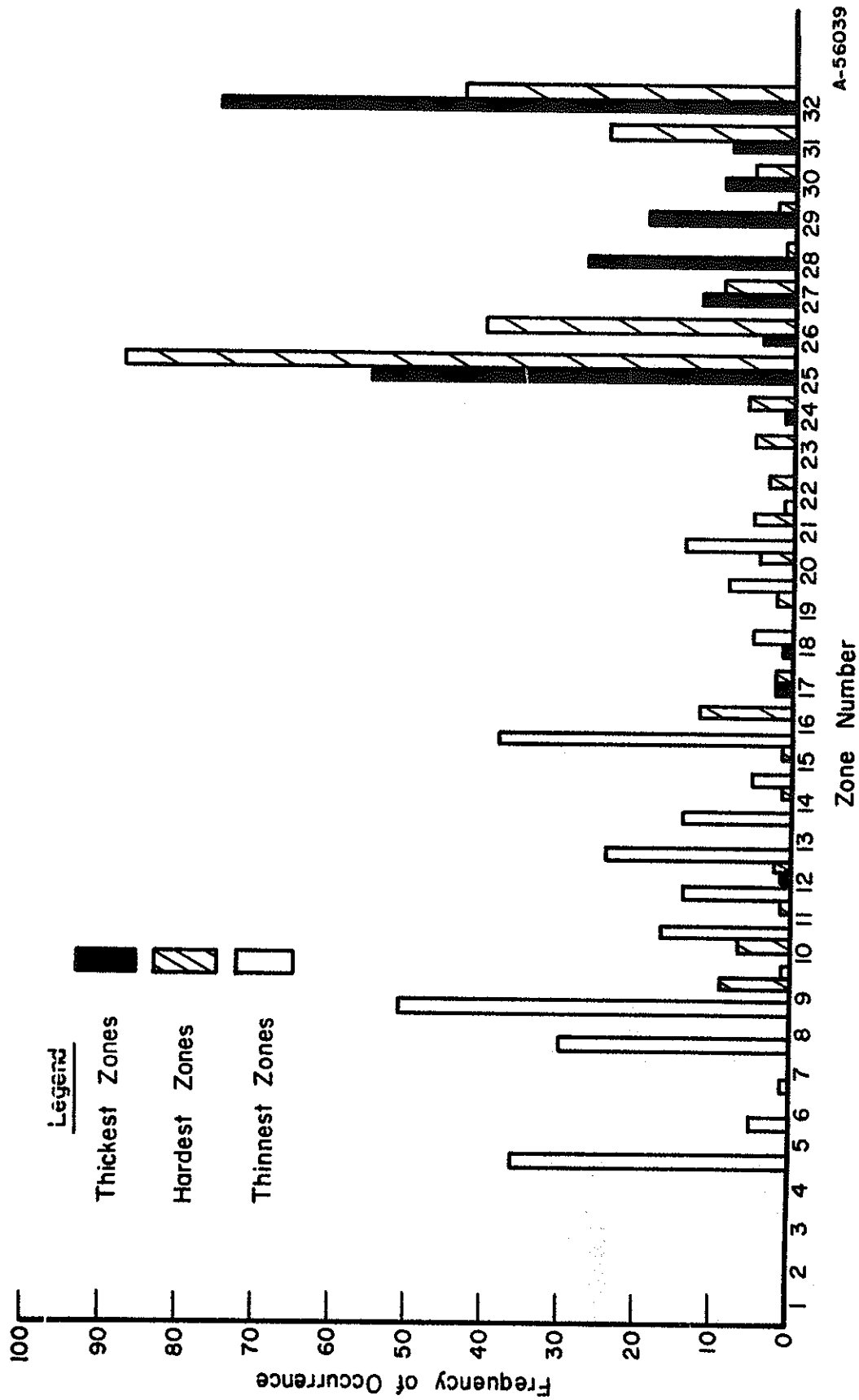


FIGURE 9. FREQUENCY OF OCCURRENCE OF ZONES BEING THE THICKEST, THINNEST, OR HARDEST IN 200 HELMETS

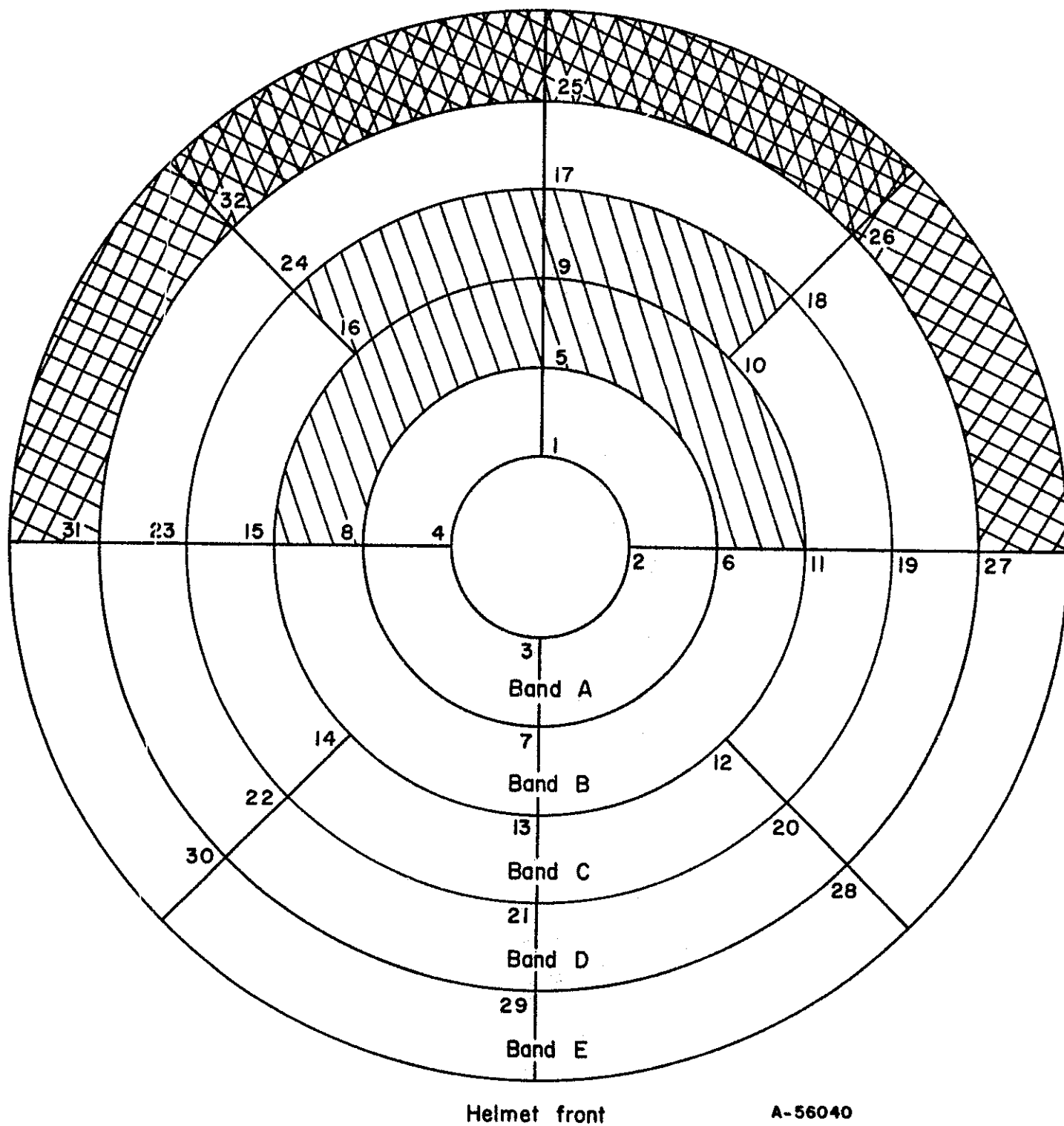
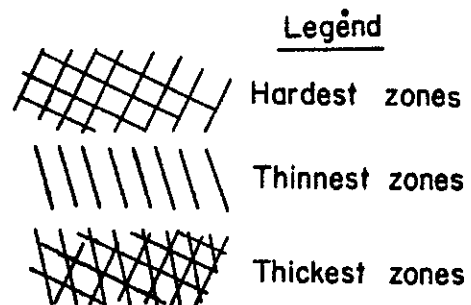


FIGURE 10. FIRING-ZONE LAYOUT SHOWING MOST FREQUENT HARD, THIN, AND THICK ZONES

in Figure 11 for a typical helmet. In this figure, Bands A through C refer to the upper section of the helmet while Bands D and E are near the rim. In the upper portion (Bands A, B, and C) there is an inverse relationship between thickness and hardness. That is, the hardness tends to increase with decreasing thickness. Such behavior is expected in stretching processes. The stretching results both in thinning and hardening. In the lower part of the helmet (Bands D and E), the hardness tends to increase with increasing thickness. This reflects an upsetting process in which the effective strain is compressive. The nature of the deformations incurred in forming helmets was further investigated in studies with gridded helmets, as discussed in a later section.

Histograms for average thicknesses of helmets and helmet blanks are shown in Figure 12. Approximate locations of the modes are shown for convenience in comparing thicknesses. By this comparison, the average reduction in thickness during forming is about 0.005 inch or 12 percent. This corresponds closely with the tabulated reductions for each helmet shown in Column 14 of Table 1A in the Appendix.

The hardness of the material increased from about 90  $R_B$  with blanks to an average of about 42  $R_C$  in the finished helmets. Figure 13 shows histograms for average hardness of the helmets and blanks. A common scale has been used for convenience in comparing the differences in hardness which resulted from the forming operation. The total spread is about 10  $R_C$  numbers for the 200 helmet and 12  $R_C$  numbers for the 200 blanks.

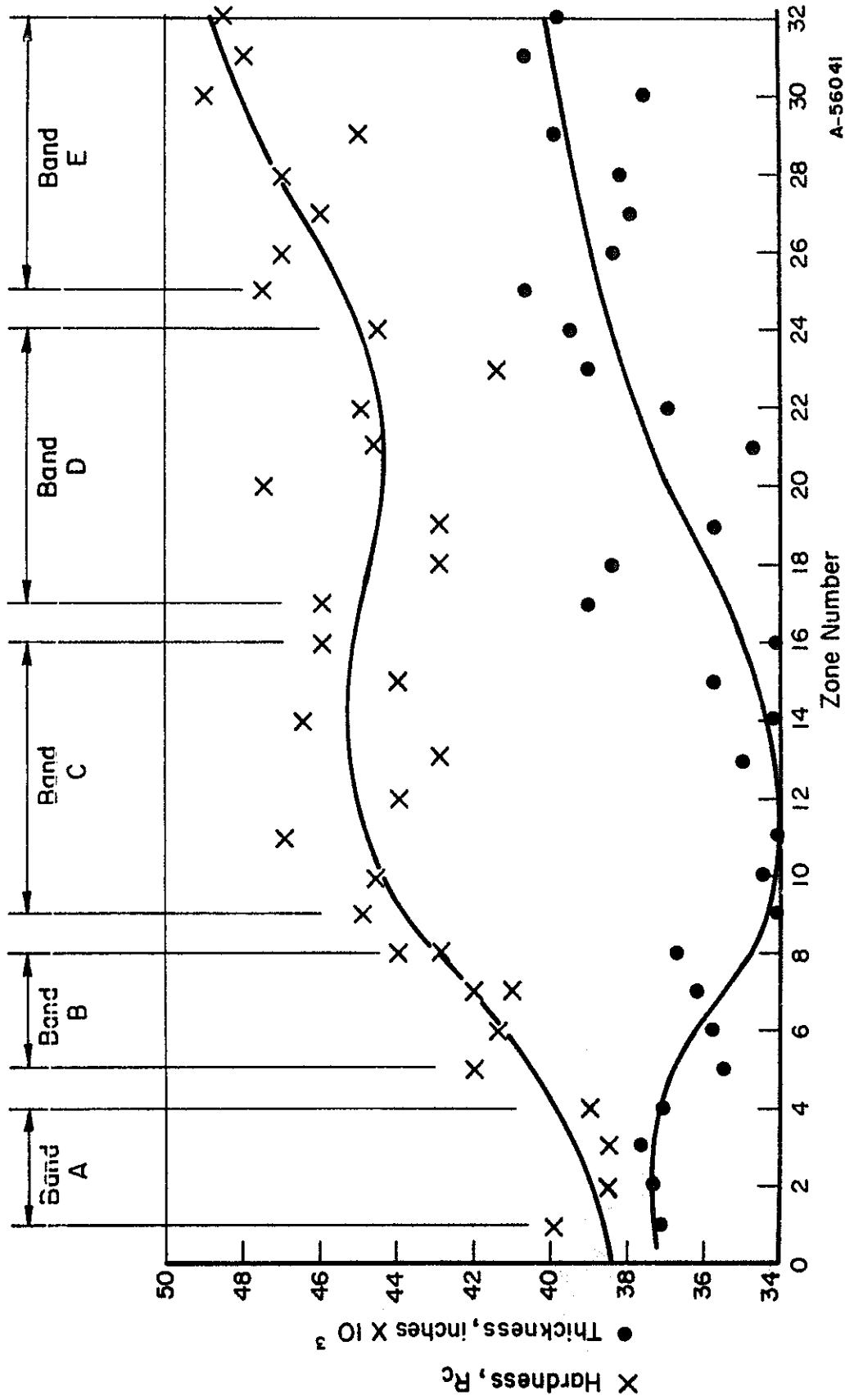


FIGURE 11. THE VARIATION IN HARDNESS AND THICKNESS FOR A TYPICAL M-1 HELMET

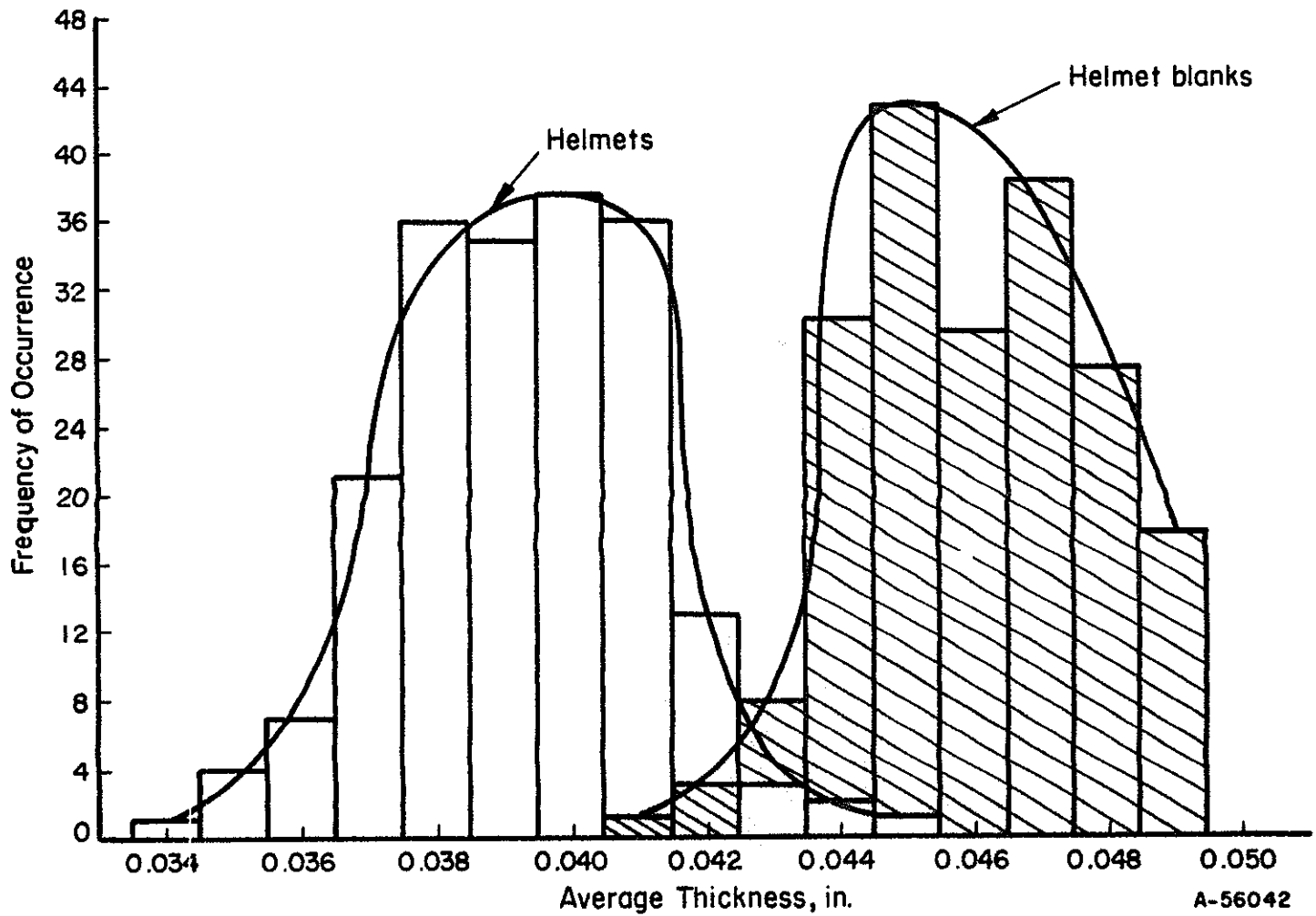


FIGURE 12. DISTRIBUTION OF THICKNESS FOR 200 HELMETS AND 200 HELMET BLANKS

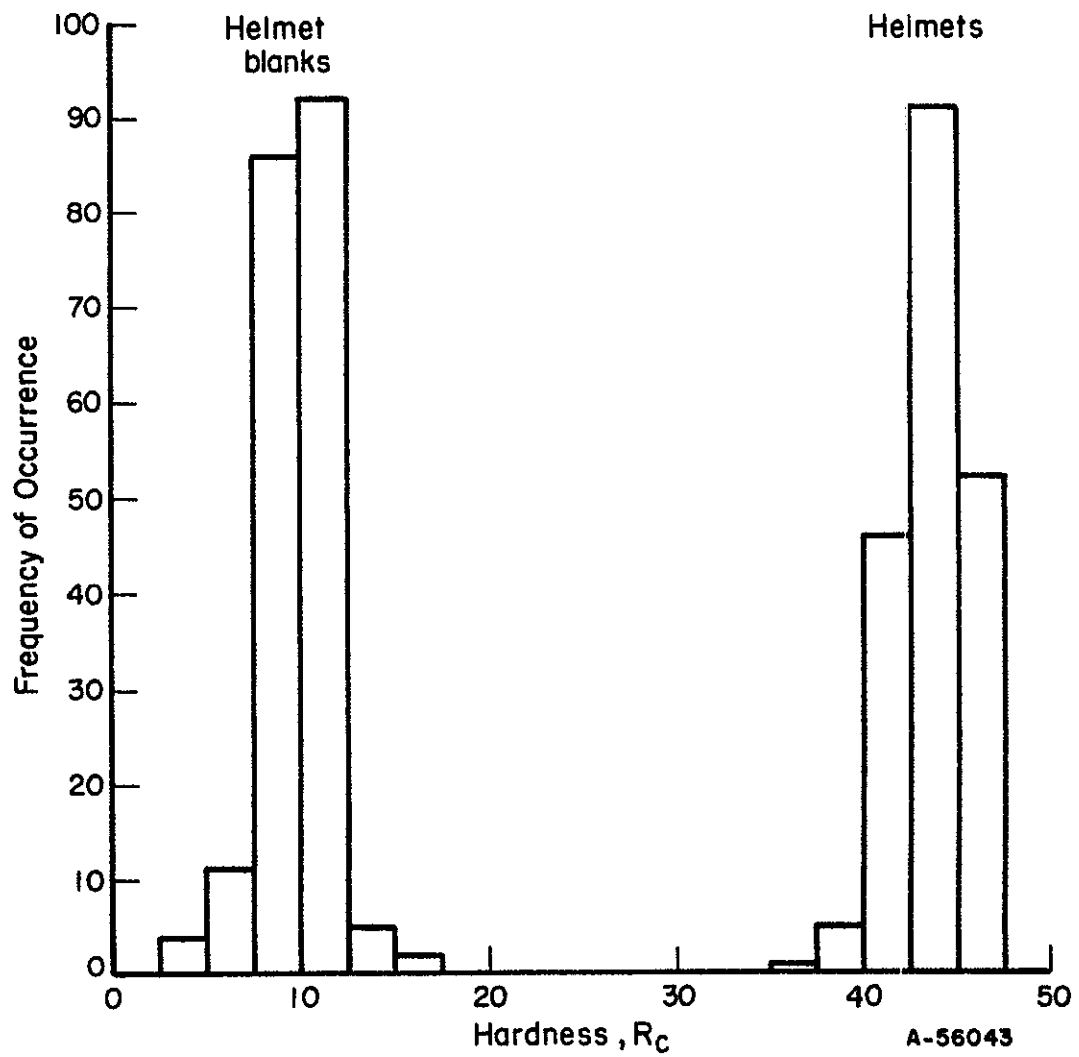


FIGURE 13. DISTRIBUTION OF AVERAGE HARDNESS FOR 200 M-1 HELMETS AND BLANKS



### Chemical Composition

Chemical analysis of the helmet material for silicon, manganese, and carbon content indicated the composition to be generally within the specifications as set forth in MIL-A-13259B (MR). Carbon content was found to be consistently on the low side of the 1.20-1.50 percent specification. About 25 percent were .05-.1 percent below the minimum. Column 9 in Table 1A lists the chemical analysis by heat number.

Histograms of the silicon, carbon, and manganese content for the 200 heats of material are shown in Figure 14.

### Metallographic Observations

All specimens exhibited a heavily cold worked microstructure which complicated the analysis. Nevertheless, it was possible to detect small differences in the amount of grain boundary carbides and in the degree of cleanliness from heat to heat. Differences in the degree of cold work were also noted. The most significant difference noted, however, was that some sections contained small microfissures (up to about 0.01 inch deep) at the surface. These fissures were similar to tears and may have resulted during the forming operation or during sectioning and removing from the helmet proper. Such fissures could well detract from the ballistic properties of the material. cursory examination suggested that about 25 percent of the sections exhibited such fissures. The fissures occurred in areas which had been the more heavily cold worked.

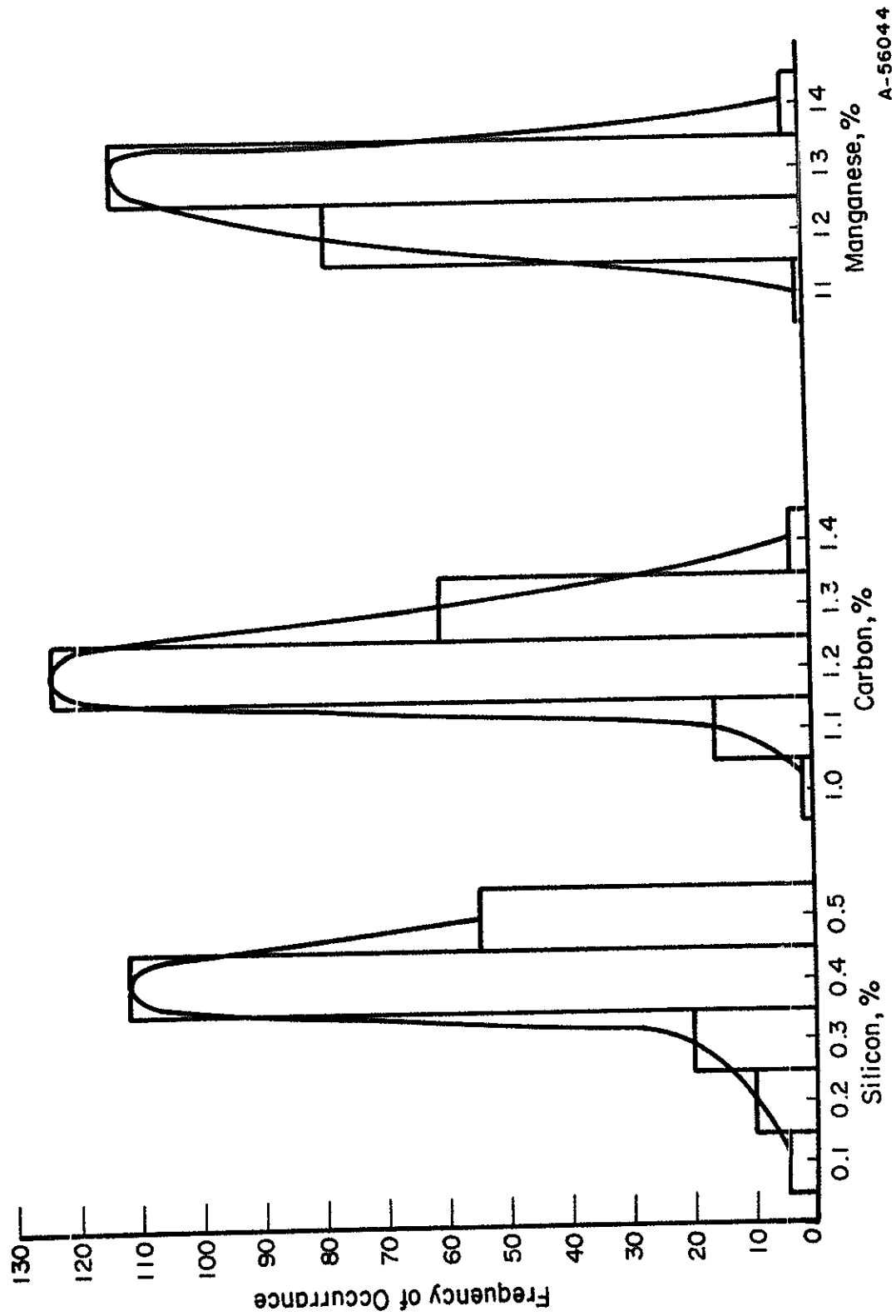


FIGURE 14. DISTRIBUTION OF SILICON, CARBON, AND MANGANESE  
FROM 200 HEATS OF HELMET STEEL

It was not possible in the sections examined to determine if the surfaces were decarburized; the presence of martensite at the deformed surfaces could not be ascertained.

#### Mechanical Properties of Helmet Blanks

The yield stress, tensile strength, total elongation and hardness after fracture for 200 helmet blanks are listed in Table 1A, Columns 5 through 9 in the Appendix. These properties were determined in a direction transverse to and longitudinal with the rolling direction of the blank.

The tensile properties were found to be reasonably uniform. Figure 15 shows the distribution of the tensile stress for the 200 helmet blanks. The longitudinal and transverse strengths are combined since no significant directional effects on the strength were observed.

The uniform elongation tended to be from 2 to 5 percent lower in the transverse direction than in the longitudinal (rolling) direction.

#### Ballistic Properties

Ballistic-test results were obtained on 202 helmets and 200 helmet blanks. The data obtained included (1) zone number, (2) projectile velocity, and (3) penetration or non-penetration. Approximately 45 shots were fired into each helmet and 15 into each blank. As noted previously, actual thickness readings, rather than the average of 3 for each zone, were used to determine firing sequence for the helmets. This resulted in improved estimates of firing velocities to be used. A complete set of ballistic data for the helmets and blanks is furnished separately from the report.

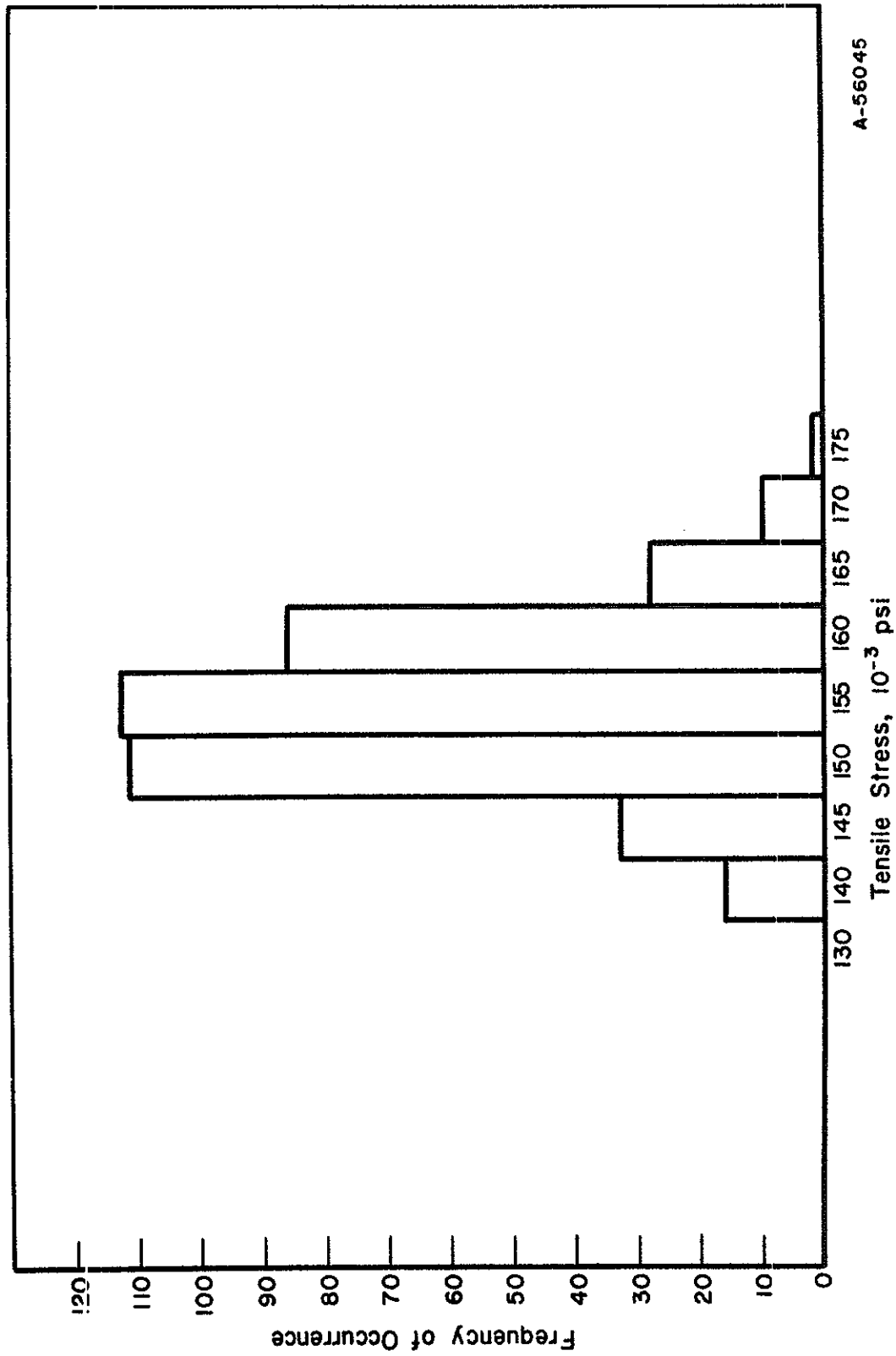


FIGURE 15. DISTRIBUTION OF TENSILE STRESS FOR 200 HEATS OF M-1 HELMET MATERIAL

A  $V_p$  50 as specified in MIL-STD-662A\* was calculated for each helmet and helmet blank. These values are included in Table A1, Columns 10 (blanks) and 12 (helmets). Figure 16 shows the distribution of  $V_p$  50's for the 200 helmets and blanks. The helmet  $V_p$  50's show a near normal distribution, whereas the distribution for helmet blanks is skewed toward the higher values. Of special interest, however, is a comparison of the modes; the  $V_p$  50 of the helmet blanks is about 350 fps higher than that of the helmets.

In the calculation of a  $V_p$  50 for the entire helmet, the lowest velocity penetration shots were almost always found in the thinner sections (located in the upper part of the helmet), while the highest velocity nonpenetration shots were found in the thicker sections (located in the lower part of the helmet). In effect, the  $V_p$  50 calculated for the whole helmet represents a combination of at least two material conditions.

In order to obtain  $V_p$  50's for material with a narrower range of properties,  $V_p$  50's were calculated for the upper and lower sections of each helmet. Referring to Figure 10, Bands A, B, and C were considered as the upper section, and D and E as the lower section. This division generally grouped the thin-hard and the thick-hard zones of the helmets.

The calculated  $V_p$  50 values and average thickness and hardness of each section are shown in Table A2 of the Appendix.

---

\* The  $V_p$  50 is defined as the average of the 5 lowest penetration velocities and the 5 highest non-penetration velocities, provided that the total spread among these values is less than 125 feet per second. If the spread is greater than 125 fps, the  $V_p$  50 is the average of the 7 lowest penetration velocities and the 7 highest non-penetration velocities.

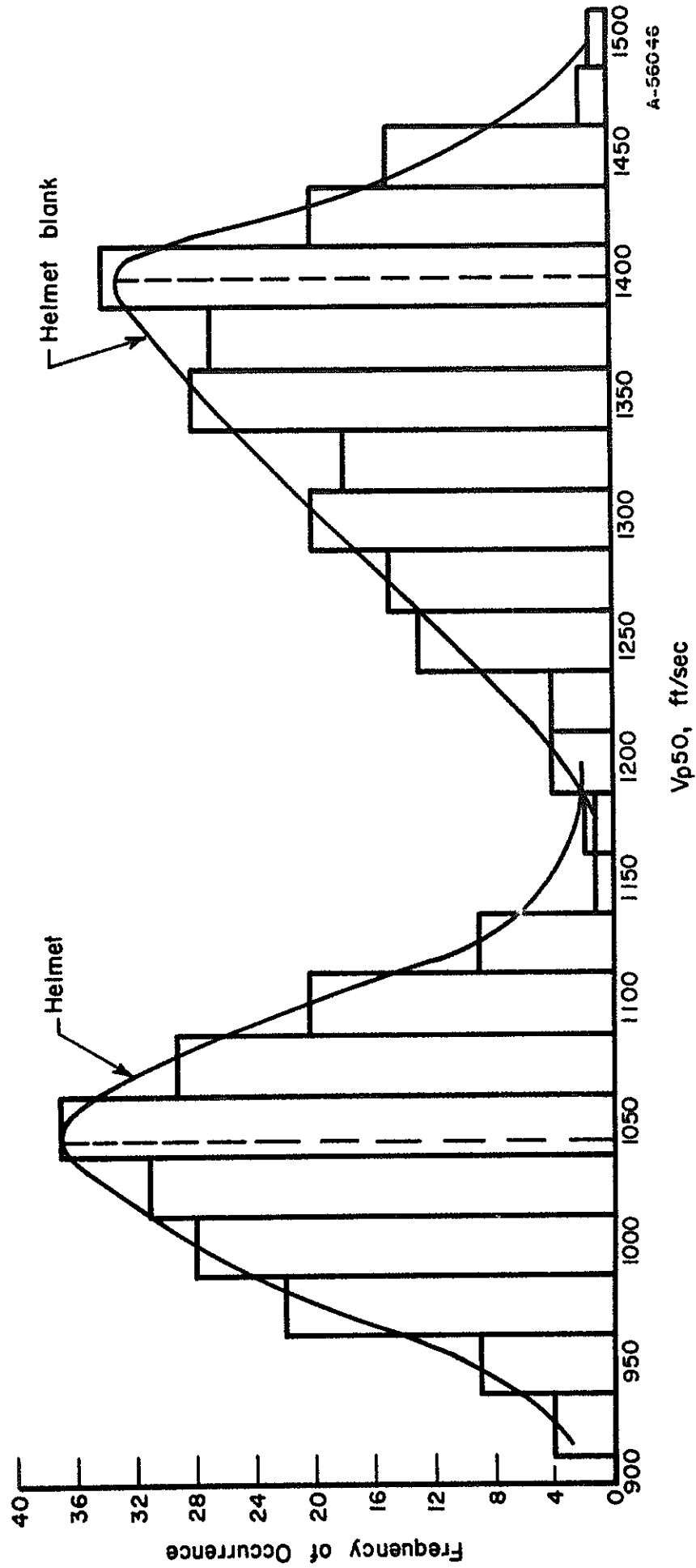


FIGURE 16. Vp50 DISTRIBUTION FOR 200 M-1 HELMETS AND HELMET BLANKS

In an attempt to establish the ballistic properties of specific areas in M-1 helmets, a  $V_p$  50 was also determined for each of 96 areas into which the helmets had been divided, using data from all 200 helmets. These values are listed in Table A3 of the Appendix.\* The lowest  $V_p$  50 measured in this way was 908 ft/sec, occurring at the right end of Zone 9, one of the thin sections of the helmet.

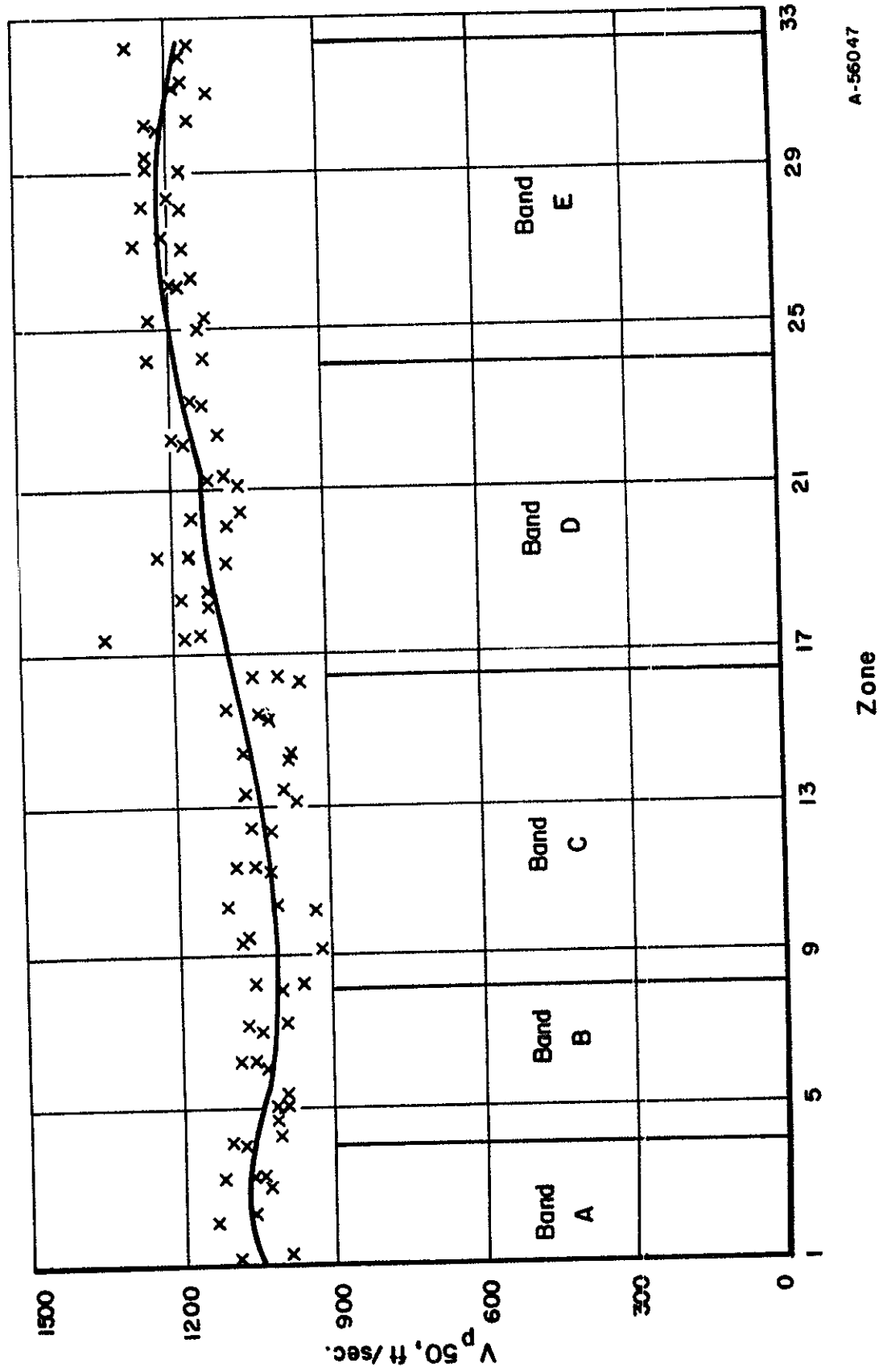
A plot of  $V_p$  50 versus zone number of the helmets is shown in Figure 17. The thinnest area of the helmet (Band C) has the lowest  $V_p$  50's. The total range of  $V_p$  50's is from about 900 to 1225 ft/sec., a spread of 325 ft/sec.

#### CORRELATIONS WITH $V_p$ 50

The computed  $V_p$  50's were plotted against the various parameters studied. In considering the relationships it should be remembered that the variations of these parameters were generally limited to very small ranges. In addition, all helmets studied had  $V_p$  50's greater than 900 fps, the minimum acceptable value. The conclusions drawn are valid only for the ranges studied and should not be extrapolated outside these ranges. The results of these plots are presented in the following paragraphs.

---

\* The average hardnesses and thicknesses reported in Table A-3 are based only on the respective values of the 10 (or 14) areas used to compute the  $V_p$  50. In all previous tables, the average hardnesses and thicknesses were computed using all pertinent data. Thus, the average thickness of a helmet in Table A-1 is based upon the measurements of all 96 zones in that helmet even though only 10 of these were used to compute the  $V_p$  50.



A-56047

FIGURE 17.  $V_{p50}$  VERSUS ZONE NUMBER FOR 96 ZONES IN M-1 HELMETS



Thickness  $V_p$  50 Correlations

Figures 18 through 22 show the variation of  $V_p$  50 with thickness. Least squares lines and correlation coefficients (R) are indicated in each figure. A summary of these  $V_p$  50 versus thickness correlations is presented in Table 1.

A considerable amount of scatter in the data is apparent in each of the above figures as indicated by the correlation coefficients. However, a distinct increase in  $V_p$  50 with increasing thickness is apparent in each curve. Considering the scatter, the differences in slopes and intercepts of the least squares lines for data obtained from the helmets are not considered to be excessive. In fact, in the vicinity of the thickness ranges actually studied, the lines representing whole helmets, and the upper and lower sections are remarkably close. This is seen from Figure 23 where the least squares lines have been plotted over the approximate thickness ranges they represent. With respect to the lines obtained from helmet data, the greatest discrepancy in  $V_p$  50 is about 75 feet per second. This discrepancy occurs at an extreme thickness and is between  $V_p$  50's for whole helmets and for individual zones. Part of this difference may be associated with the different methods used to compute average thicknesses for these two bodies of data (see footnote, page 36). This difference in methods of computing average thickness may also account for the relatively high correlation coefficient (low scatter) associated with the  $V_p$  50 thickness line for individual zones.

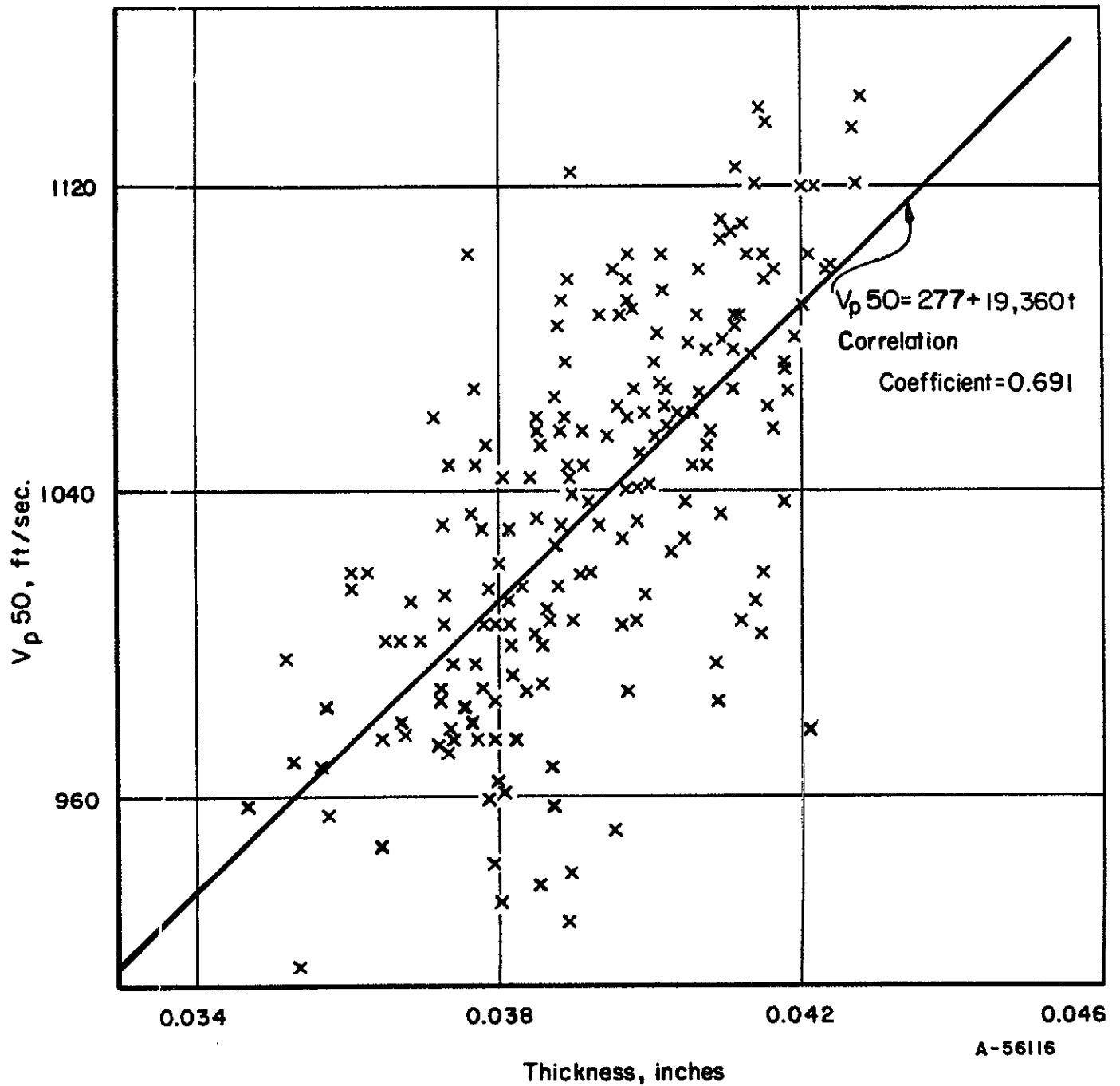


FIGURE 18. VARIATION OF COMPOSITE  $V_p 50$  WITH AVERAGE HELMET THICKNESS

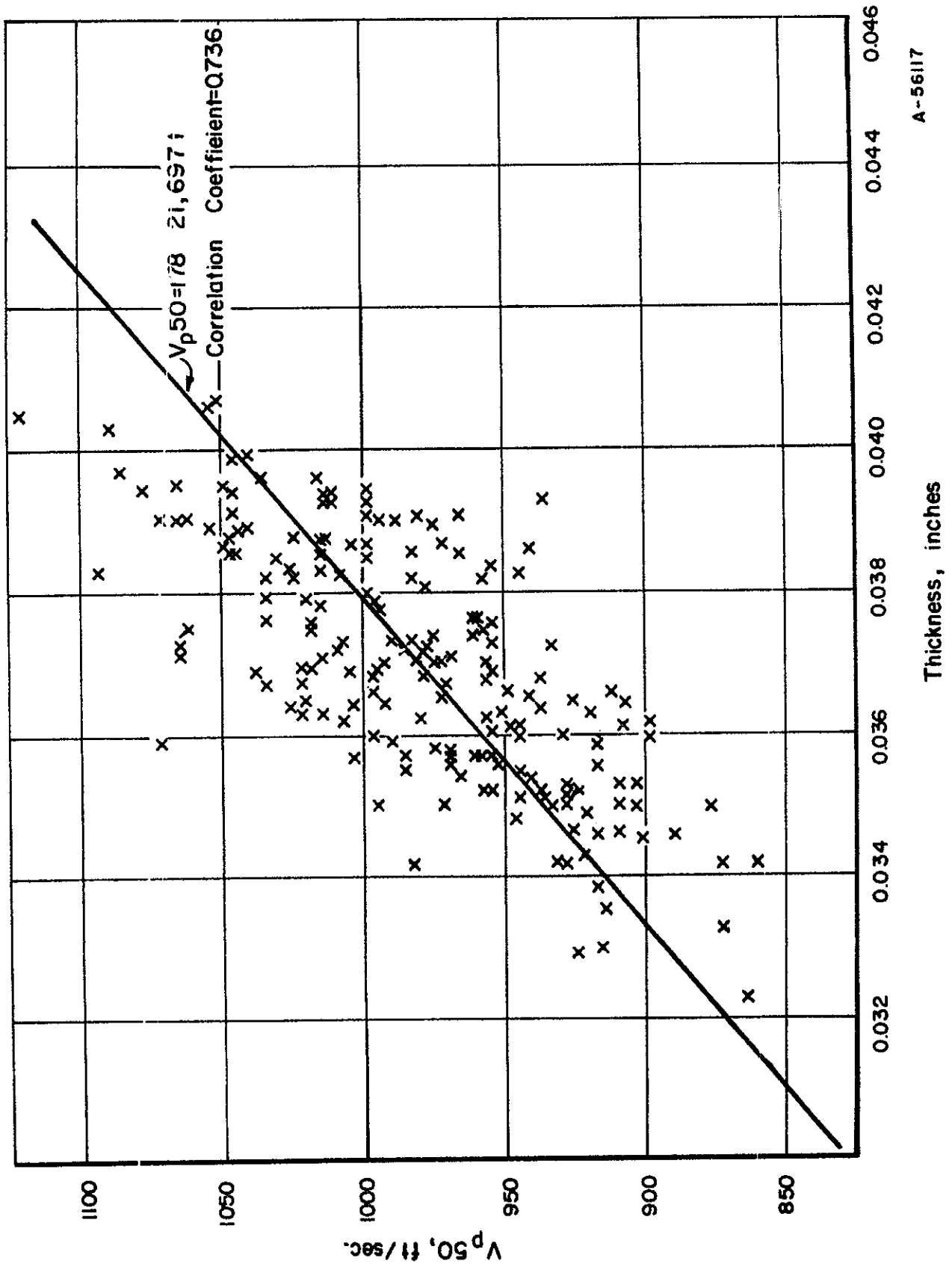
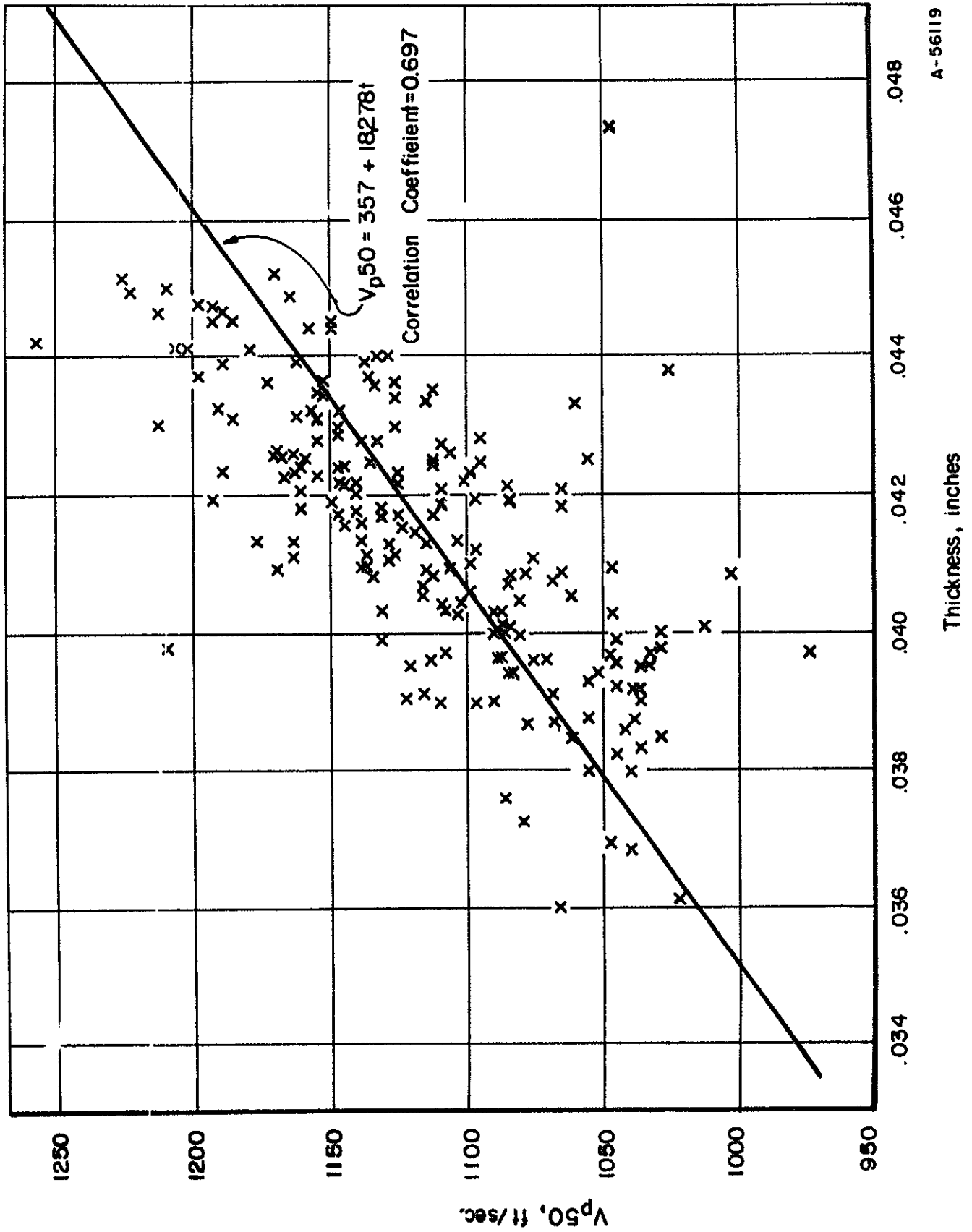


FIGURE 19. EFFECT OF THICKNESS ON THE  $V_{p50}$  FOR UPPER SECTION (BANDS A, B, AND C) OF 200 M-1 HELMETS



A-56119

FIGURE 20. EFFECT OF THICKNESS ON THE  $V_{p50}$  FOR LOWER SECTION (BANDS D AND E) OF 200 M-1 HELMETS

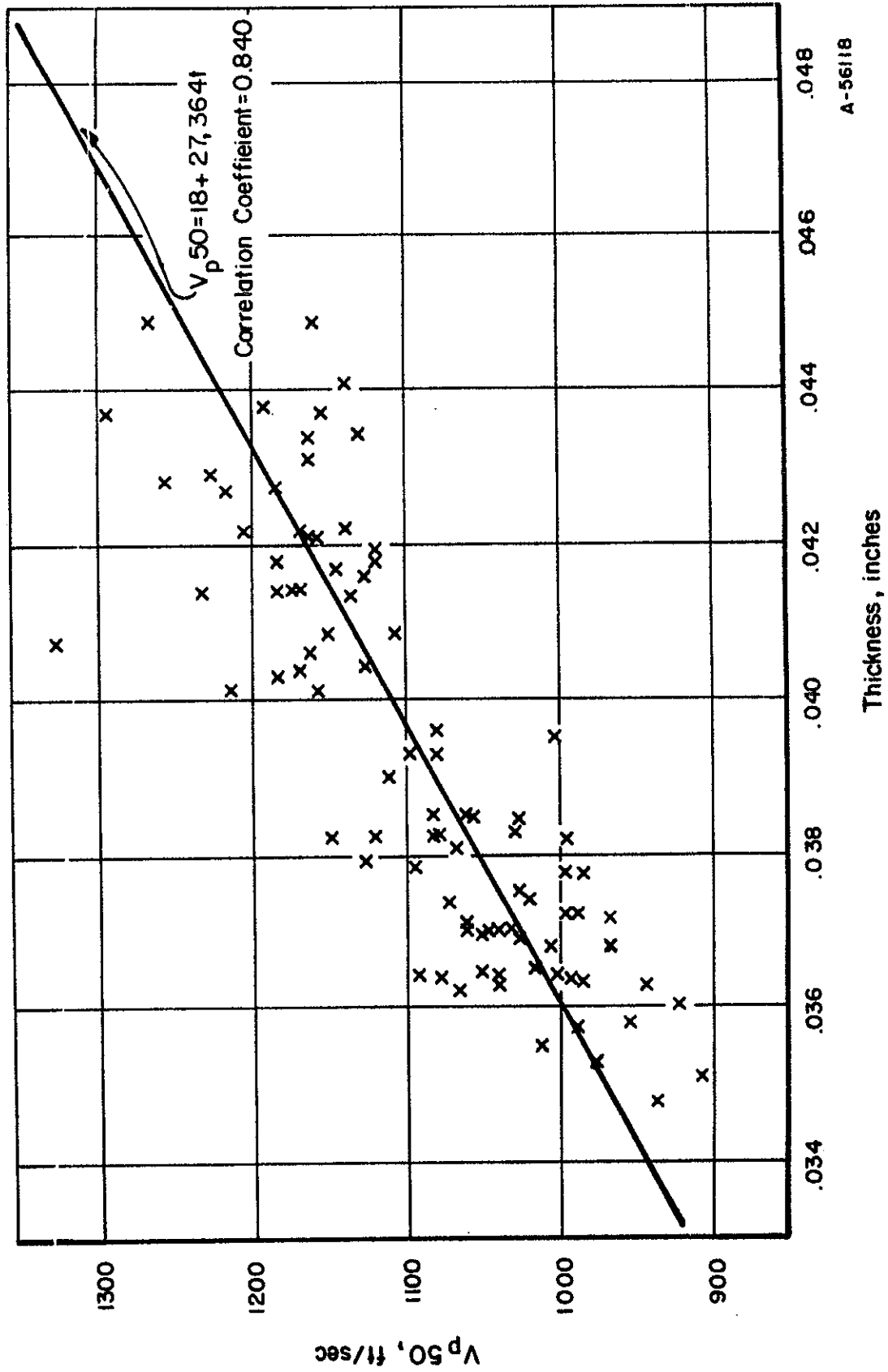


FIGURE 21. THE EFFECT OF THICKNESS ON THE  $V_p 50$  FOR  
96 ZONES IN EACH OF 200 HELMETS

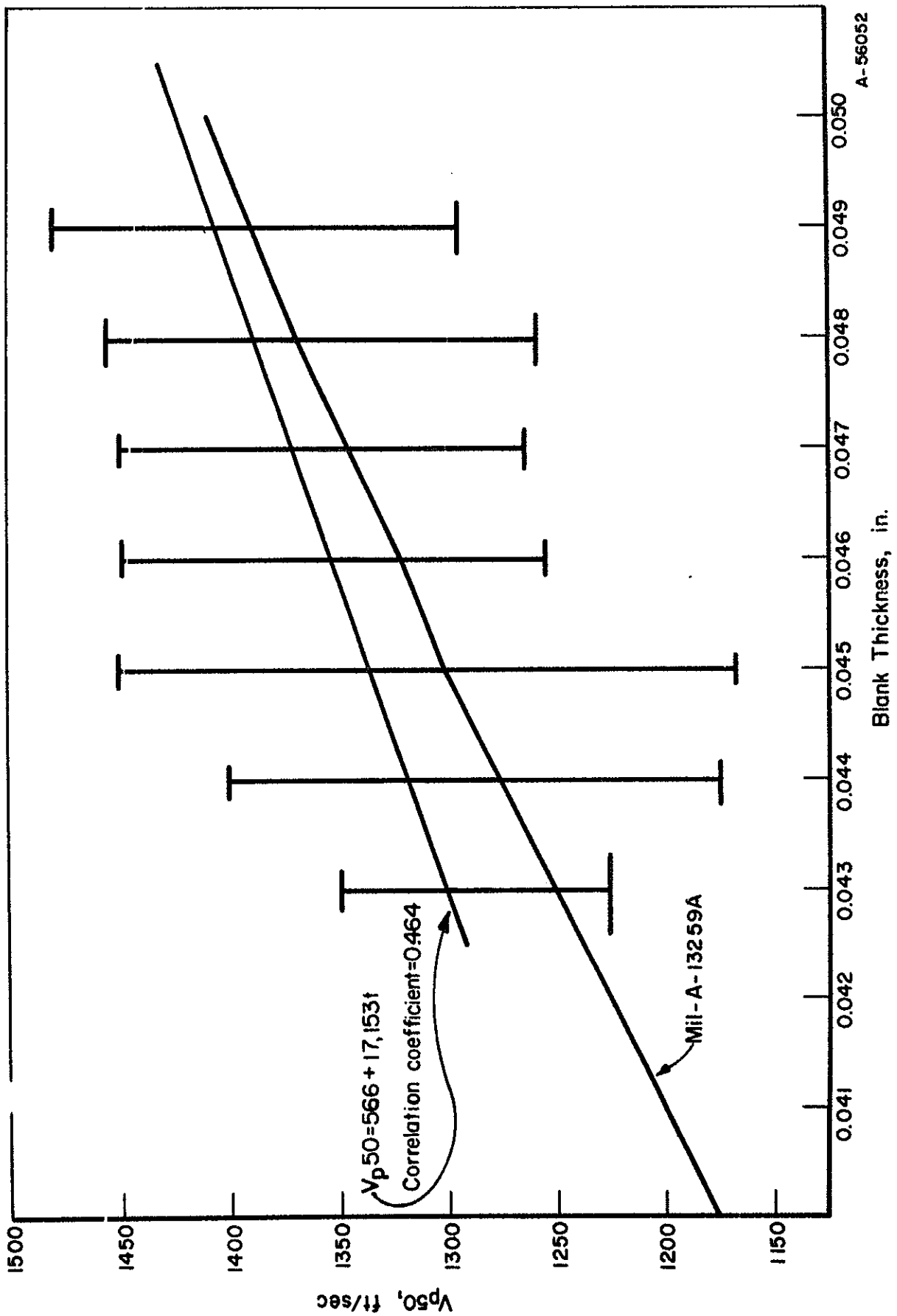
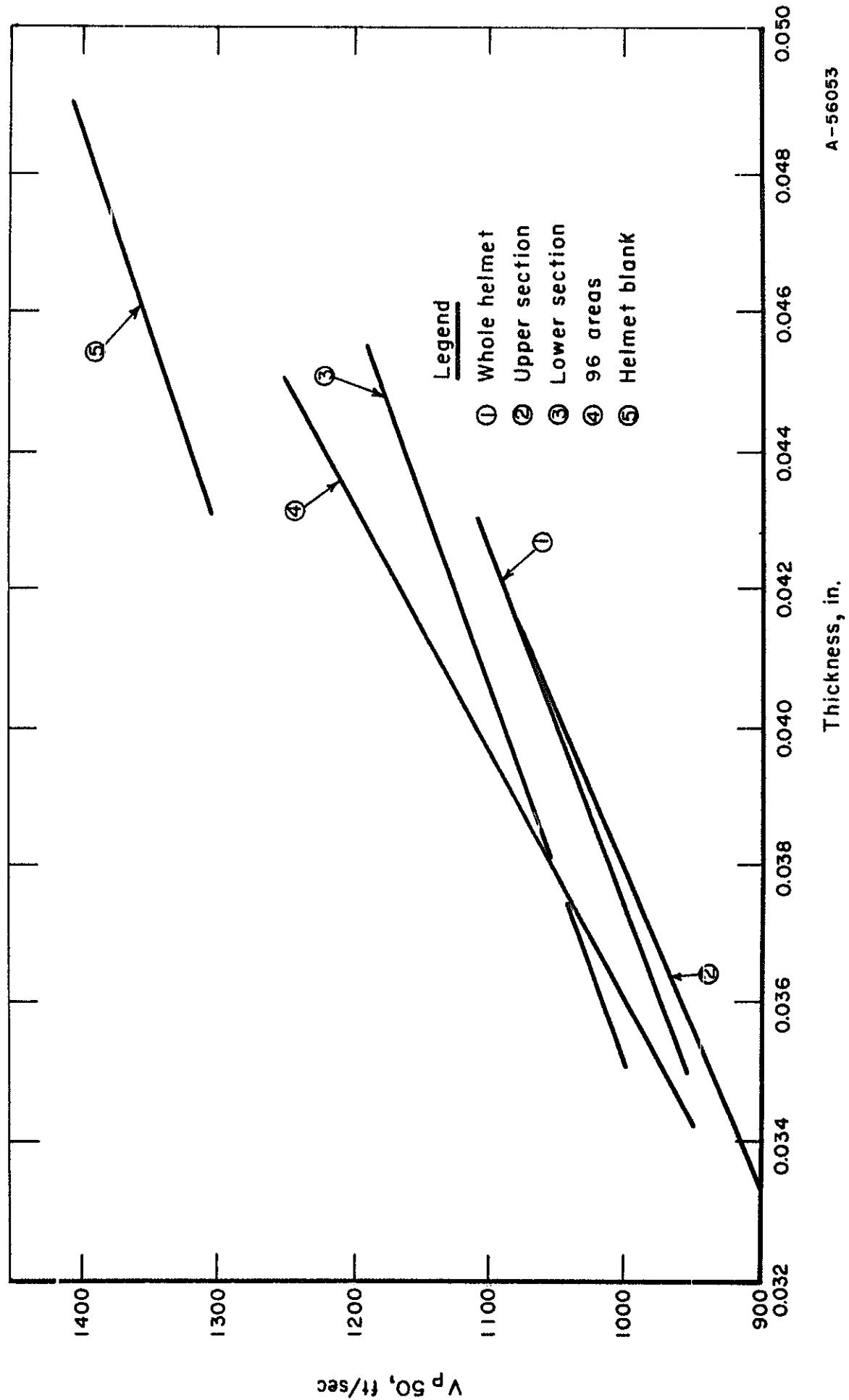
FIGURE 22. THE EFFECT OF THICKNESS ON THE  $V_{p50}$  OF M-1 HELMET BLANKS

TABLE 1. SUMMARY OF  $V_p$  50 VERSUS THICKNESS CORRELATIONS  
FOR M-1 HELMETS AND HELMET BLANKS

	Experimental Range of Thickness, inch	Equation of Least Squares Line*	Correlation Coefficient
Whole Helmet(Fig.18)	0.035-0.043	$V_p$ 50=277+19,360t	0.691
Upper Section(Fig.19)	0.033-0.041	$V_p$ 50=178+21,697t	0.736
Lower Section(Fig.20)	0.036-0.045	$V_p$ 50=357+18,278t	0.697
96 Areas (Fig.21)	0.035-0.045	$V_p$ 50= 18+27,364t	0.840
Helmet Blank (Fig.22)	0.043-0.049	$V_p$ 50=566+17,153t	0.464

$$\text{Correlation Coefficient} = \frac{N \Sigma(V_p 50) t - \Sigma(V_p 50) \Sigma t}{\sqrt{[N \Sigma t^2 - (\Sigma t)^2] [N \Sigma(V_p 50)^2 - (\Sigma V_p 50)^2]}}$$

\*Thickness, t, in inches.



A-56053

FIGURE 23. COMPARISON OF THICKNESS AND  $V_{p\ 50}$  FOR HELMETS AND BLANKS



The least squares line for the blanks is distinctly separated from the lines obtained from helmet data. An explanation for this is given in the next section.

It should be noted that although the least squares line for the  $V_p$  50 of blanks is above the specification value included in Figure 22 from Table II, MIL-A-13259B(MR), the individual data extend well below the specified lower acceptable limit. In fact, a very significant number of the helmet blanks would be below Military Specifications.

#### Hardness - $V_p$ 50 Correlations

A plot of hardness and  $V_p$  50 for the 96 areas is shown in Figure 24. The total range of hardness is 11  $R_c$  numbers. Over this limited range, and with the relatively large distribution in readings, the  $V_p$  50 appears to be insensitive to hardness. Similar plots using data from whole helmets and blanks also indicated a lack of correlation between  $V_p$  50 and hardness.

A significant correlation with hardness was found, however, over a larger range of hardness values. A direct comparison of  $V_p$  50 and thickness for the helmets and for helmet blanks is shown in Figure 23. As noted earlier, it can be seen that the helmet blanks are distinctly more resistant to ballistic penetration than are the helmets. The fact that a smooth curve cannot be drawn to include both helmet and helmet blank data, implies that some parameter other than thickness is operative. Of the parameters studied, only thickness and hardness

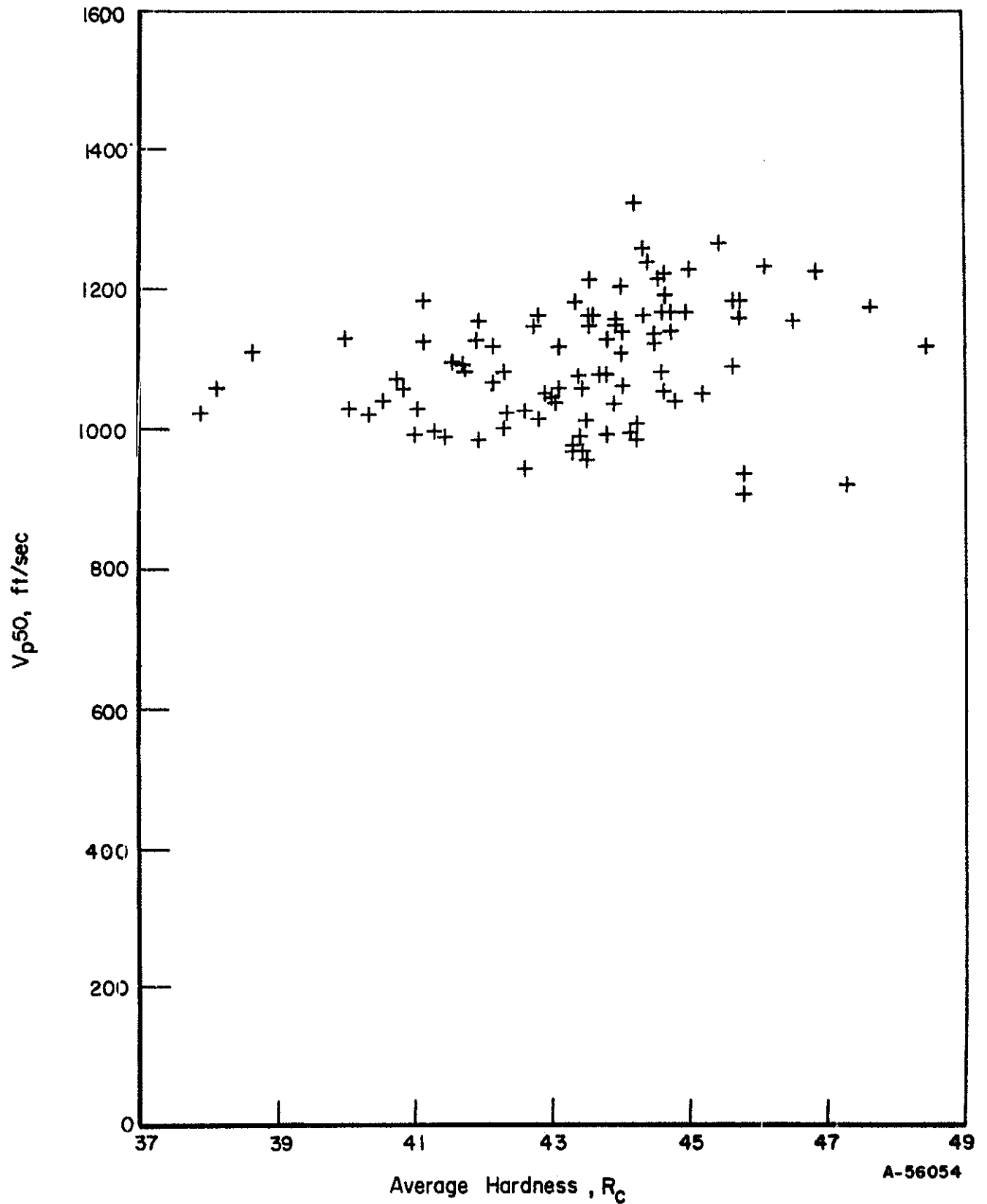


FIGURE 24. EFFECT OF HARDNESS ON THE  $V_{p50}$  FOR 96 ZONES IN EACH OF 200 HELMETS

were significantly different for helmets and blanks.\* Since thickness cannot account for the difference in  $V_p$  50, it seems reasonable to ascribe the differences to hardness. The implication is that for the range studied,  $V_p$  50 decreases with increasing hardness. The sensitivity of the relationship, however, is not sufficient to allow detection within the very narrow ranges of hardness of either helmets or blanks.

#### $V_p$ 50 Correlations with other Parameters

No influence of carbon, silicon, and manganese content on the  $V_p$  50 of the helmets was detected, as indicated by Figures A1 through A3 in the Appendix. Similarly, variations in tensile properties of the helmet blanks do not appear to influence the helmet  $V_p$  50 as shown in Figure A4. The small ranges of each of these properties and scatter in the  $V_p$  50 data could have masked any correlation which might exist. Larger property ranges may indicate a definite influence on the  $V_p$  50. A plot of  $V_p$  50 of blanks versus  $V_p$  50 of corresponding helmets (i.e., blanks and helmets from the same heat of steel) also revealed no direct correlation. This is especially significant since it indicates that inspection on the blanks will not provide direct information on helmet performance.

---

\* It can, of course, be argued that the tensile properties and perhaps the microstructure also differ between helmets and blanks. These differences, however, will be reflected in hardness. This point is developed in the discussion of forming.

### HELMET DEFORMATION STUDIES

In order to understand better the effects of forming the helmet on material properties, a series of helmet blanks was procured for detailed study. The objectives of this study included the following items:

- (1) To determine the pattern of deformation in various parts of the helmet, and to correlate these deformations with the observed hardness and mechanical-property values.
- (2) To determine whether the orientation of the rolling direction of the steel was an important factor in the mechanical properties of the helmet.
- (3) To investigate whether the mechanical and ballistic properties of a helmet could be predicted from a knowledge of the properties of the blank and the manufacturing process.

Eight blanks were selected for this study. Measurements of average hardness and thickness were made on each blank, after which a grid of 1-inch squares was scribed on one surface. In each case, the grid pattern was oriented 0 or 45 degrees to the rolling direction. The helmet blanks then were taken to Ingersoll and formed into helmets. The blanks were oriented in the dies such that the rolling direction was parallel, perpendicular, or at 45 degrees to the front-back axis of the helmet. Normal production procedures were used, including the shearing off of the excess metal at the rim, and exposing the formed helmet to the heating cycle used for baking the paint (the test helmets were not painted, however). Figure 25 shows the appearance of the gridded blank and the final appearance of the finished helmet.

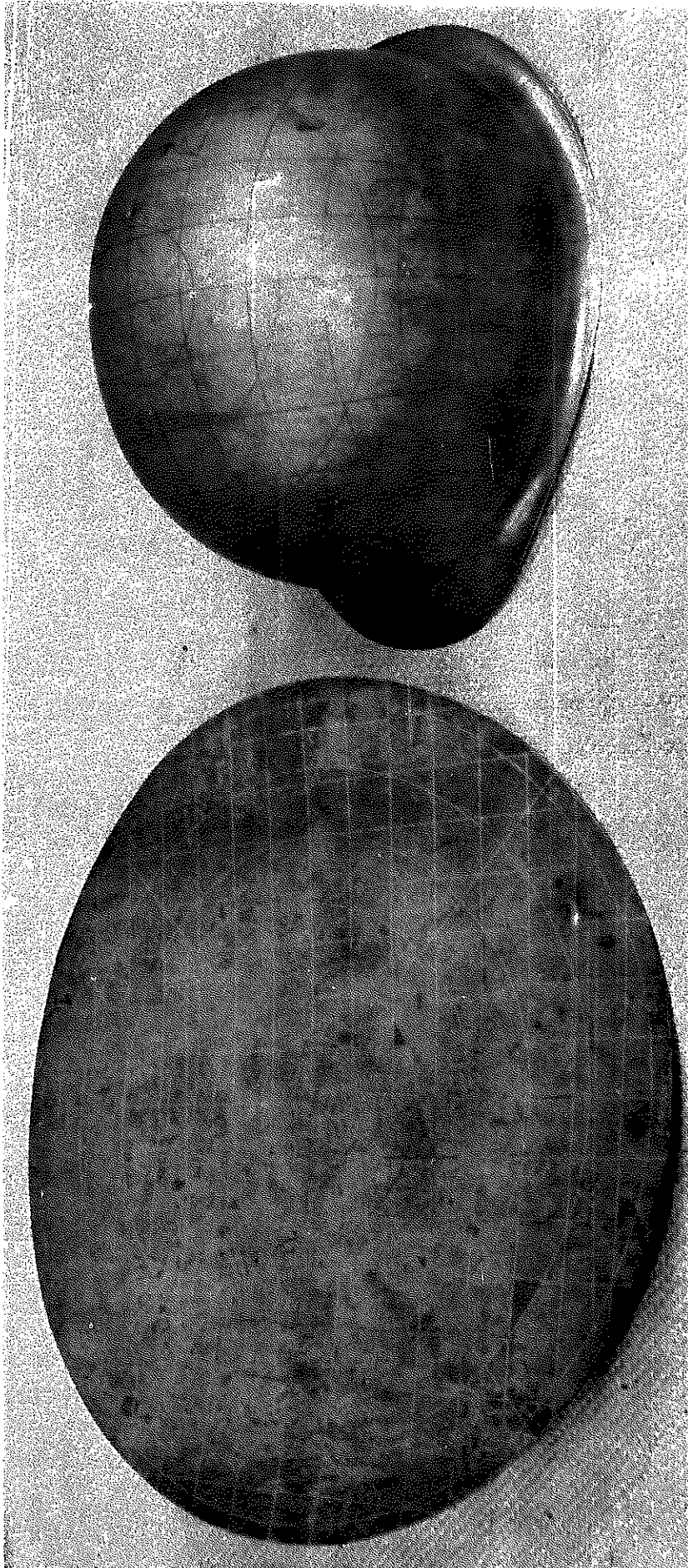


FIGURE 25. GRIDDED BLANK AND HELMET

Measurements of hardness and thickness then were made at the center of each of the original grid squares. These data are shown in Figures 26 through 33, on which the upper number represents the thickness (inches x 1000) and the lower number the Rockwell "C" hardness. The deformations at each grid point were measured along each of the original 1-inch gage lengths. The results are shown on maps of the original grids in Figures 34 through 41. The numbers shown represent the ordinary or engineering strain values expressed as percentages, positive or negative. The upsetting or compressive strains around the circumference are apparent as negative strain values.

The effective strain at the center of each grid square was computed by averaging the strains on opposite sides of each square to obtain values of  $e_1$  and  $e_2$ . These values first were converted to natural strains by the relation  $\epsilon = \ln (1+e)$ ; the effective strain was then computed from the expression:

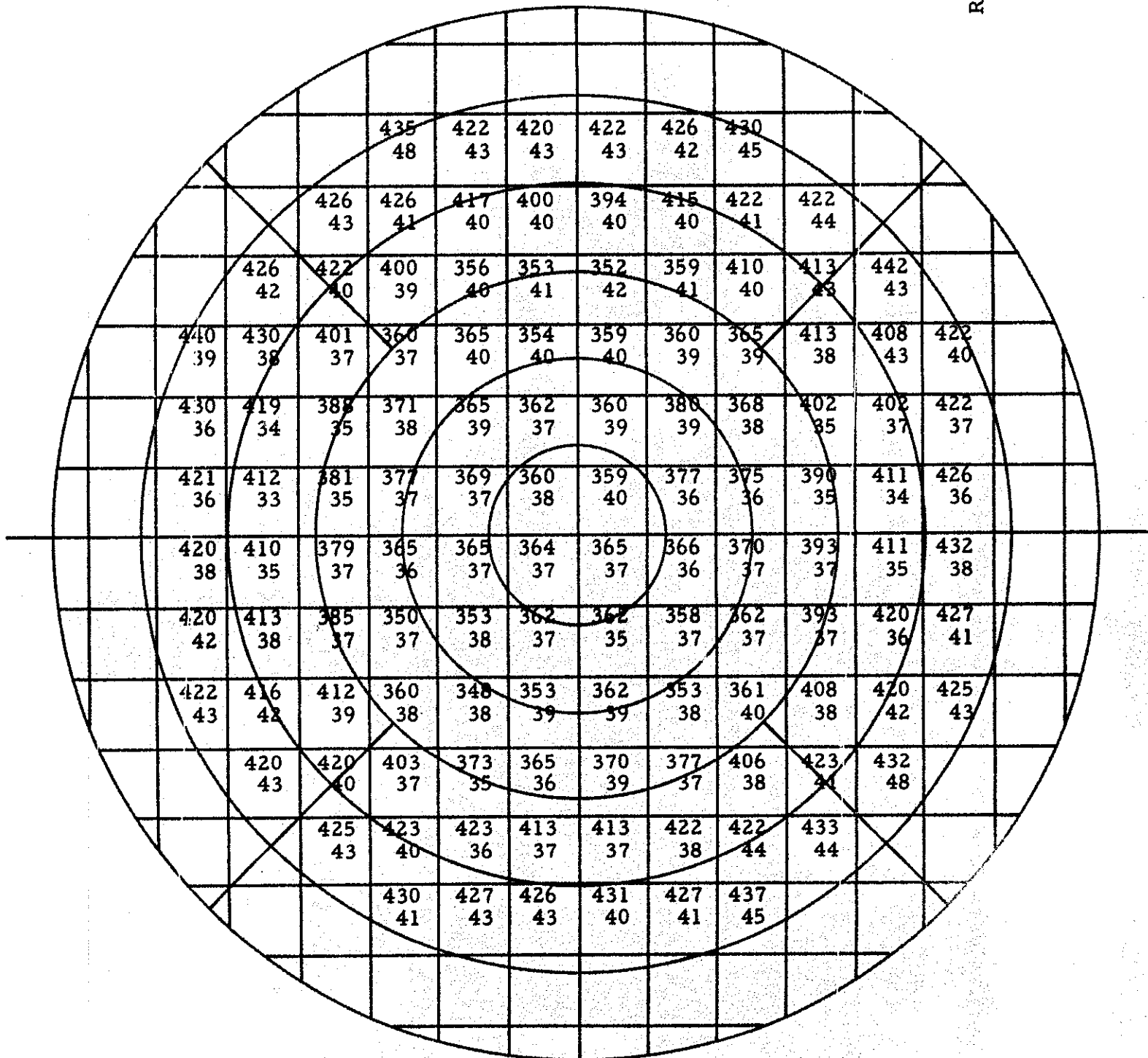
$$\bar{\epsilon} = \frac{\sqrt{2}}{3} \sqrt{\epsilon_1^2 + \epsilon_1\epsilon_2 + \epsilon_2^2}$$

These computations were programmed and performed on a desktop computer, and the results were used as described in the following sections.

#### Effect of Rolling Direction on Properties

Polycrystalline metals are known to develop a preferred orientation or texturing during many metal-working operations, such as wire drawing or rolling. In some instances, the texturing is sufficient

Rolling direction



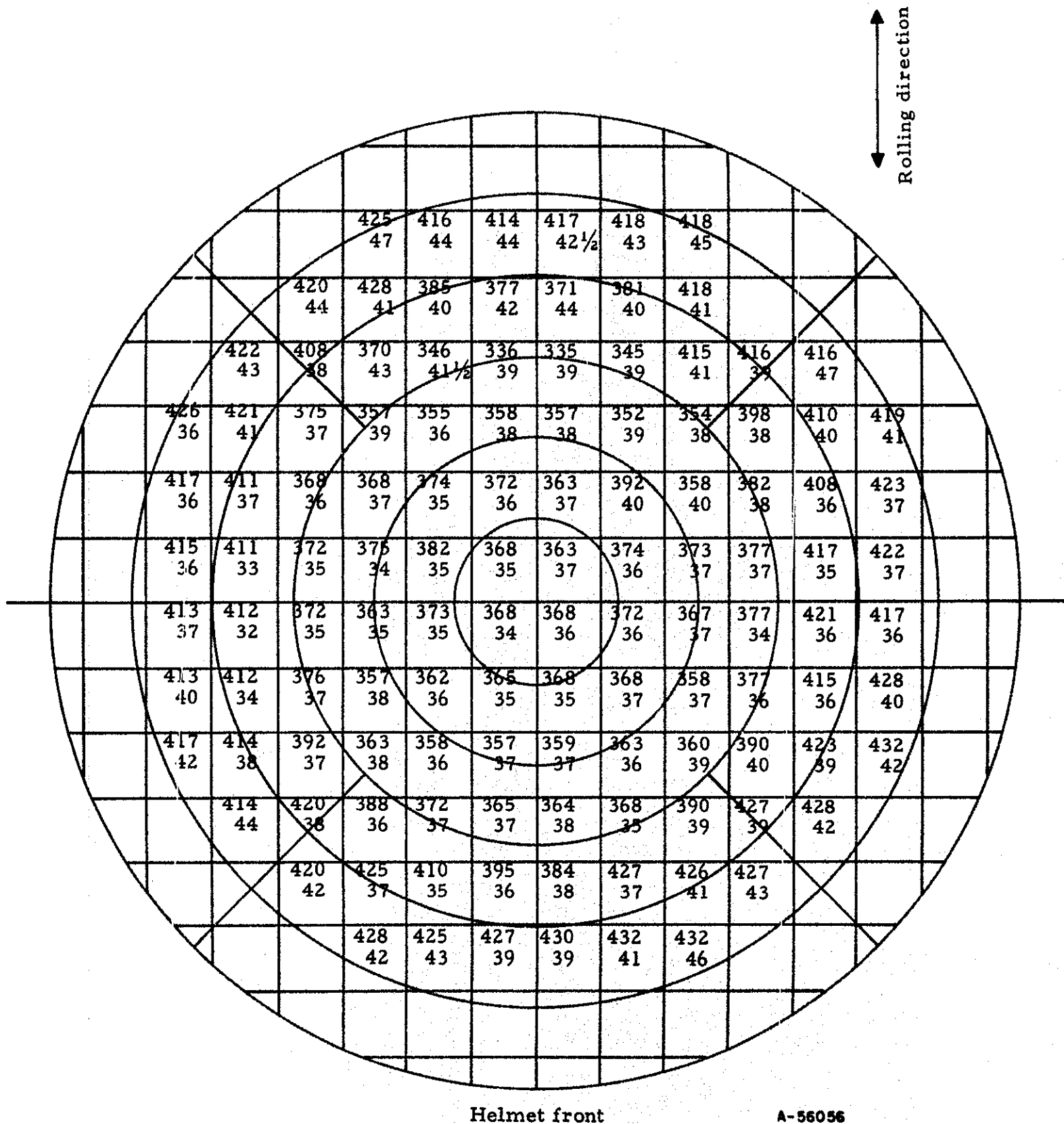
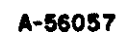


FIGURE 27. HARDNESS AND THICKNESS DATA ON HELMET M326A





**FIGURE 28. HARDNESS AND THICKNESS DATA ON HELMET I334B**

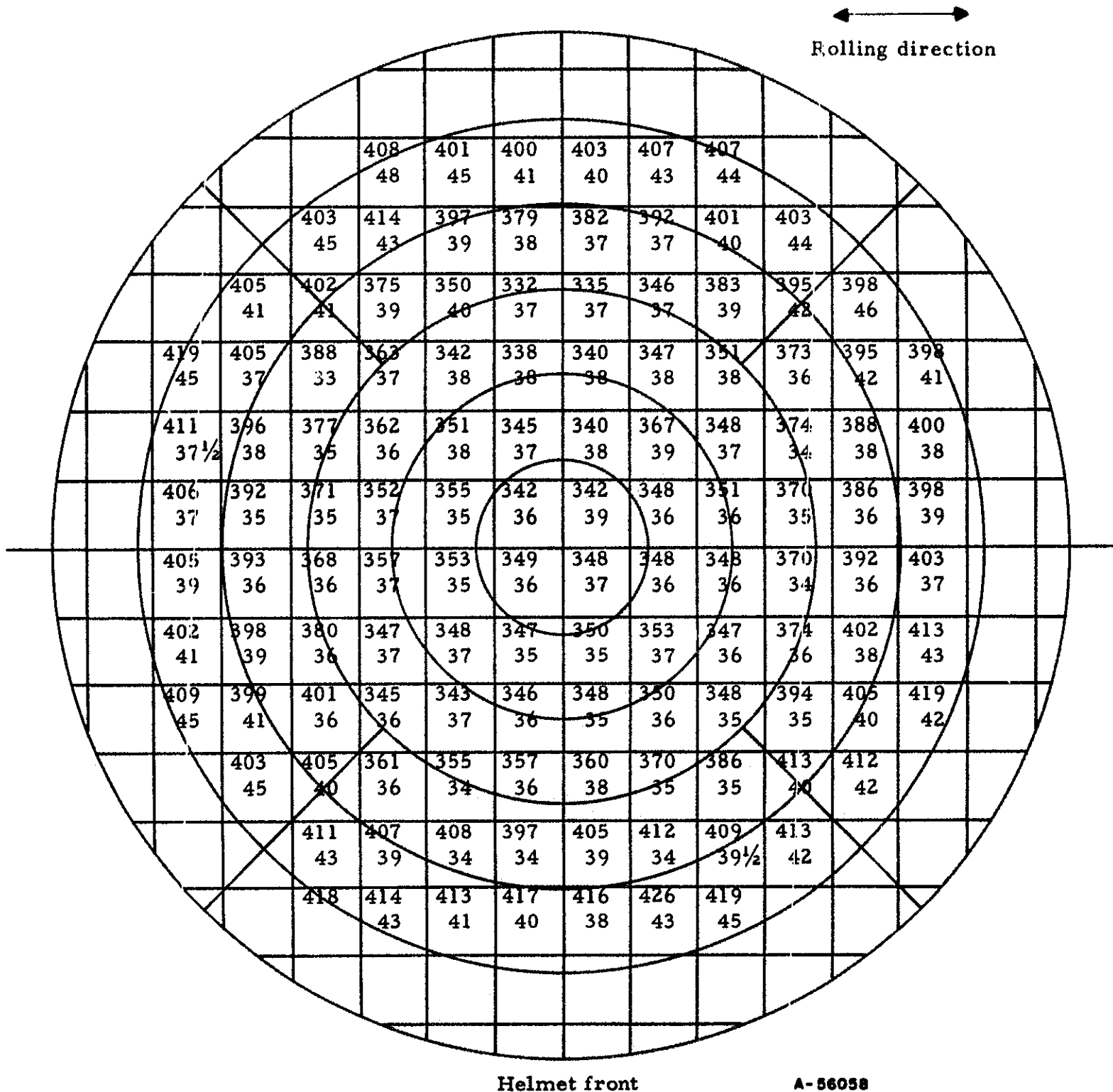


FIGURE 29. HARDNESS AND THICKNESS DATA ON HELMET I2491

↔  
Rolling direction

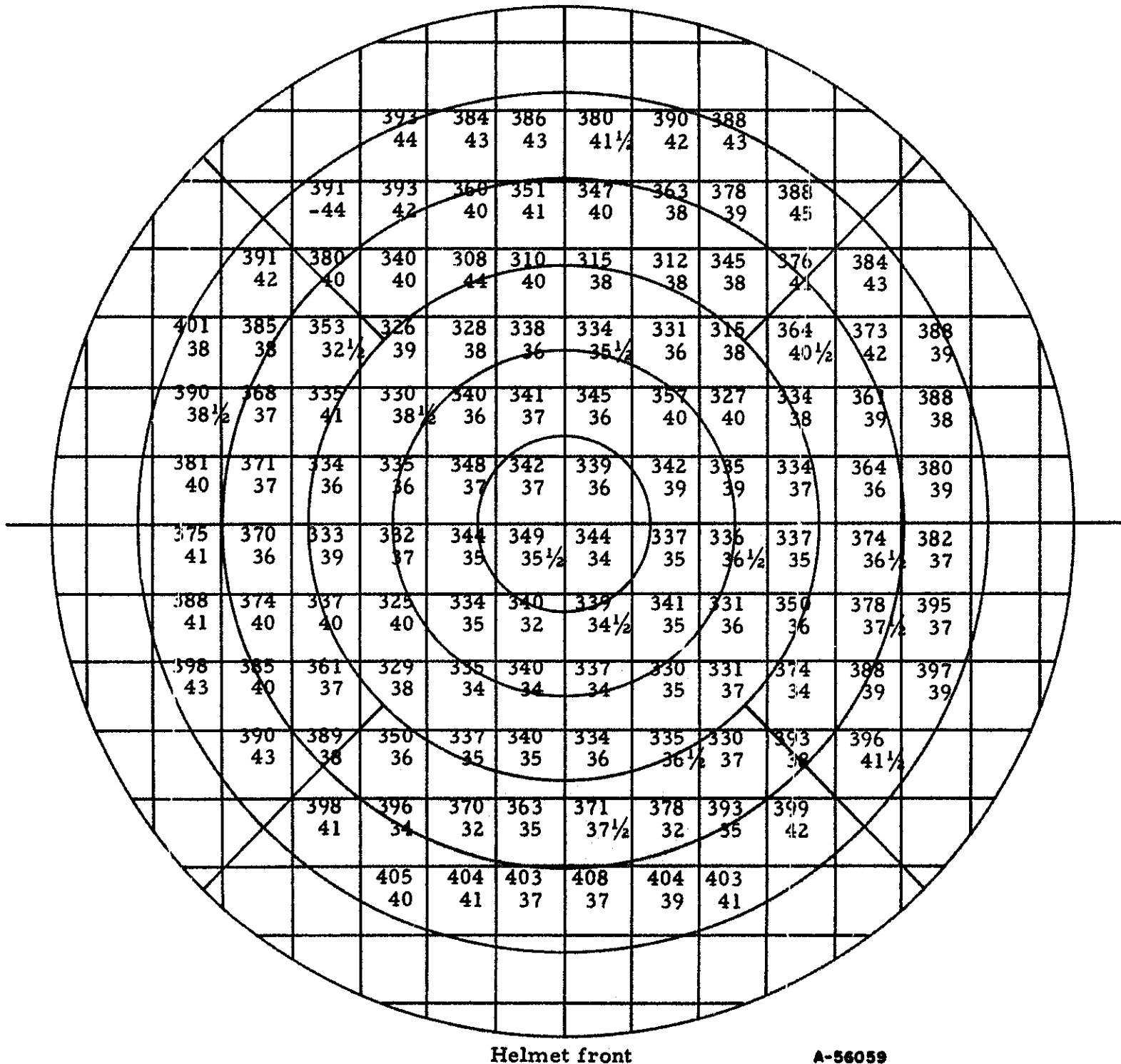
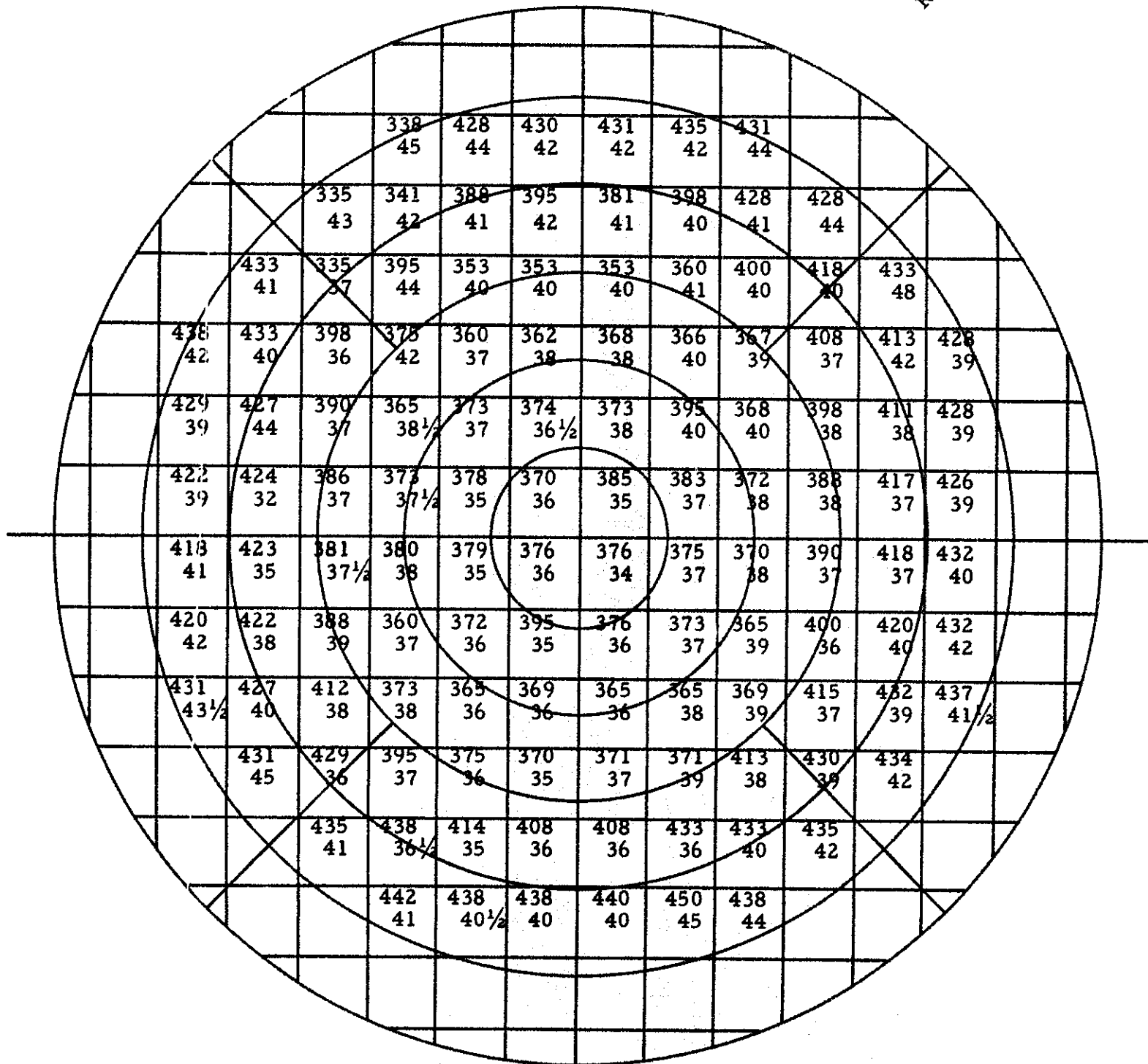


FIGURE 30. HARDNESS AND THICKNESS DATA ON HELMET I2505

**A-56060**

FIGURE 31. HARDNESS AND THICKNESS DATA ON HELMET I6674

Rolling direction



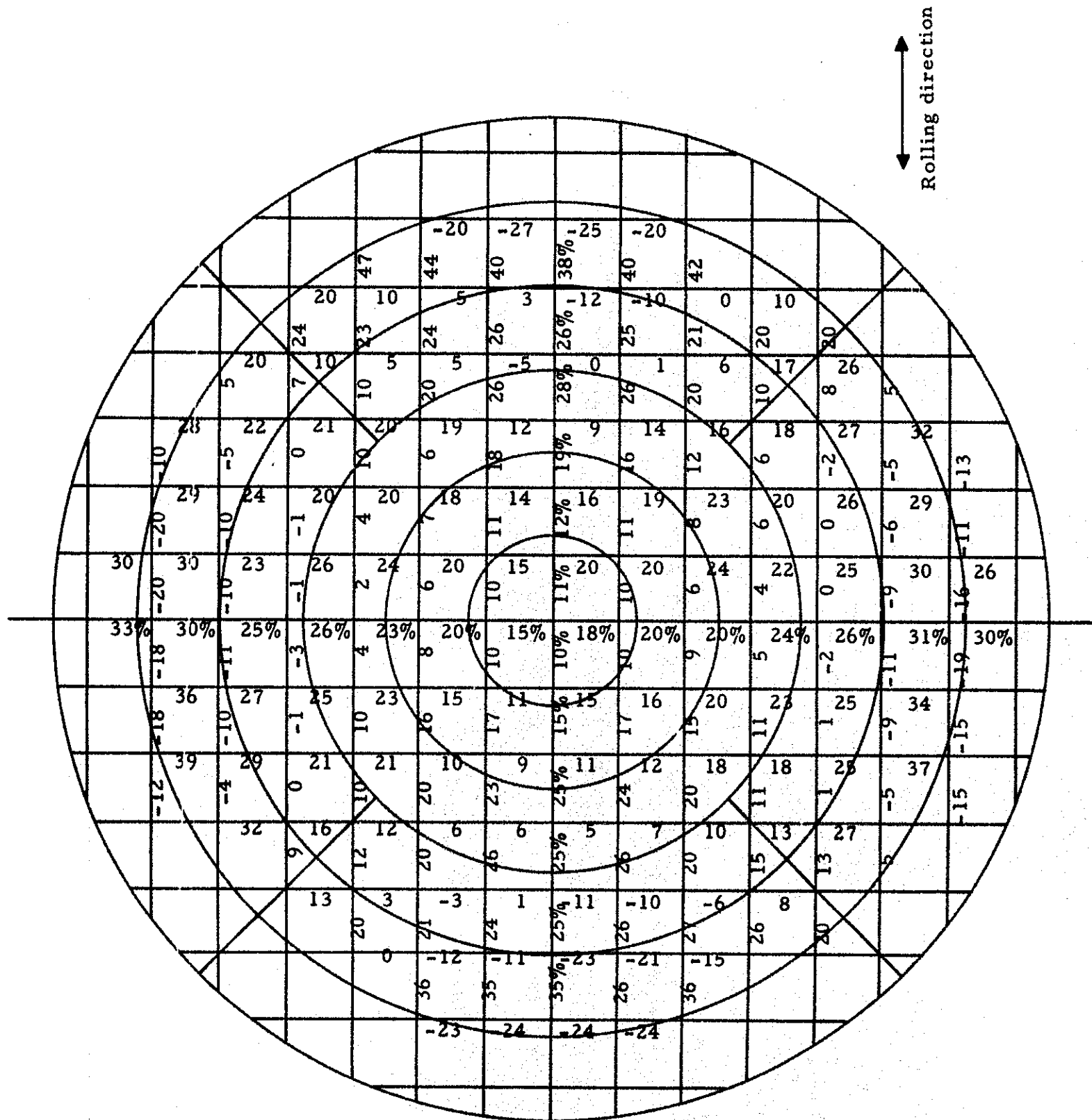
Helmet front

A-58061

FIGURE 32. HARDNESS AND THICKNESS DATA ON HELMET I7421



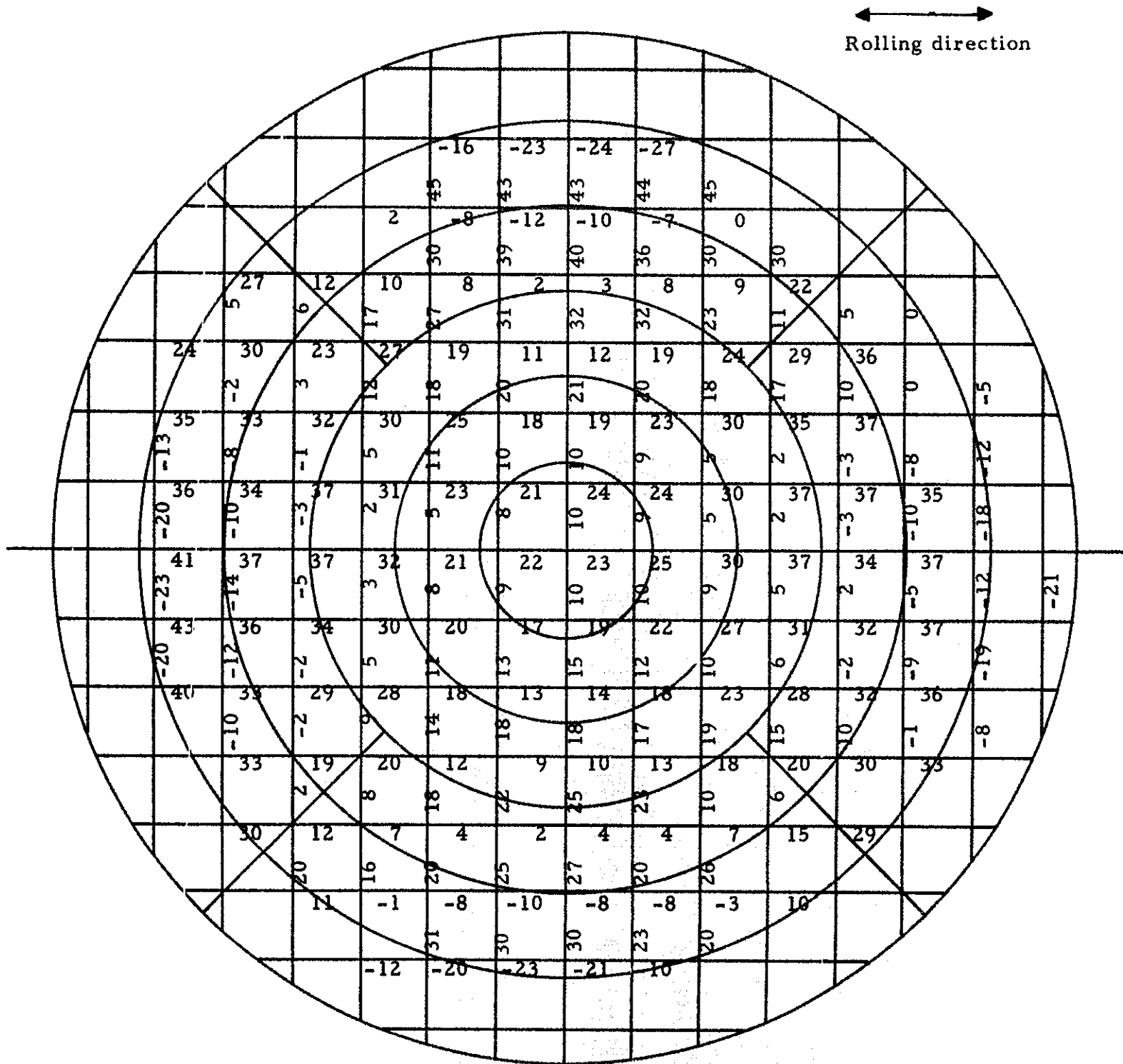
FIGURE 33. HARDNESS AND THICKNESS DATA ON HELMET I9926



Helmet front

A-56063

FIGURE 34. DEFORMATIONS OF 1-INCH GRIDS IN HELMET M322B

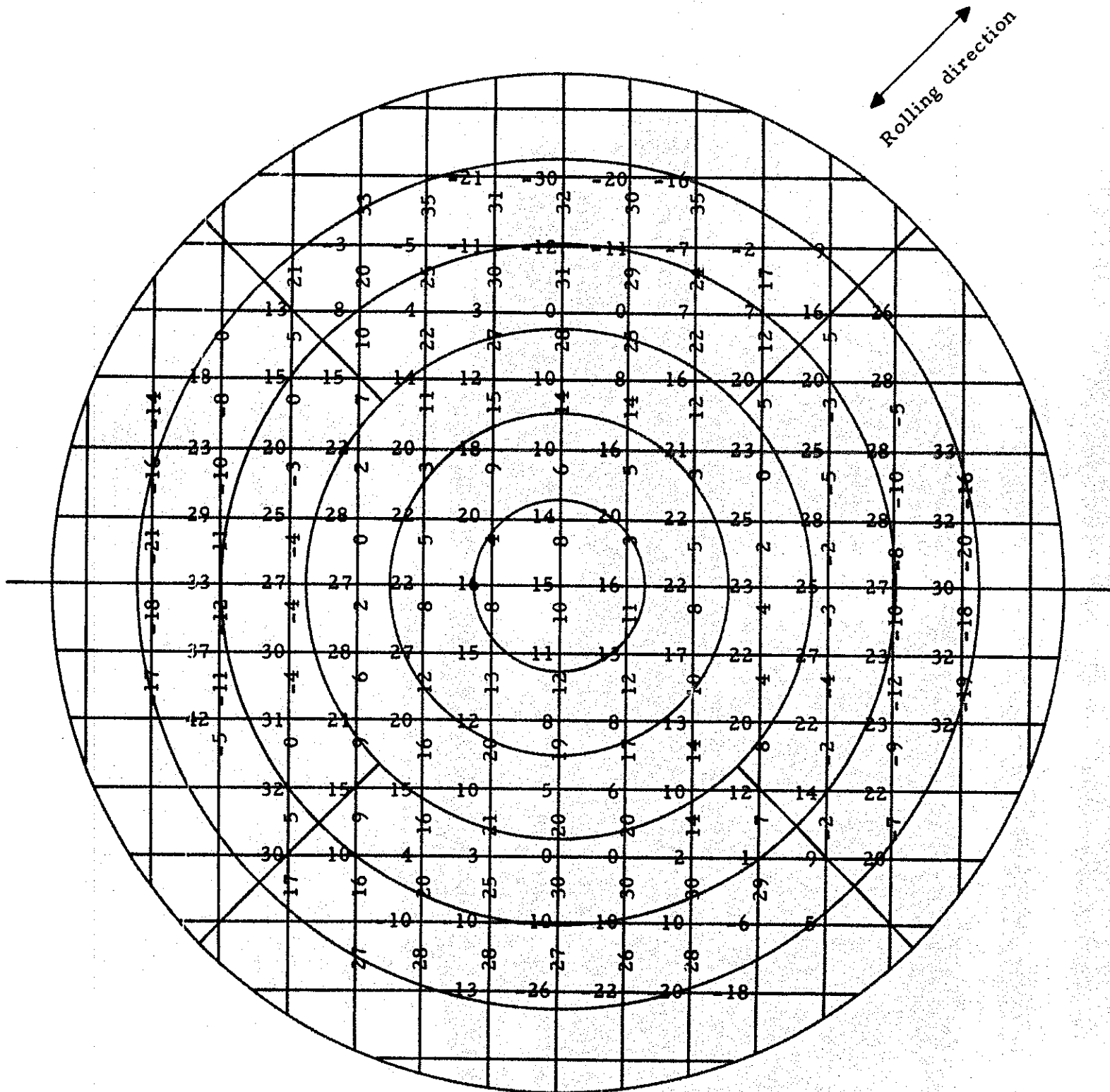


Helmet front

A-56064

FIGURE 35. DEFORMATIONS OF 1-INCH GRIDS IN HELMET 12505





Helmet front

A-56065

FIGURE 36. DEFORMATIONS OF 1-INCH GRIDS IN HELMET 19926

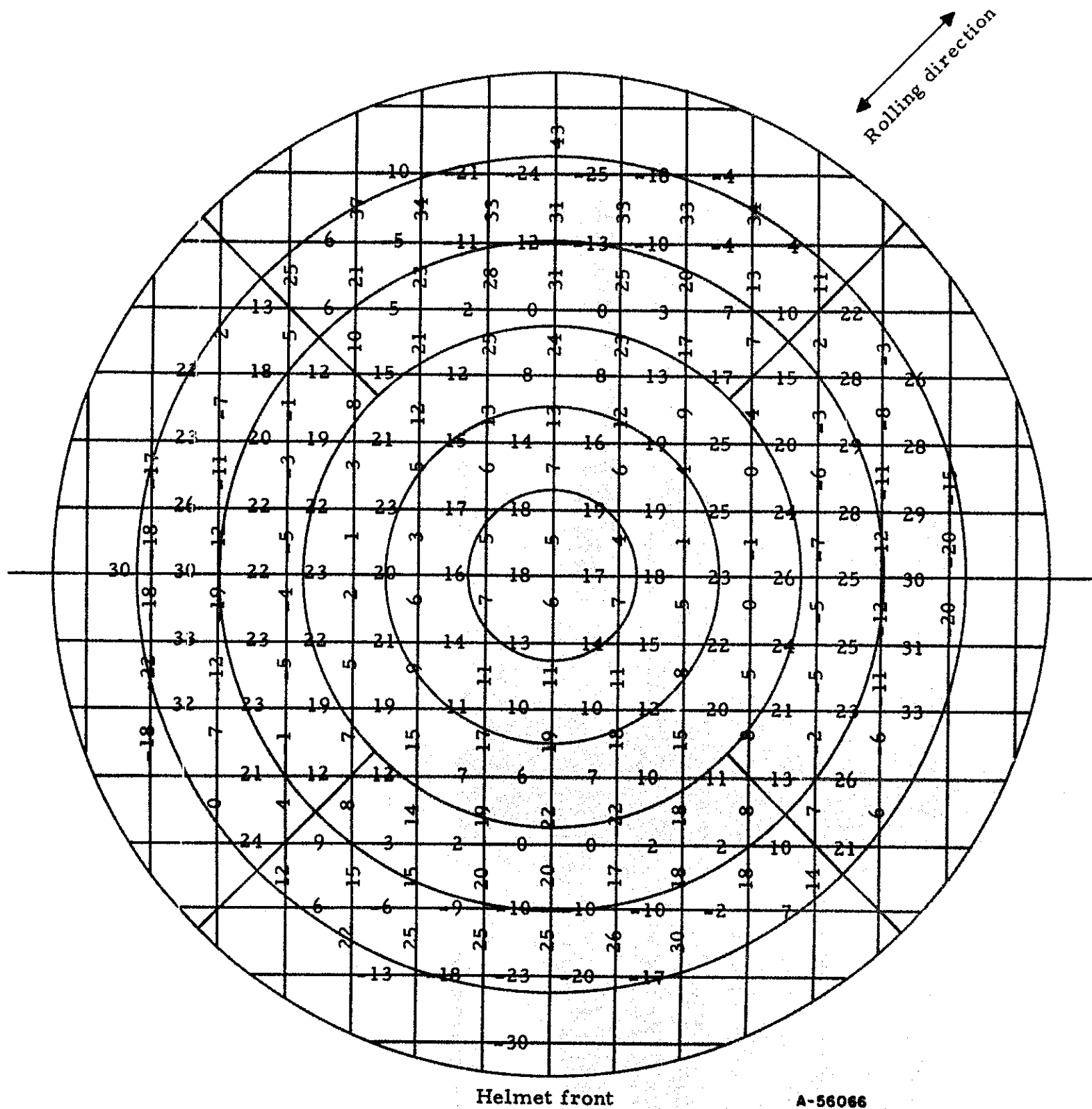
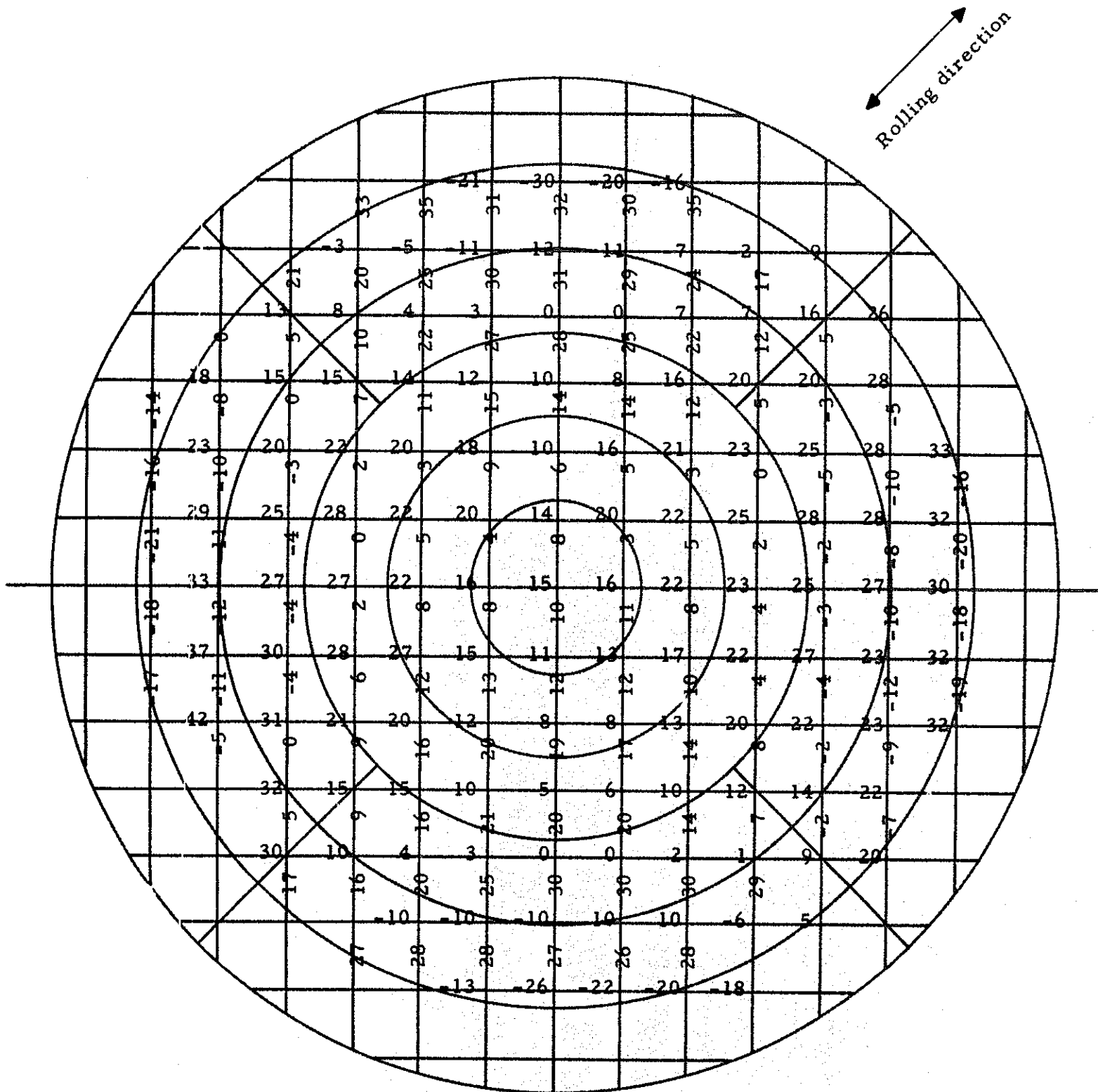


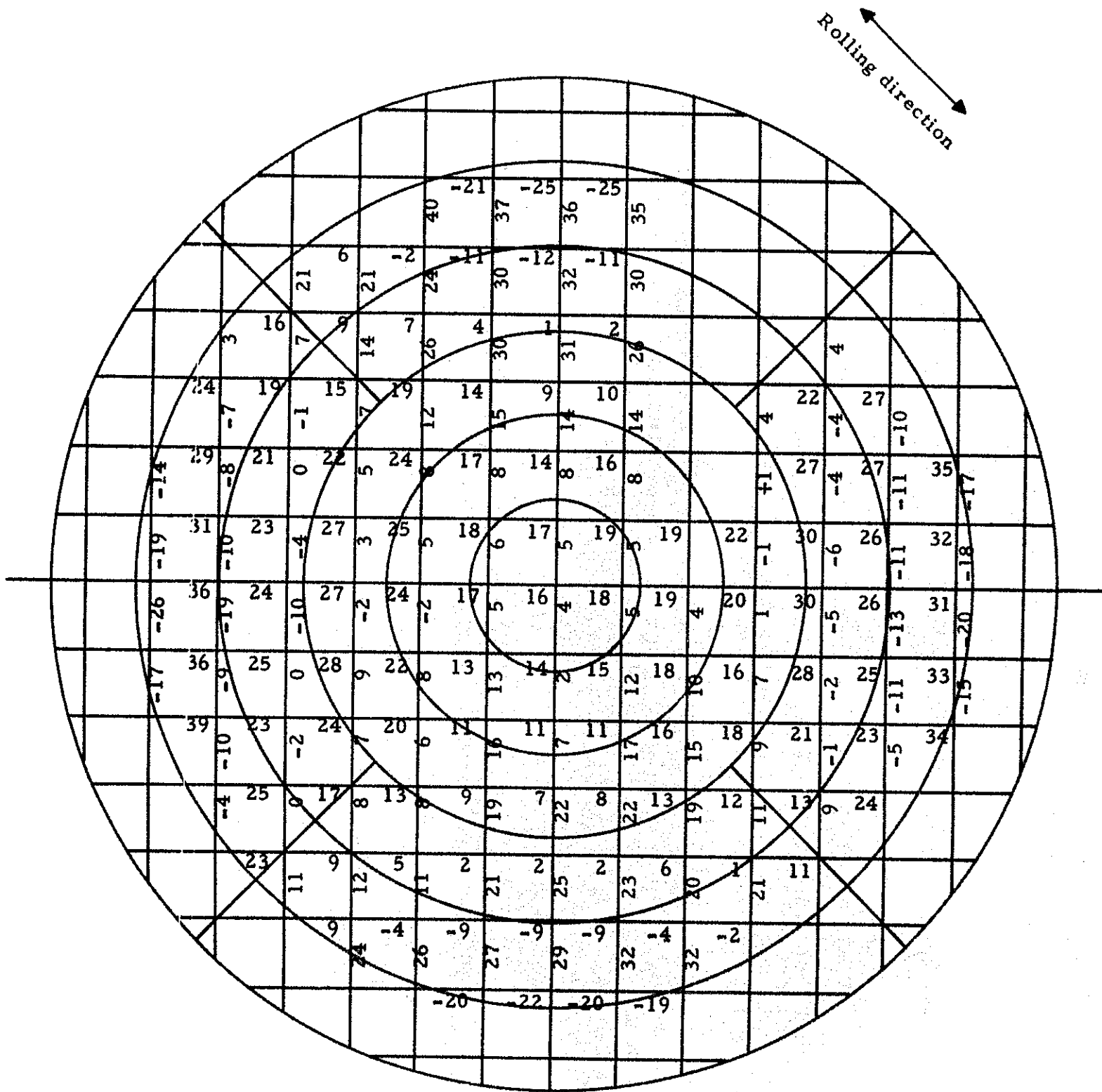
FIGURE 37. DEFORMATIONS OF 1-INCH GRIDS IN HELMET I7421



Helmet front

A-56065


FIGURE 36. DEFORMATIONS OF 1-INCH GRIDS IN HELMET 19926

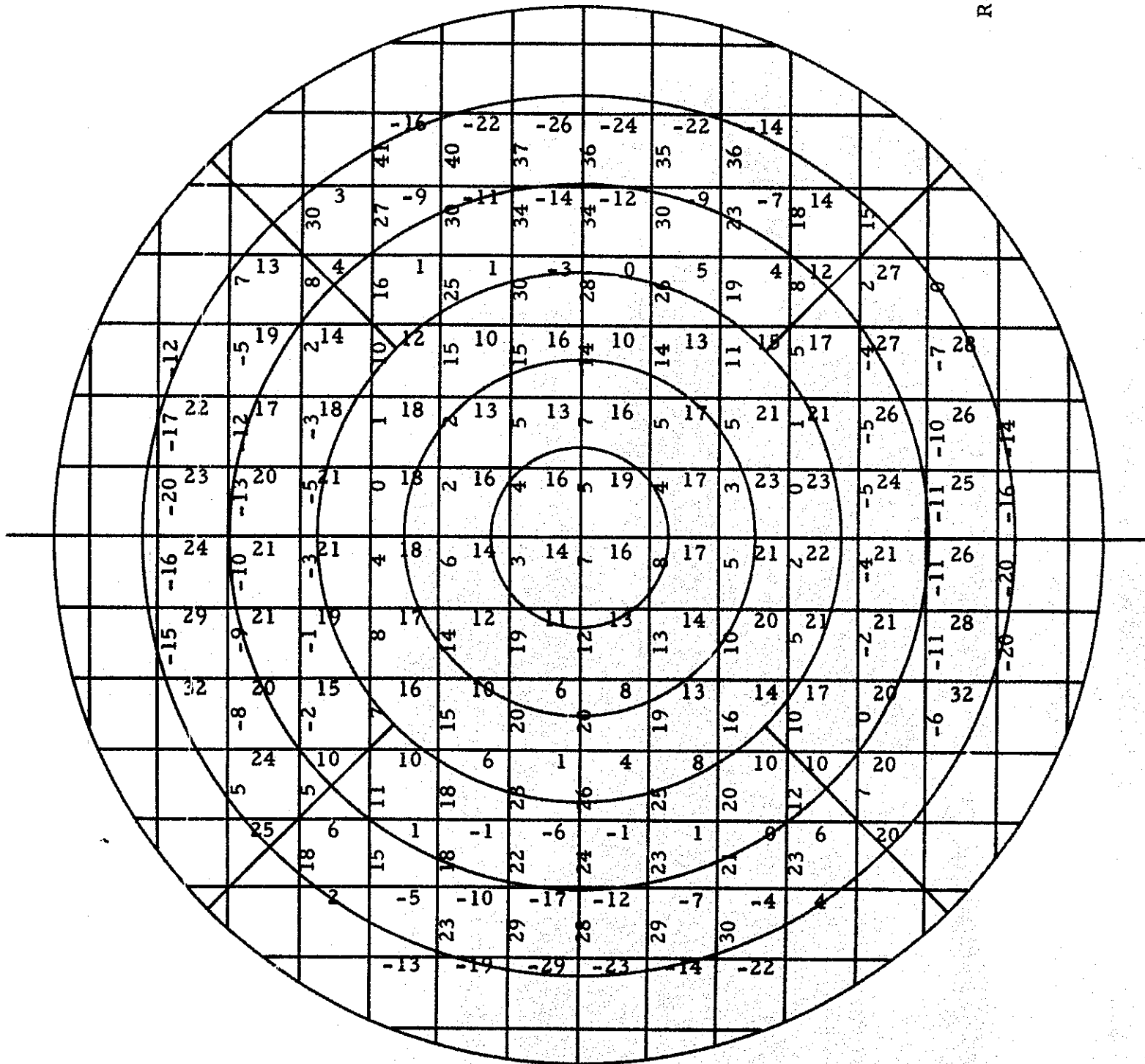


Helmet front

A-56068

FIGURE 39. DEFORMATIONS OF 1-INCH GRIDS ON HELMET M334B

Rolling direction  


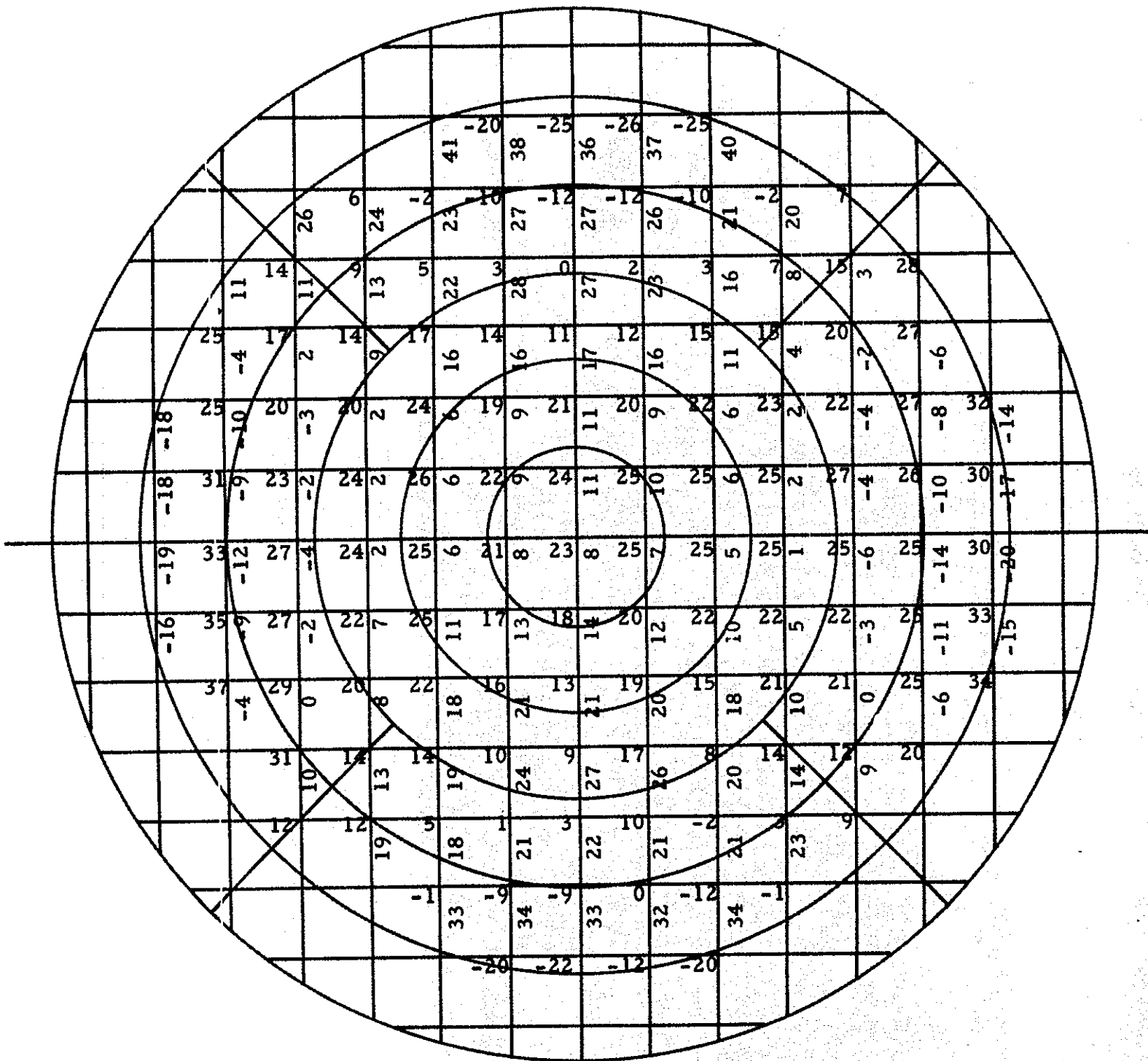


Helmet front

A-56069

FIGURE 40. DEFORMATIONS OF 1-INCH GRIDS IN HELMET M326A

↔  
Rolling direction



Helmet front

A-56070

FIGURE 41. DEFORMATIONS OF 1-INCH GRIDS IN HELMET J2491

to cause subsequent problems in forming; the development of earing in deep-drawing steel is a typical example. To examine the possibility that this effect might be significant in the deformation of a helmet during drawing, the test helmets were formed with the rolling direction parallel, perpendicular, and at 45 degrees to the front-to-back plane of symmetry. The true strain values ( $\epsilon_1$ ,  $\epsilon_2$ , and  $\bar{\epsilon}$ ) then were plotted for the corresponding grid points on the left and right sides of the plane of symmetry.

It was reasoned that if a significant effect of texturing were present, the data points would be symmetric about a 45-degree line on the graph only for the cases in which the rolling direction was parallel or normal to the plane of symmetry for the helmet. For the third case, in which the rolling direction was at 45 degrees, the points should be skewed.

The results of these studies are summarized in Figures 42-49 in which it can be seen that no significant effect of rolling direction on the symmetry of the deformation pattern is observed. This observation of a plane of symmetry can be of considerable importance in further studies, and will be commented on again in a later section.

#### Stress-Strain Behavior

It is well known that when most metals are plastically deformed at room temperature they become harder and stronger. This effect is usually termed work hardening or work strengthening. In many instances, the shape of the stress-strain curve or flow curve obtained in a tension test can be approximated by an expression

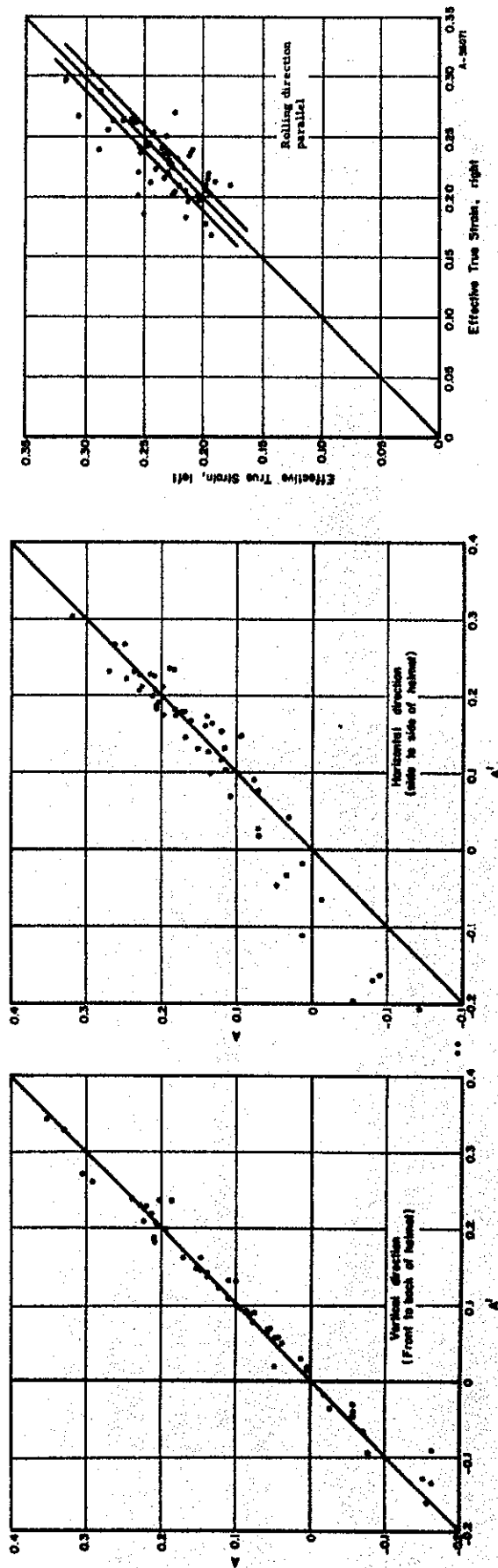


FIGURE 42. HELMET NO. M322B PLOTS OF TRUE STRAINS ON 1-INCH GRIDS, COMPARING LEFT (A) TO RIGHT (A') SYMMETRY



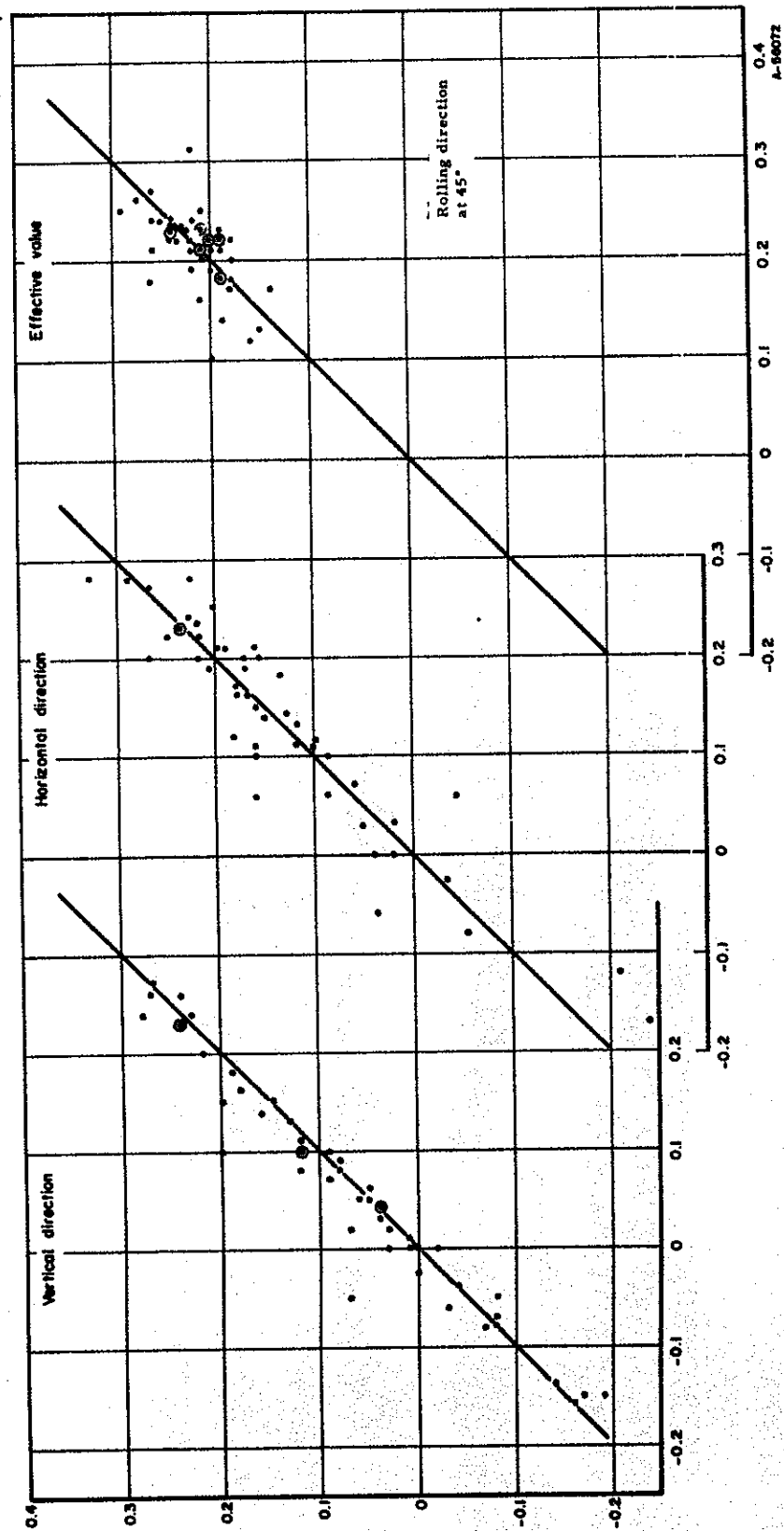


FIGURE 43. PLOTS OF TRUE STRAINS ON 1-INCH GRIDS FOR HELMET I-9926, COMPARING LEFT TO RIGHT SYMMETRY

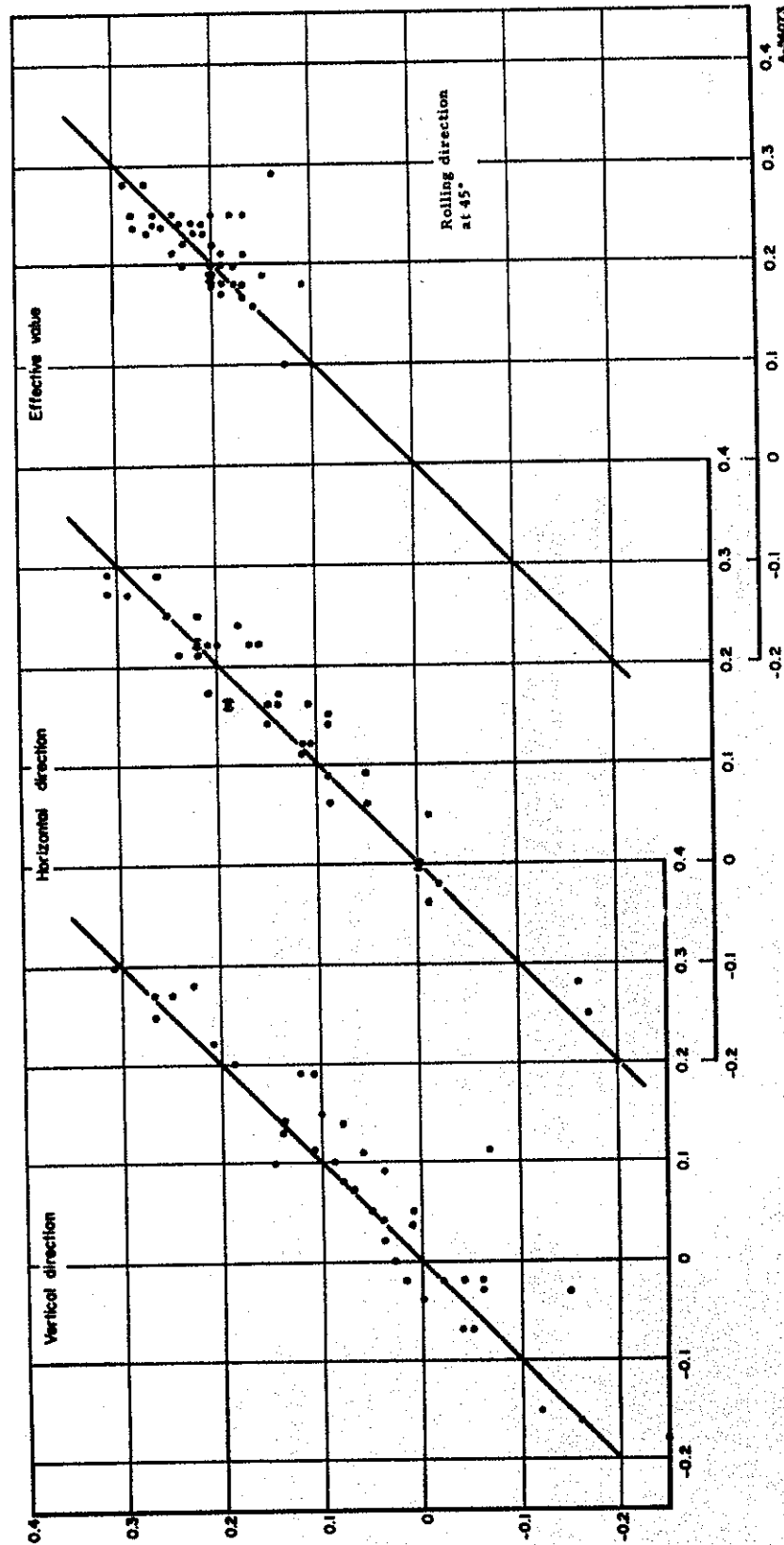


FIGURE 44. PLOTS OF TRUE STRAINS ON 1-INCH GRIDS FOR HELMET M334B,  
COMPARING LEFT TO RIGHT SYMMETRY

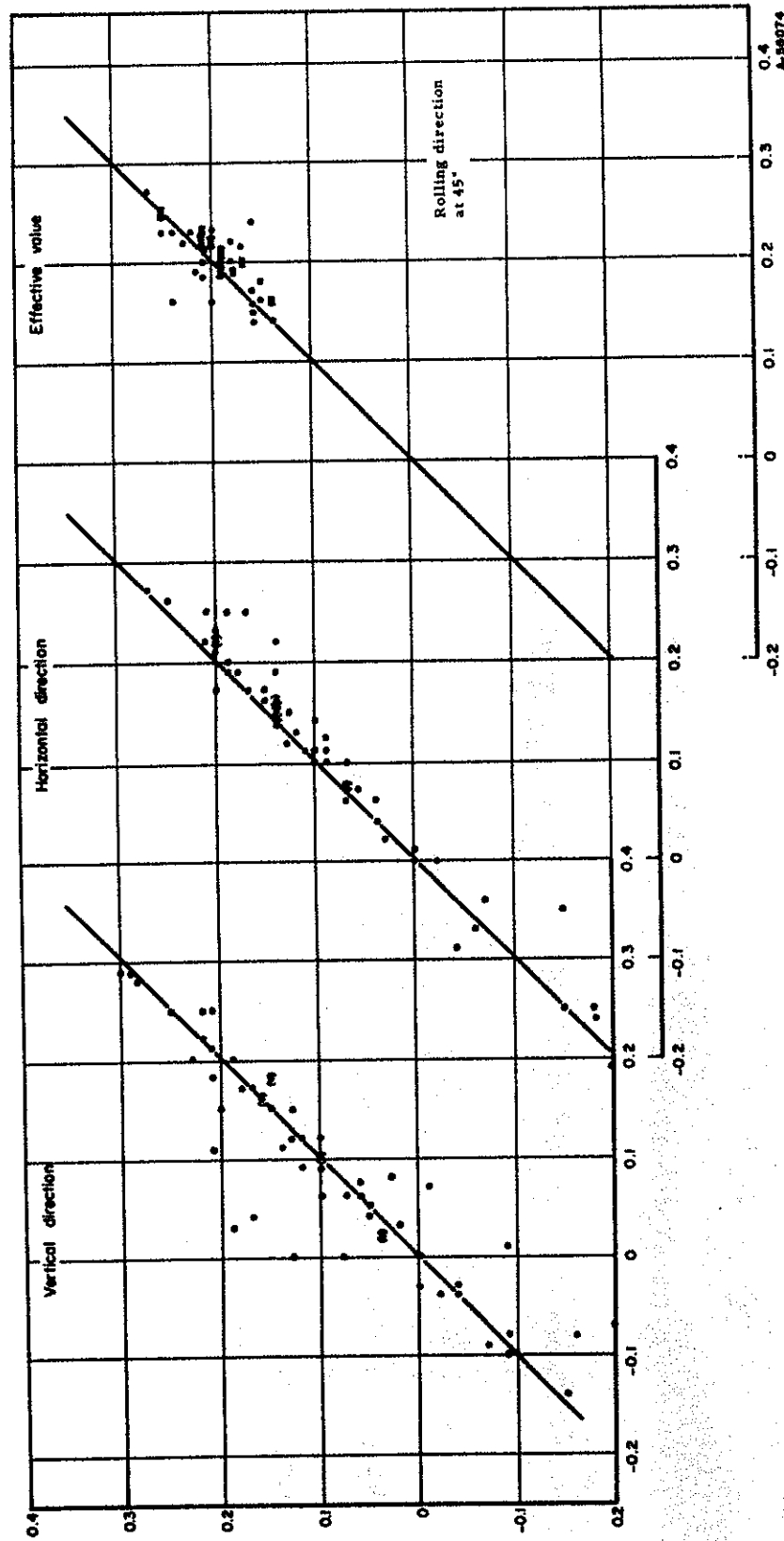


FIGURE 45. PLOTS OF TRUE STRAINS ON 1-INCH GRIDS FOR HELMET 1-7421,  
COMPARING LEFT TO RIGHT SYMMETRY

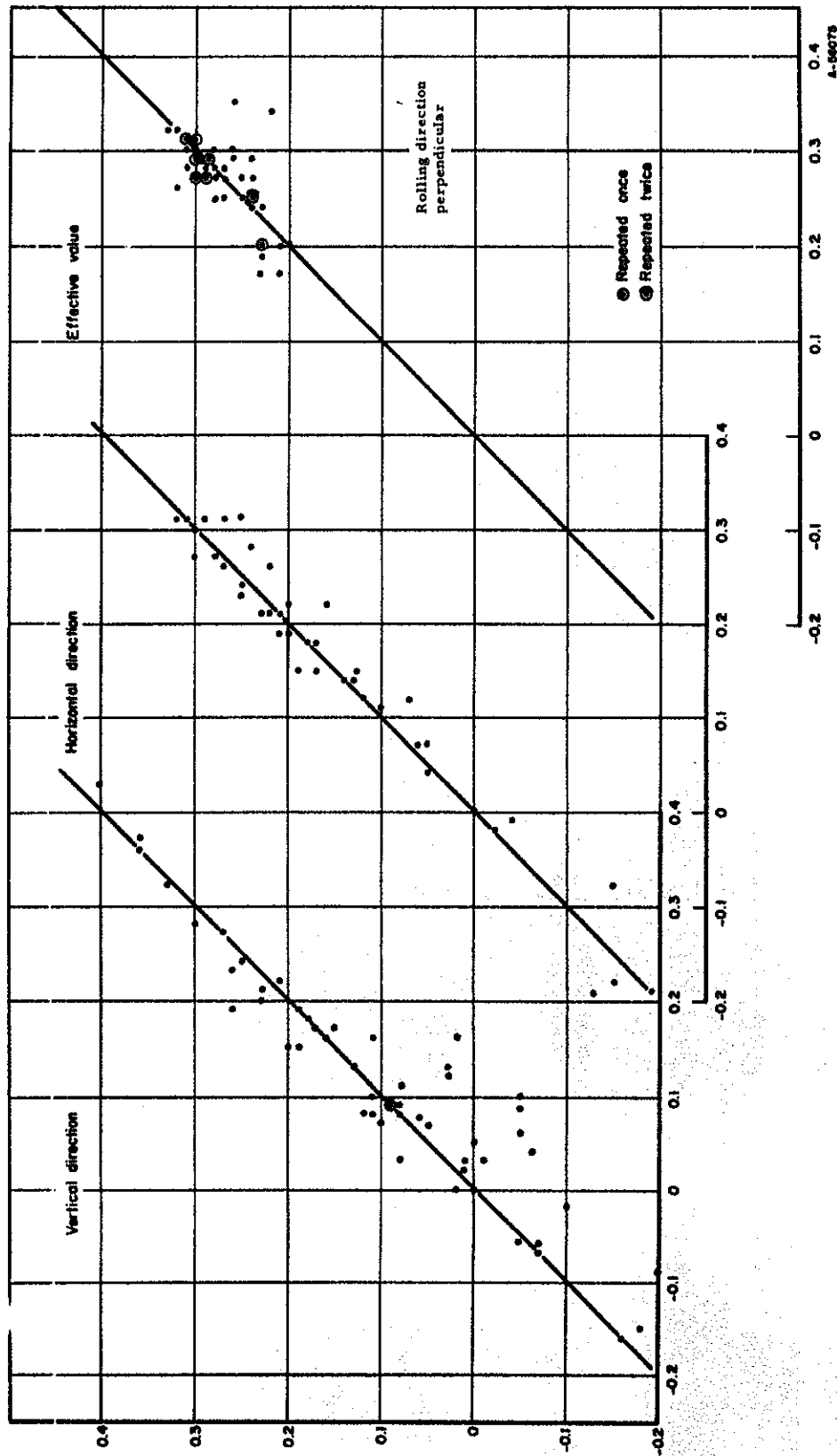


FIGURE 46. PLOTS OF TRUE STRAINS ON 1-INCH GRIDS FOR HELMET I-2505, COMPARING LEFT TO RIGHT SYMMETRY

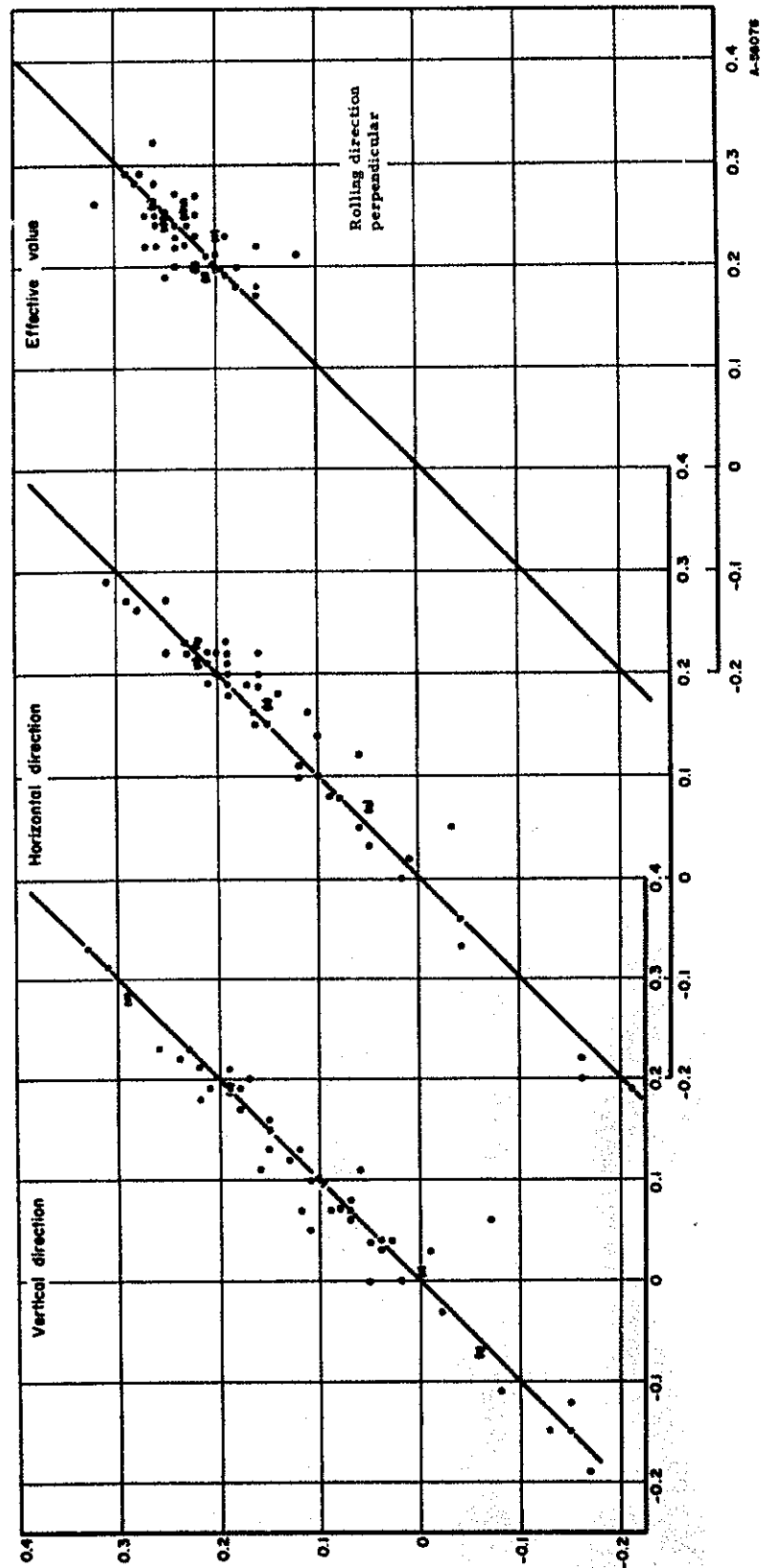


FIGURE 47. PLOTS OF TRUE STRAINS ON 1-INCH GRIDS FOR HELMET I-2491,  
COMPARING LEFT TO RIGHT SYMMETRY

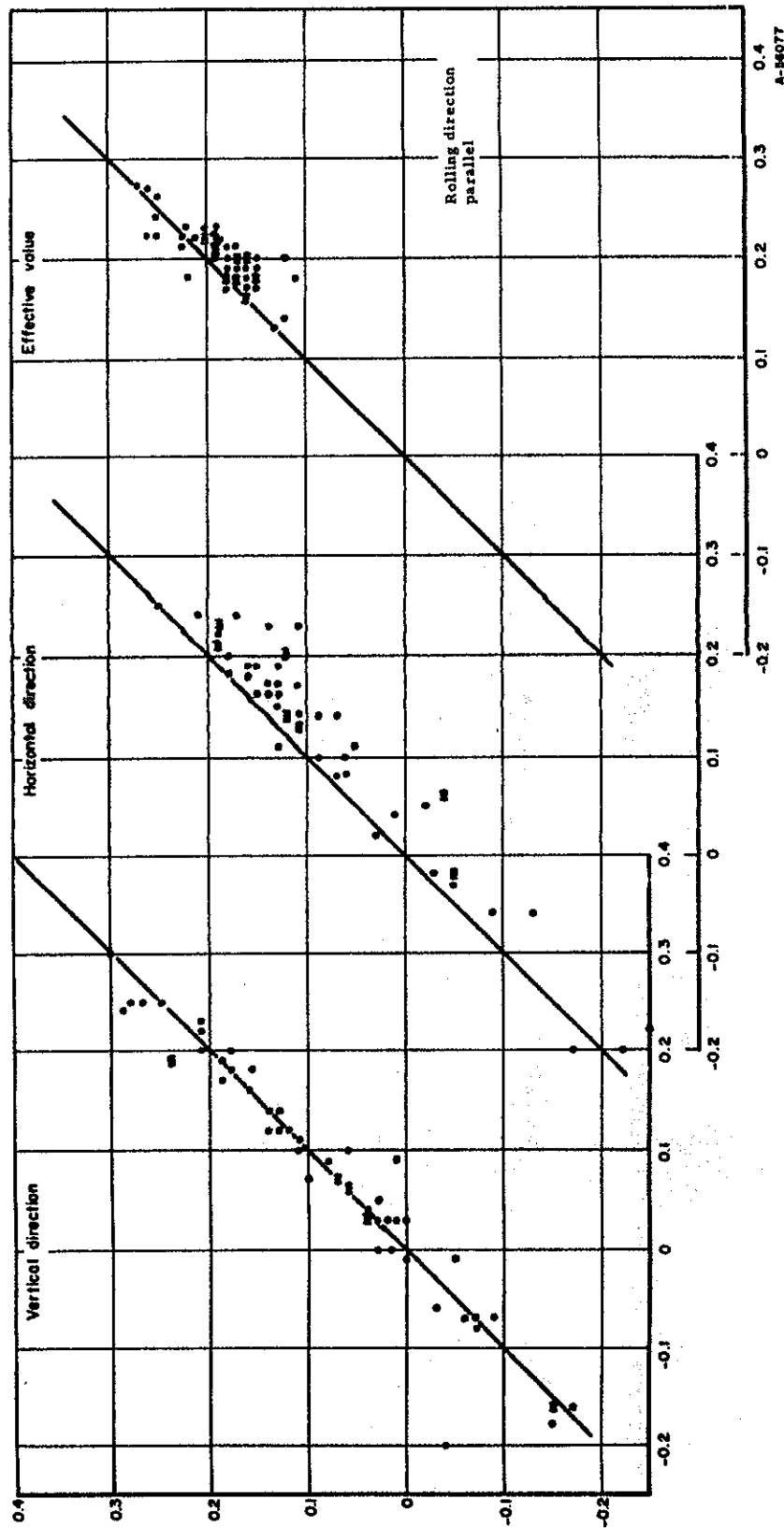


FIGURE 48. PLOTS OF TRUE STRAINS ON 1-INCH GRIDS FOR HELMET I-6674, COMPARING LEFT TO RIGHT SYMMETRY

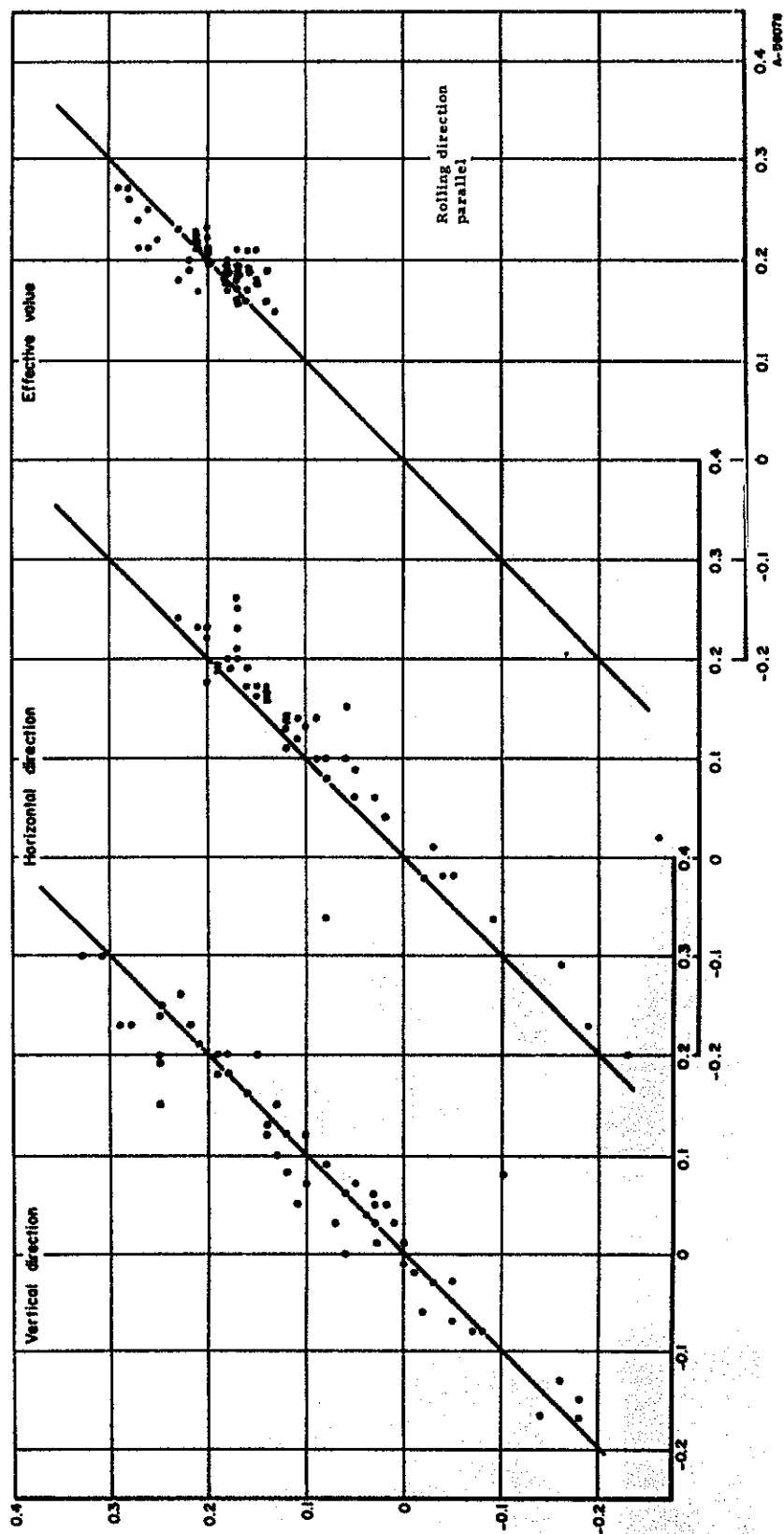


FIGURE 49. PLOTS OF TRUE STRAINS ON 1-INCH GRIDS FOR HELMET M326A,  
COMPARING LEFT TO RIGHT SYMMETRY

in the form:  $\sigma = K\epsilon^n$ , in which  $\sigma$  is the true stress,  $\epsilon$  is the true strain, and  $K$  and  $n$  are material constants known as the flow coefficient and the flow exponent, respectively. The form of this equation is such that a plot of  $\log \sigma$  vs  $\log \epsilon$  results in a straight line of slope  $n$ , and with an intercept at  $\epsilon = 1.0$  of  $\sigma = K$ .

The data for obtaining the flow curve can be provided from simultaneous measurements of tensile load and either area or extension between gage marks on the tensile specimen. The values of  $\sigma$  (the true stress) and  $\epsilon$  (the true strain) are calculated from the expressions:

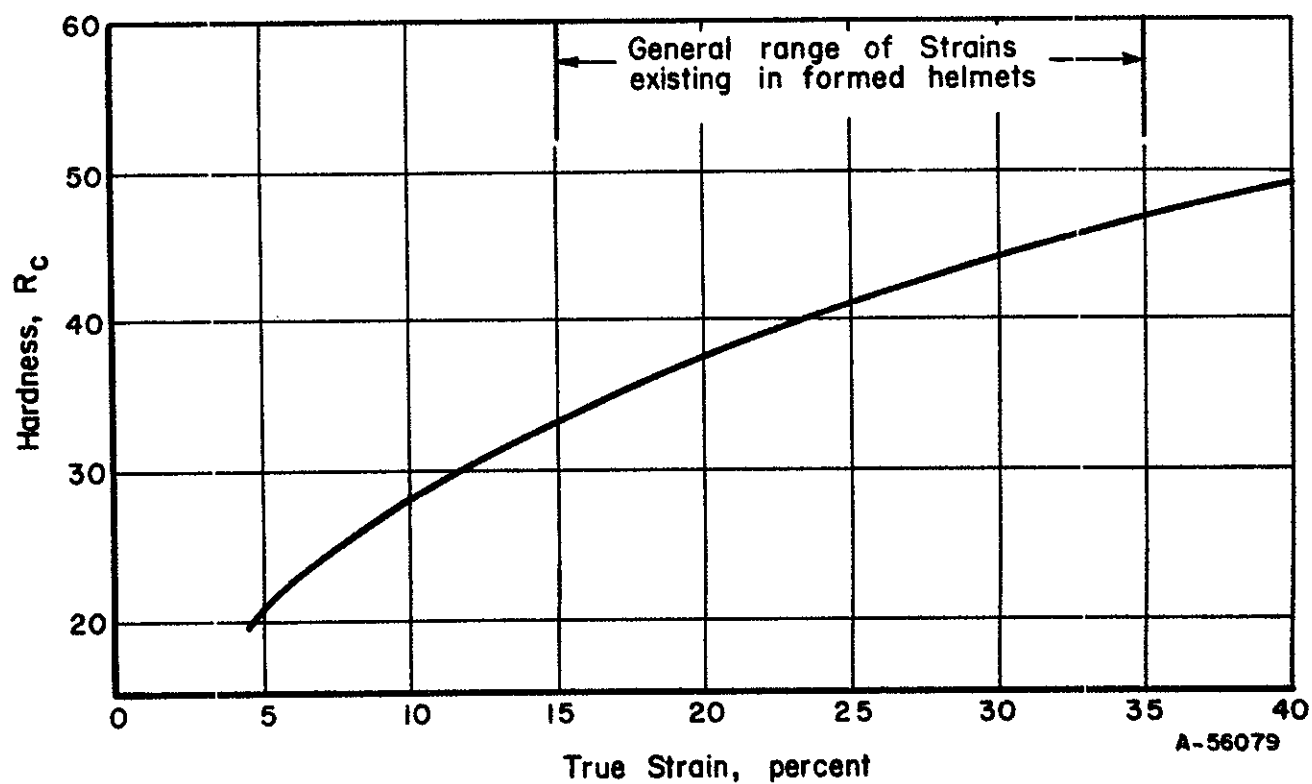
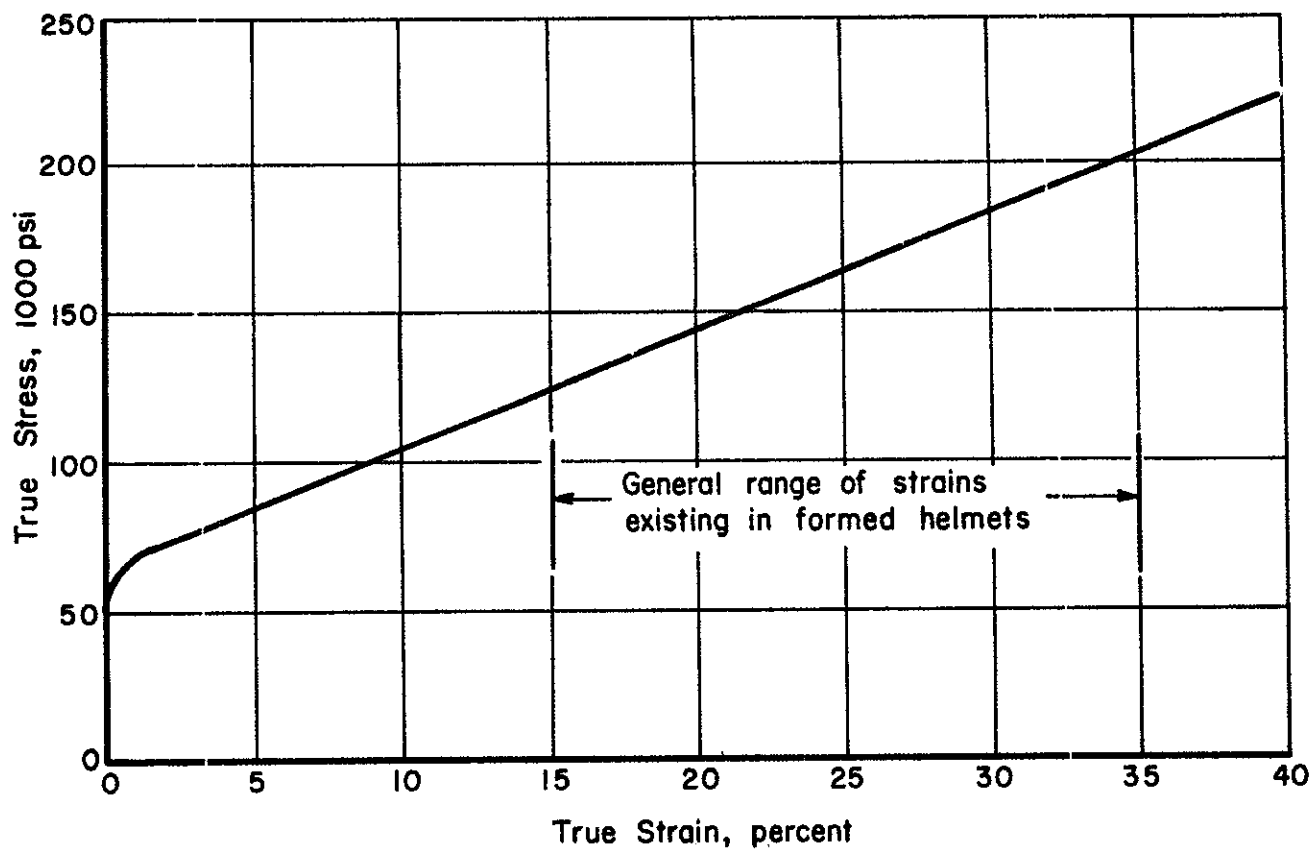
$$\sigma = P/A = \frac{P}{A_0} \left( \frac{A_0}{A} \right) = S \left( \frac{A_0}{A} \right) = S \left( \frac{l}{l_0} \right) = S (1 + e)$$

$$\epsilon = \ln \left( \frac{A_0}{A} \right) = \ln \left( \frac{l}{l_0} \right) = \ln (1 + e)$$

In the equations above,  $S$  and  $e$  represent the ordinary or engineering values of stress and strain, respectively.

A similar method can be used to express the hardness of a material after straining, since there is generally a monotonic relationship between flow stress and hardness. This relationship can be a useful one here, because hardness measurements on the helmet or helmet blank are nondestructive and are relatively easy to conduct. Thus, a tensile test made on a sample of work-hardenable material can be used to provide test data for a flow curve (a plot of true-stress vs true-strain) as well as for a plot of hardness vs true-strain; and further, the two curves should be similar. This is illustrated in Figure 50, in which hardness and load measurements were made on





A-56079

FIGURE 50. EFFECT OF STRAIN ON FLOW STRESS AND HARDNESS OF HELMET STEEL

individual specimens over a range of strains. The same data are presented on logarithmic coordinates in Figure 51.

The situation for a cold-drawn helmet is more complex, and considerably more difficult to analyze. First, the strains are biaxial, or applied in two directions in the plane of the sheet, rather than uniaxial, as in a tension test. Second, the work hardening undergone by the metal is a function of the path of straining as well as the amount. This means that the final hardness of a section may not be predictable from measurements of initial and final dimensions alone. For the portions of the helmet near the center, most of the straining undergone is biaxial tension. For these sections, the effective strain can be expressed by the equation:

$$\bar{\epsilon} = \frac{2}{\sqrt{3}} \sqrt{\epsilon_1^2 + \epsilon_1\epsilon_2 + \epsilon_2^2},$$

in which  $\epsilon_1$  and  $\epsilon_2$  are the true strains in mutually perpendicular directions. In the sections near the rim of the helmet, tensile deformation in the radial direction is accompanied by compressive deformation (upsetting) in the circumferential direction. This results in relatively high values of thickness and low values of computed effective strain, even though the amount of work hardening is high. This effect is illustrated by the plots of Figure 10, in which the hardness vs thickness points are seen to lie in distinct groups depending upon their location in the helmet.

The effect is further illustrated by the data shown in Figure 52, in which hardness and effective strain are plotted in each grid section of a single helmet. The curve superimposed upon the data points is taken from Figure 50. It can be seen that although the data

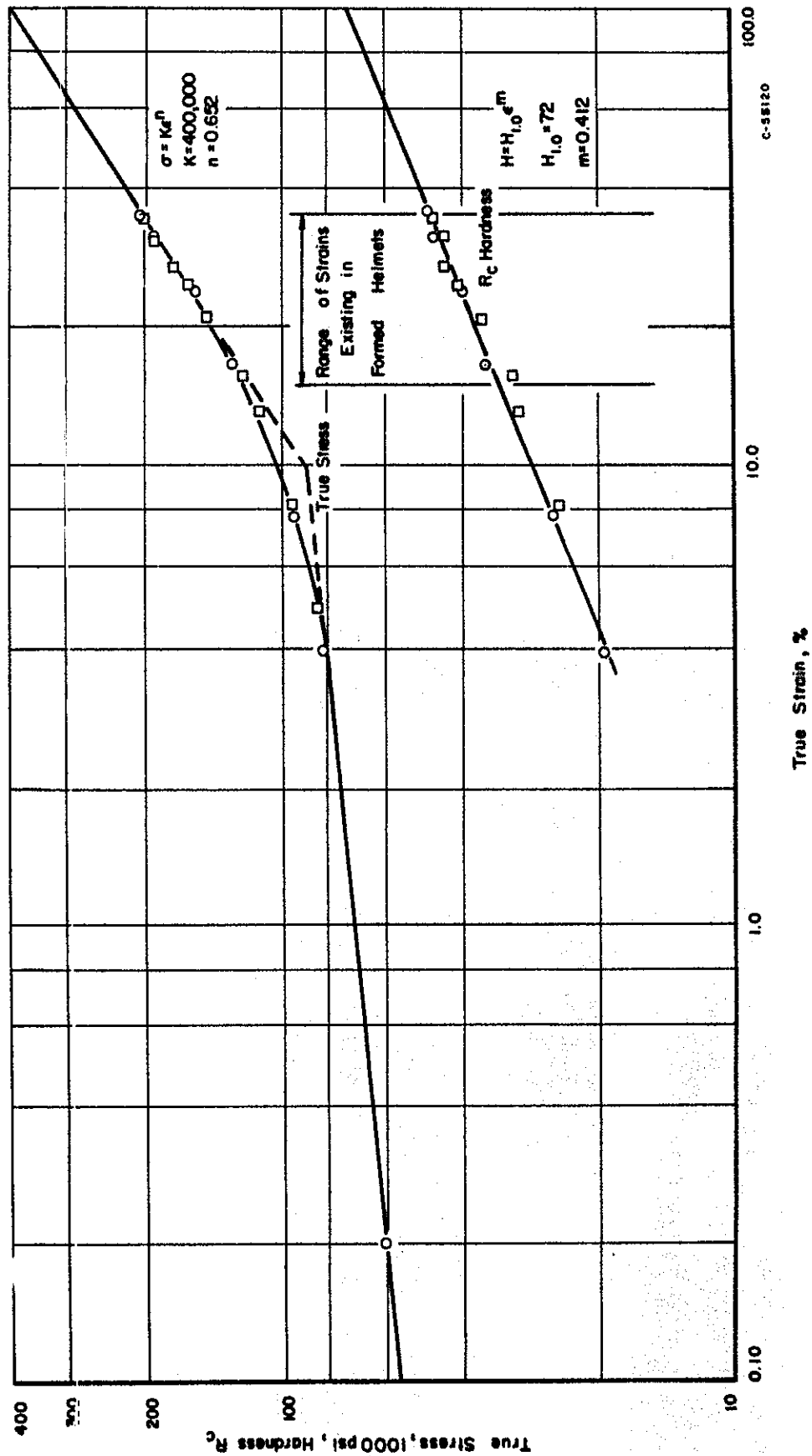


FIGURE 51. EFFECT OF STRAIN ON FLOW STRESS AND HARDNESS OF HELMET STEEL

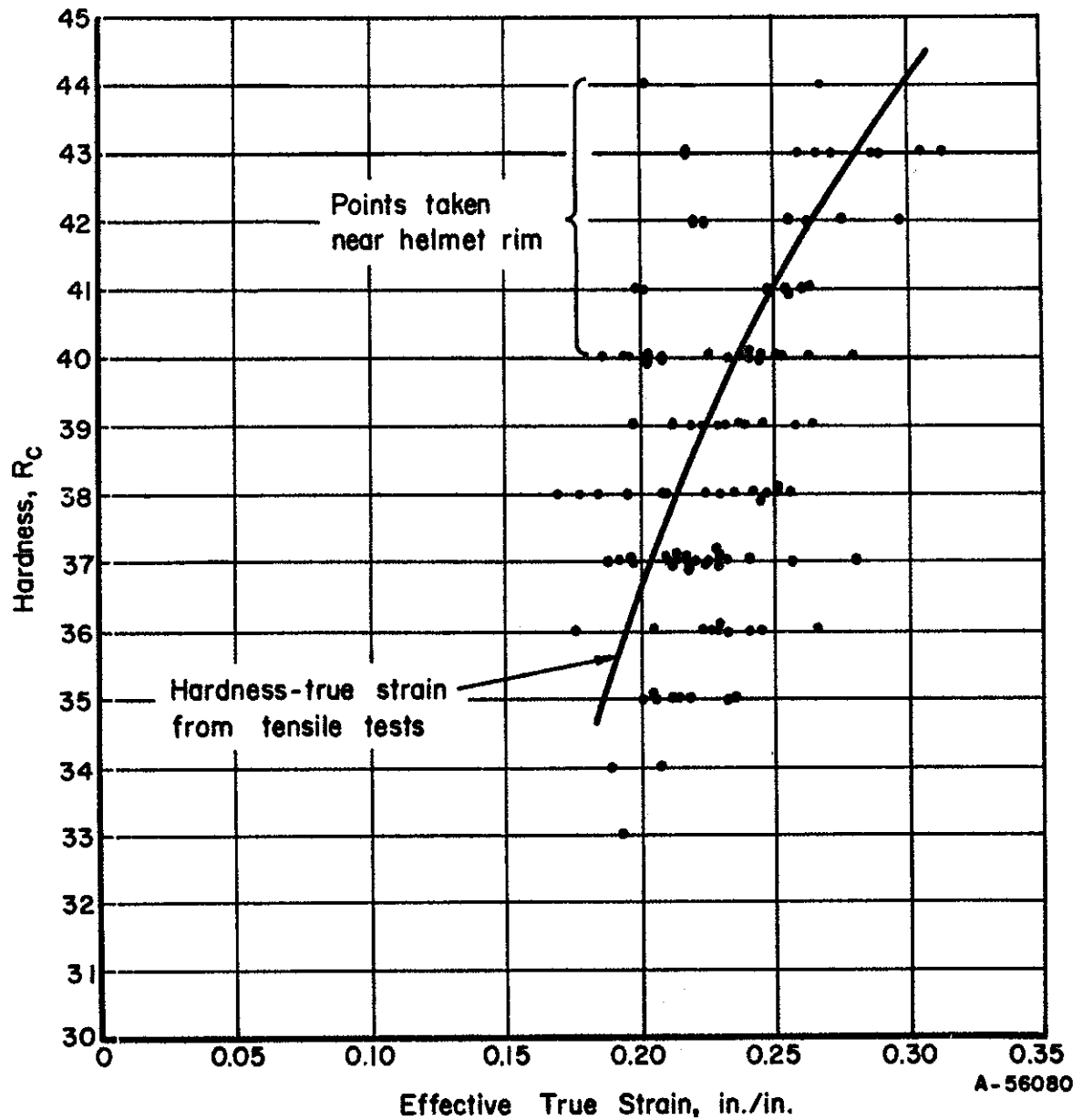


FIGURE 52. HELMET NO. M322B, PLOTS OF  $R_c$  HARDNESS VS EFFECTIVE TRUE STRAINS

points conform reasonably well with the superimposed curve, there are many points well separated from it. Examination of the individual data points reveals that those points displaced above and to the left are all from the rim section of the helmet. The data points taken from near the center of the helmet correspond well with the generalized hardness-deformation curve.

Another method in computing the effective true strain is from thickness measurements, in which the true strain at a point is taken equal to  $\ln t_0/t$ , where  $t_0$  is the initial thickness and  $t$  is the thickness after straining. This method has the advantage of simplicity, since it is not necessary to use grid measurements to calculate the true strain values. It also tends to separate strongly the points of biaxial tension straining from those where upsetting is involved, in much the same way as hardness vs thickness measurements were shown to fall in distinct groups. In Figure 53, the hardness vs true strain points are shown for the central 36 grid squares only, avoiding measurements near the outer rim. These are seen to group well about the hardness-true strain curve developed from tension tests.

## DISCUSSION

### Observations on the Helmet

An important accomplishment of this study has been the insight gained into the helmet itself. Detailed studies have defined the variations in thickness and material properties within the helmet and have related these to the forming process.

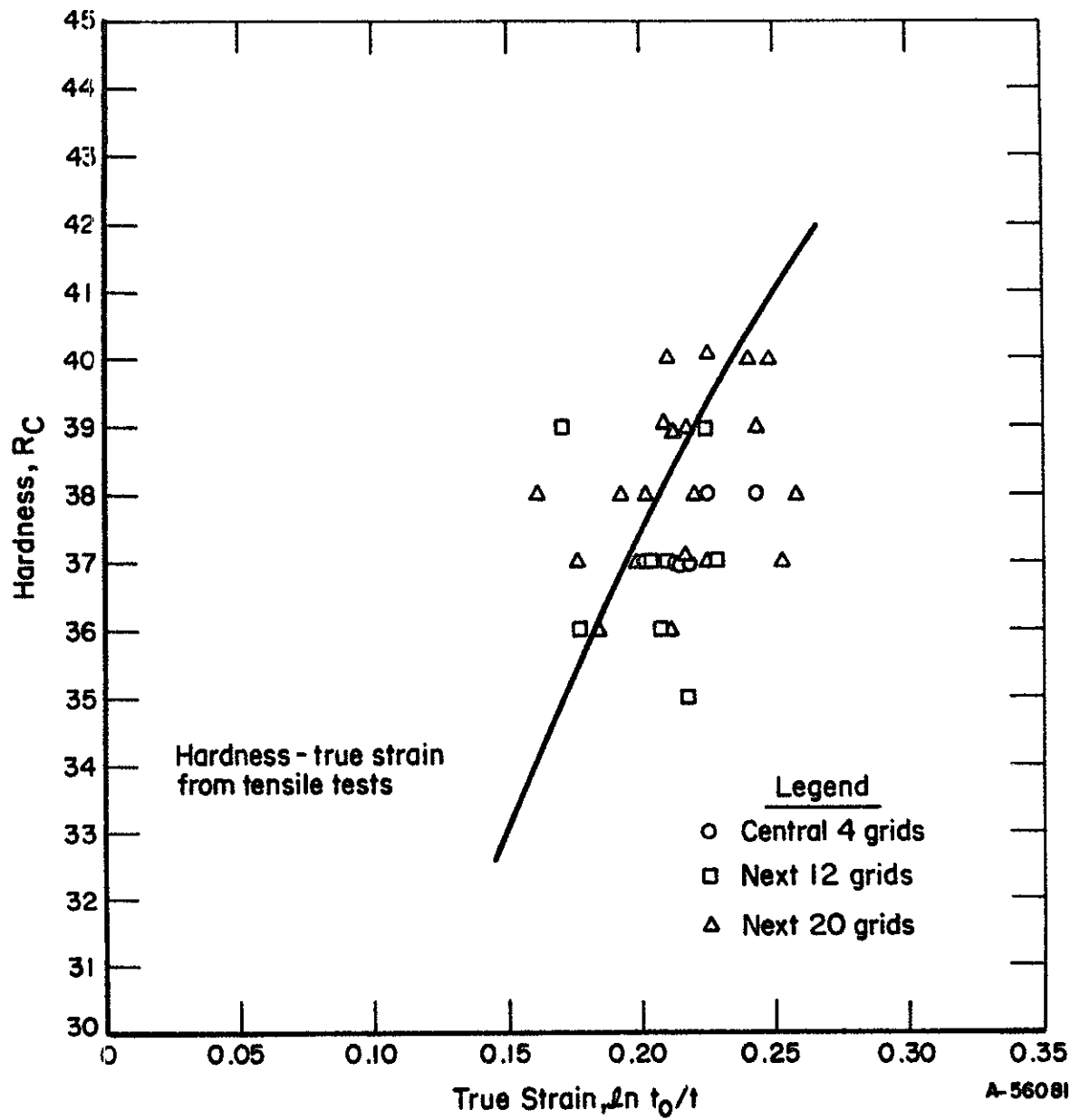


FIGURE 53. PLOT OF  $R_C$  HARDNESS VS  $\ln t_0/t$  FOR HELMET M322B

The studies in which gridded blanks were formed into helmets have shown the deformation patterns in a formed helmet. It was observed that the upper section of the helmet is formed mainly by a stretching process, whereas the lower (rim) section is formed by a stretching-upsetting process. Thus, the upper section of a helmet is appreciably thinner and harder than the blank from which it was drawn while the lower section is nearly as thick but appreciably harder than the blank.

A reasonably strong correlation of hardness with thickness was found in the upper section of the helmet; a decrease in thickness corresponding with an increase in hardness. In the lower section, hardness and thickness correlations were less obvious, but hardness tended to increase with increasing thickness, reflecting the stretching-upsetting deformation pattern in this part of the helmet. Reduction of thickness during forming was in the range of 20 to 25 percent in the upper section, whereas 2 to 5 percent was noted in the lower section.

In addition to the distinct differences between upper and lower sections, variations in hardness and thickness were observed within relatively small areas of the helmets. Significant variations in thickness were noted, especially in the upper section. The thickness of zone 5, for instance, generally varied about 0.004-inch from end-to-end. (A distance of about 2-1/2 inches).

Another important observation was the side-to-side symmetry of the deformation pattern. It was found that the deformation pattern is, within statistical variation, symmetrical about a

central front-to-back line regardless of the orientation of the rolling direction of the blank with respect to this line. One of the implications of this finding is that future studies could be justifiably limited to one side of a helmet.

Such close correspondance in deformation patterns did not exist between the front and back halves of the helmet (see Figure 10). The implications of these observations on the  $V_p$  50 are considered below.

#### Observations on the $V_p$ 50

##### Experimental Problems\*

Early in the program it was found that it would be difficult to maintain full compliance with the velocity control requirements of MIL-STD-622A. Variations in the diameter of the .22 Cal. projectiles presented differences in drag with the rifle barrels from shot to shot. Although the projectiles were within the tolerance of  $\pm 0.002$ , it became necessary to segregate the highs and the lows to improve velocity control.

Another problem area was the .22 L.R. rim-fire case. The small capacity of this case limits the choice of powders which can be used to those of the high intensity, fast burning types. In addition, the rim-fire primer is less uniform in intensity of combustion and ignition time than a center-fire case.

---

\* The comments on experimental problems associated with the  $V_p$  50 are drawn from the report by American Machine and Foundry Company.



Precise velocity control is required to make efficient use of the  $V_p$  50 test. To test the M-1 helmet which has a variable thickness range, the velocity of each shot must be closely predicted to obtain a penetration or non-penetration. This becomes very difficult and as a result of this difficulty, about 45 shots were required for each helmet.

#### Computation Procedure

The  $V_p$  50 is computed on the basis of the five lowest penetration and five highest non-penetration velocities. For materials with a variable thickness, such as the M-1 helmet, the penetration velocities used to compute the  $V_p$  50 will usually come from the thinner sections and the non-penetration velocities from the thicker sections.

A variety of  $V_p$  50's can be obtained from any given helmet depending on the sections of the helmet selected for firing. This was demonstrated in this study by dividing the helmet into upper and lower sections. As was seen in Figure 23,  $V_p$  50's computed for the upper (thinner) section were consistently below those of the lower (thicker) section, while the  $V_p$  50 for the whole helmet fell in between these values. Using only the upper section, eight of the 200 helmets did not meet the specified minimum  $V_p$  50 of 900 fps, whereas the  $V_p$  50 for the whole helmet was above the minimum requirements in all cases.

Combining these observations with the observations of the symmetry of the deformation pattern made earlier, certain conclusions can be drawn.

(1) Shots fired into the helmet from the front and back should provide the same  $V_p$  50 as for the whole helmet.

(2) A  $V_p$  50 based upon shots fired only into the front half will not be the same as a  $V_p$  50 for the back half.

(3) The minimum  $V_p$  50 within a helmet will be obtained from the helmet back, near the crown.

(4) The maximum  $V_p$  50 will be obtained from the helmet back, near the rim.

In the early stages of this study, we were quite skeptical about the value of a  $V_p$  50 as an effective index of ballistic performance of helmets. The skepticism was based, in large part, upon the wide range of  $V_p$  50 values obtainable from apparently similar bodies as well as upon the effect of material variations within the helmet. As the analysis proceeded, however, it became reasonably clear that the average  $V_p$  50's for a number of helmets can be an effective tool if enough independent values are obtained. Thus, considering the data of Figures 18 through 22, the wide scatter among  $V_p$  50's presents a rather discouraging picture. "Averaging" these values (as by a least squares fit), however, reveals systemic differences in the ballistic performance which are explained in terms of material characteristics. This observation is quite significant in terms of the use of the  $V_p$  50 for quality control of helmets. The  $V_p$  50 based upon one, or even a few, helmets is not a reliable index of helmet lot. On the other hand, the average  $V_p$  50 of a large number of helmets can provide a reasonable (if arbitrary) base line for evaluating some other inspection parameter.

Effects of Parameters Studied on  $V_p$  50

The parameters studied were thickness, hardness, chemical composition, microstructure, and tensile stress-strain properties. The objective of studying the first two parameters (thickness and hardness) was to determine the effects of their variations within and among helmets and blanks. The objective of studying the other parameters was to study the effects of heat-to-heat material variations. Two factors must be emphasized in considering the findings. First, the parameters studied may not be the only ones which affect the ballistic performance of helmets. Other, less obvious factors may have caused some of the scatter in  $V_p$  50's.

The second important point is that the conclusions drawn apply only to the range of the parameters encountered in the study. These ranges have been indicated in histograms for each of the parameters. As an example, the heat-to-heat variations in carbon, silicon, and manganese content had no detectable effect on either helmet or blank  $V_p$  50. Greater variations in these elements undoubtedly would affect ballistic performance. However, as long as the helmet material is made to current compositional specifications, small deviations in composition (at least of the three elements studied) will not affect ballistic performance.

This point was brought out strongly in the case of hardness. For the range of hardnesses found among blanks, no correlation between hardness and  $V_p$  50 of the blanks was observed. Similarly, the range of hardnesses found both within single helmets and among the

200 helmets was sufficiently small (about 10  $R_c$  hardness numbers) that no correlation with  $V_p$  50 was detectable. On the other hand, the difference between average hardness of blanks and helmets was sufficiently great (about 30 to 40  $R_c$  numbers) to account for the considerably higher  $V_p$  50's of the blanks. One of the implications of this observation is that, while hardness variations among (or within) helmets are not sufficient to warrant the use of this parameter as an index of  $V_p$  50, a significant improvement in helmet performance might result from "softening" (e.g., by annealing) helmets.\*

Of the parameters studied, only thickness was found to have both a sufficiently wide range and a sufficiently great effect on  $V_p$  50 to be of value as an index of ballistic performance. The sensitivity of  $V_p$  50 to thickness is about 20 fps per .001 inch. Thus, for helmets produced to current specifications, strong evidence has been developed to indicate that thickness could serve as an acceptance criterion for quality control.

It was also established that quality control of helmets must be based on measurements made on the helmets themselves. The relationship between  $V_p$  50 of helmets and blanks is not sufficiently strong to allow prediction of the helmet  $V_p$  50 from that of the blank.

---

\* A proposal recommending further study of this effort is being prepared.

### RECOMMENDATIONS FOR PHASE III

The study indicates that  $V_p$  50 is sufficiently sensitive to thickness to justify the use of thickness as a quality control parameter for M-1 helmets. The use of thickness will have many advantages over the current  $V_p$  50 test. The inspection procedure can be non-destructive, inexpensive and relatively rapid. Equally important, it is conceivable that the use of thickness will permit 100 percent inspection. This can assure that no sub-standard helmet will be accepted and that no good helmets will be rejected.\*

Two basic questions remain to be answered before thickness can be instituted for quality control: Where should thickness be measured and how should it be measured? These questions are not entirely independent. Thus, the best measurement technique may be such as to be most appropriate for a certain spot (or area) of the helmet. None the less, some of the basic issues involved in these two questions are treated independently below.

First, where should the measurements be made? The fact that thickness proved to correlate well with several selected areas (including the overall average thickness of the helmet) is fortunate. It indicates that there is reasonable latitude in selecting a "reference" area. This will be important if the measurement technique selected is such

---

\*The  $\epsilon$  would, of course, be an optimum condition. In fact, some compromises would be required in setting the actual specifications. If set "tight", no poor helmets would be accepted but some good helmets might be rejected. If the specifications are "loose", some sub-standard helmets might be accepted. This situation, of course, applies to any inspection.

as to require the use of a particular area. On the other hand, it is possible that some locations may reflect the helmet  $V_p$  50 with greater sensitivity than others. If so, these would be most desirable. Also, it may be found desirable to specify the minimum thickness allowable in a helmet. This would be analogous to specifying a minimum  $V_p$  50 for any area within a helmet, rather than a minimum  $V_p$  50 for the helmet as a whole, as is presently done. That the possibility for doing this is good is indicated by the relatively little scatter and the high sensitivity of the  $V_p$  50 versus thickness graph for individual zones (Figure 21).

Several possible answers also exist to the question of how to measure thickness. Among the desirable features of a thickness measurement system are high speed, minimum interruption to production, and simplicity (skilled workers should not be required). A micrometer or dial gage technique similar to the one used in this study could be employed, especially if only a small number of measurements need be taken on each helmet. A more sophisticated technique might include eddy currents, radiation, or ultrasonics. These would have the advantage of allowing automation and, perhaps, provide over all average thickness if such proved desirable.

Data obtained in the present study will be used as a criterion of the effectiveness of the various thickness measuring procedures studied.

A proposal recommending study of these factors as part of the Phase III effort will be submitted after further discussing with Natick personnel. Following the establishment of a measurement

procedure (where and how to measure thickness), the study will center on reducing this procedure to practice. It is anticipated that this will be done in cooperation with helmet manufacturers to assure that the measurements will result in a minimum interruption to the production line.

rev 2 Aug 67  
WAF 8/8/67

APPENDIX





TABLE A-1. (Continued)

Blanks										Helmets					
(1)	(2)	(3)	(4)	(5)	(6)	(7)	(8)	(9)	(10)	(11)	(12)	(13)	(14)		
Blank and Helmet Number	Average Thickness, inches	Tensile Specimen Orientation	As Received, R <sub>c</sub>	Hardness After Tensile Test, R <sub>c</sub>	0.2% Offset Yield Stress, 10 <sup>3</sup> psi	Maximum Stress, 10 <sup>3</sup> psi	Elongation in 2 inches, percent	Chemical Analysis, percent			Average Hardness, R <sub>c</sub>	Average Thickness, inches	V, 50, ft/sec	Average Reduction in Thickness, percent	
								Si	Mn	C					
I 4452	0.0415	L T	91.4	47.0 44.5	63.5 62.2	148 147	46 44	0.51	12.1	1.14	1252	40.3	0.0385	1030	7.2
M 322C	0.0459	L T	88.6	46.3 45.5	59.2 61.8	146 150	45 43	0.32	12.0	1.29	1256	43.6	0.0376	1031	18.1
M 341B	0.0452	L T	91.1	50.2 48.8	65.0 63.4	163 160	62 53	0.45	12.9	1.25	1256	43.3	0.0373	1044	17.5
I 9923	0.0447	L T	91.8	48.6 46.0	63.7 65.2	154 151	53 47	0.38	12.0	1.24	1257	41.2	0.0386	965	13.6
I 6663	0.0478	L T	90.3	49.5 48.0	59.7 61.5	151 151	54 52	0.48	12.0	1.17	1259	42.1	0.0416	1034	13.0
I 6926	0.0443	L T	91.1	47.7 47.0	56.8 61.2	144 146	56 49	0.42	12.6	1.14	1260	40.1	0.0406	1095	8.4
I 2502	0.0424	L T	88.8	50.2 49.8	62.2 54.7	156 160	70 70	0.24	13.8	1.20	1262	36.9	0.0372	1010	12.3
I 7422	0.0451	L T	90.7	49.5 47.2	57 50	155 154	70.0 59.5	0.44	12.6	1.21	1264	43.4	0.0389	1036	13.7
I 6244	0.0476	L T	90.7	48.6 43.7	54 45	154 159	61.3 64.0	0.40	12.5	1.21	1265	43.7	0.0414	1136	13.0
I 6665	0.0471	L T	90.0	48.0 49.1	50 48	152 153	64.0 63.6	0.47	12.35	1.24	1268	46.8	0.0406	1043	13.8
I 6673	0.0433	L T	89.5	45.8 43.5	48.5 41	150 147	62.3 63.8	0.41	13.3	1.26	1268	42.9	0.0372	1003	14.1
I 7423	0.0464	L T	89.5	49.0 52.8	57 57	158.5 158	65.5 59.6	0.47	12.9	1.27	1270	Not available			

TABLE A-1. (Continued)

Blanks															Helmets		
(1)	(2)	(3)	(4)	(5)	(6)	(7)	(8)	(9)			(10)	(11)	(12)	(13)	(14)		
Blank and Helmets Number	Average Thickness, inches	Tensile Specimen Orientation	As Received, R <sub>p</sub>	Hardness After Tensile Test, R <sub>c</sub>	0.2% Offset Yield Stress, 10 <sup>3</sup> psi	Maximum Stress, 10 <sup>3</sup> psi	Elongation in 2 inches, percent	Chemical Analysis, percent			V 50 ft/sec	Average Hardness, R <sub>c</sub>	Average Thickness, inches	V 50, ft/sec	Average Reduction in Thickness, percent		
								Si	Mn	C							
I 7575	0.0465	L T	90.9	49.0 46.0	59 51	153 150	62.2 59.7	0.52	12.9	1.12	1272	45.3	0.0383	986	17.7		
M 339A	0.0466	L T	91.6	49.2 50.0	57 53	158 158	62.5 63.0	0.33	12.5	1.26	1279	44.1	0.0381	1040	18.2		
I 4463	0.0438	L T	90.1	49.7 50.3	62 57	156 162	63.2 62.8	0.38	11.6	1.29	1280	41.0	0.0396	1093	9.6		
I 6323	0.0475	L T	91.3	49.3 48.5	54 54	148 154.2	65.5 62.5	0.42	12.9	1.14	1280	44.9	0.0388	925	18.3		
I 9131	0.0449	L T	91.8	46.5 47.3	45 46	145 147	64.0 63.0	0.42	12.6	1.31	1280	41.7	0.0378	1013	15.8		
M 324C	0.0440	L T	87.9	44.7 45.3	59 49	151 148.5	58.0 57.4	0.43	13.1	1.17	1281	42.0	0.0386	1061	12.3		
I 9922	0.0443	L T	89.1	46.3 46.7	46 46	149 150	64.4 60.5	0.38	12.1	1.20	1284	42.8	0.0393	1051	11.3		
I 8241	0.0467	L T	91.6	50.0 50.3	53 47	155 157.5	63.7 62.1	0.42	12.55	1.26	1285	44.8	0.0422	1095	9.7		
I 6233	0.0464	L T	92.2	46.5 50.1	62 57	157 158	61.7 62.6	0.48	12.95	1.20	1288	43.6	0.0405	1043	12.7		
I 6652	0.0477	L T	90.3	49.0 45.5	63 50	159 153	64.3 62.6	0.40	13.0	1.04	1288	45.2	0.0410	1089	14.1		
I 6246	0.0475	L T	91.0	47.0 47.8	48 47	149 151	61 64	0.40	12.45	1.20	1289	41.0	0.0413	1009	13.1		
I 9082	0.0463	L T	90.4	47.8 47.7	59 53	157.5 155	65.4 62.6	0.42	12.95	1.23	1289	40.9	0.0426	1131	8.0		

TABLE A-1. (Continued)

Helmets															
(1) Blank and Helmet Number	(2) Average Thickness, inches	(3) Tensile Specimen Orientation	Blanks					Helmets							
			(4) As Received, R <sub>g</sub>	(5) Hardness After Tensile Test, R <sub>g</sub>	(6) 0.2% Offset Yield Stress, 10 <sup>3</sup> psi	(7) Maximum Stress, 10 <sup>3</sup> psi	(8) Elongation in 2 inches, percent	(9) Chemical Analysis, percent			(10) V <sub>50</sub> ft/sec	(11) Average Hardness, R <sub>C</sub>	(12) Average Thickness, inches	(13) V <sub>50</sub> , ft/sec	(14) Average Reduction in Thickness, percent
								Si	Mn	C					
M 323A	0.0426	L T	88.6	43.2 45.8	46 44	143 145	56.7 64.0	0.35	11.82	1.19	1292	43.2	0.0369	1007	13.4
I 5643	0.0462	L T	91.2	47.5 50.5	64 51	166 160.5	66.6 65.2	0.39	12.95	1.27	1292	43.5	0.0372	985	
M 325B	0.0449	L T	89.3	46.6 42.8	47 38	149 142	66.7 61.0	0.42	11.95	1.25	1294	48.1	0.0346	955	23.0
I 6924	0.0440	L T	90.1	47.3 47.5	63 53	159 157	61.0 60.5	0.44	12.8	1.27	1296	40.5	0.0381	1026	13.3
I 9084	0.0494	L T	90.7	49.2 47.7	58 51	148 149	58.4 63.2	0.39	12.9	1.10	1296	43.2	0.0400	1077	19.0
I 7735	0.0442	L T	88.4	47.0 46.5	53 50	151 150	66 57.4	0.53	12.3	1.17	1298		Not available		
I 2706	0.0461	L T	89.8	45.5 45.5	46 43	140 145	58.6	0.39	12.7	1.15	1299	45.0	0.0378	1003	18.0
I 2932	0.0452	L T	87.7	49.2 47.3	50 48	155 157	62.2 64.0	0.40	12.1	1.29	1300	40.2	0.0375	976	17.0
I 6935	0.0444	L T	88.4	49.0 48.5	55 53	159.5 157	64.0 61.9	0.46	12.8	1.21	1300	40.7	0.0389	938	12.4
M 337D	0.0441	L T	89.3	47.7 39.3	53 51	144 142	61.8 61.2	0.40	12.95	1.08	1302	45.3	0.0380	1002	11.6
M 335D	0.0464	L T	90.2	46.3 46.7	47 47	146 150	59.0 59.4	0.41	12.32	1.18	1306	44.1	0.0379	930	18.3
I 2914	0.0446	L T	84.3	46.7 47.7	51 43.5	142 150	53.3 63.5	0.30	11.9	1.30	1306	44.1	0.0379	930	15.0



TABLE A-1. (Continued)

Blanks														Helmets			
(1)	(2)	(3)	(4)	(5)	(6)	(7)	(8)	(9)			(10)	(11)	(12)	(13)	(14)		
Blank and Helmets Number	Average Thickness, inches	Tensile Specimen Orientation	As Received, $R_p$	Hardness After Tensile Test, $R_g$	0.2% Offset Yield Stress, 10 <sup>3</sup> psi	Maximum Stress, 10 <sup>3</sup> psi	Elongation in 2 inches, percent	Chemical Analysis, percent			$V_{50}$ ft/sec	Average Hardness, $R_c$	Average Thickness, inches	$V_{50}$ ft/sec	Average Reduction in Thickness, percent		
								Si	Mn	C							
I 5663	0.0476	L T	90.2	47.3 47.8	55 57	152 152	62.5 59.2	0.45	12.7	1.25	1321	39.3	0.0420	1085	11.8		
I 2694	0.0451	L T	90.0	49.8 46.0	58 45	156 154.5	61.0 67.5	0.43	12.45	1.22	1323	43.6	0.0390	1042	13.5		
I 1825	0.0445	L T	89.2	45.8 44.3	43 43	149 152	62.2 62.3	0.33	12.25	1.24	1325	46.0	0.0363	945	20.2		
I 6315	0.0465	L T	89.6	42.5 46.0	42 50	138 149	60.5 61.3	0.49	12.55	1.26	1326	46.3	0.0372	970	20.0		
M 3358	0.0437	L T	89.2	45.3 45.7	48 42	155 148	59.6 61.8	0.38	12.45	1.20	1328	43.3	0.0381	998	12.8		
I 7733	0.0453	L T	89.5	45.6 47.1	48 48	143 150	58.5 58.8	0.47	12.66	1.18	1328	43.0	0.0389	1120	14.1		
I 6636	0.0453	L T	92.8	47.3 48.8	60 54	157.5 158	62.6 62.6	0.39	12.5	1.24	1331	42.3	0.0386	1007	14.8		
I 6921	0.0433	L T	91.1	49.8 52.2	64 58.5	159 159	59.5 60.0	0.51	12.3	1.16	1334	38.7	0.0389	1036	10.2		
I 9913	0.0455	L T	90.8	49.0 48.5	59 56	160 156	67.9 63.5	0.44	12.6	1.14	1334	42.9	0.0409	1077	10.1		
I 6321	0.0473	L T	89.9	50.5 48.7	57 52	157 156	67.3 64.8	0.48	12.8	1.25	1335	44.2	0.0410	1075	15.4		
I 6631	0.0446	L T	89.0	47.3 47.2	52 46	152 148	64 61.4	0.41	12.62	1.28	1335	43.0	0.0397	1084	11.0		
I 7734	0.0459	L T	90.8	42.3 47.2	46 49	144 149	64 61.5	0.46	12.1	1.16	1336	38.4	0.0400	1064	12.8		



TABLE A-1. (Continued)

Blanks															Helmets		
(1)	(2)	(3)	(4)	(5)	(6)	(7)	(8)	(9)	(10)	(11)	(12)	(13)	(14)				
Blank and Helmets Number	Average Thickness, inches	Tensile Specimen Orientation	Hardness		0.2% Offset Yield Stress, 10 <sup>3</sup> psi	Maximum Stress, 10 <sup>3</sup> psi	Elongation in 2 Inches, percent	Chemical Analysis, percent			V 50 ft/sec	Average Hardness, R <sub>c</sub>	Average Thickness, inches	V 50, ft/sec	Average Reduction in Thickness, percent		
			As Received, R <sub>p</sub>	After Test, R <sub>p</sub>				Si	Mn	C							
I 1855	0.0441	L T	89.4	47.8 46.0	49 41	148.5 146.5	57.8 62.0	0.22	12.6	1.21	1349	41.0	0.0384	1054	12.9		
I 4461	0.0449	L T	90.8	50.3 50.8	64 63	164 170	65.0 69.0	0.38	13.57	1.28	1349	44.6	0.0395	1083	12.0		
M 340A	0.0446	L T	90.8	50.3 49.5	62 56	160 162	63.8 61.0	0.46	13.1	1.20	1350	43.5	0.0372	1028	16.6		
I 6234	0.0469	L T	90.2	44.3 51.1	52 62	151 160	63.8 66.2	0.47	12.65	1.21	1350	44.2	0.0409	1103	12.8		
I 9126	0.0462	L T	89.6	49.3 49.3	63 52	161 158	62 60.4	0.19	13.25	1.26	1350	42.9	0.0394	1085	14.7		
I 5665	0.0469	L T	91.1	53.5 51.1	64 56	167 164	63.5 65.0	0.41	12.6	1.32	1351	41.2	0.0412	1073	12.1		
M 322A	0.0441	L T	89.3	46.8 46.7	48 39	147.4 149	56.2 71.3	0.45	12.2	1.25	1352	45.3	0.0373	975	15.4		
I 2705	0.0443	L T	90.9	48.0 44.3	47 44	151 149	64.2 61.0	0.42	12.25	1.19	1355	44.5	0.0381	989	14.0		
M 335C	0.0459	L T	90.6	46.3 46.6	48 43	153 152	63.8 64.5	0.38	12.47	1.31	1356	43.2	0.0371	971	19.2		
I 6241	0.0475	L T	90.6	47.3 50.7	60 54	157 157	63.7 64.5	0.41	12.1	1.37	1357	42.0	0.0413	1001	13.1		
I 9113	0.0454	L T	91.6	48.0 45.3	58 49	161 160	70.0	0.49	12.2	1.31	1357	43.6	0.0367	974	19.2		
I 9132	0.0444	L T	88.9	47.8 44.2	48 42	150.5 147	62.1 61.8	0.41	12.35	1.22	1359	44.9	0.0380	1009	14.4		



TABLE A-1. (Continued)

(1) Blank and Helmet Number	(2) Average Thickness, inches	(3) Tensile Specimen Orientation	Blanks										Helmets			
			(4) Hardness		(5) As Received, R <sub>g</sub>	(6) 0.2% Offset Yield Stress, 10 <sup>3</sup> psi	(7) Maximum Stress, 10 <sup>3</sup> psi	(8) Elongation in 2 inches, percent	(9) Chemical Analysis, percent			(10) V <sub>50</sub> ft/sec	(11) Average Hardness, R <sub>C</sub>	(12) Average Thickness, inches	(13) V <sub>50</sub> ft/sec	(14) Average Reduction in Thickness, percent
			(4) As Received, R <sub>g</sub>	(5) After Tensile Test, R <sub>g</sub>					Si	Mn	C					
I 2702	0.0466	L T	90.4	48.0 43.3	49 46	155 150.5	63.2 60.9	0.42 0.18	12.75 12.9	1.22 1.23	1360 1362	43.9 46.4	0.0382 0.0355	1012 965	18.0 24.0	
I 1845	0.0467	L T	88.9	47.3 47.2	56 50	153 155	64.6 64.2	0.36 0.36	12.95 1.15	1363 1363	44.3 44.3	0.0372 0.0372	983 18.6			
I 2683	0.0457	L T	90.0	48.8 43.2	53 49	152 153	64.2 61.8	0.52 0.52	13.0 1.21	1363 1363	44.9 44.9	0.0408 0.0408	1107 14.1			
I 7573	0.0475	L T	89.5	49.5 48.6	55 58	154 159	60.9 62.8	0.47 0.47	13.27 1.15	1365 1365	43.6 43.6	0.0404 0.0404	1056 13.1			
I 9061	0.0465	L T	89.6	52.3 50.1	71 63	158 158	62.6 64.1	0.16 0.16	12.7 1.18	1368 1368	44.6 44.6	0.0376 0.0376	1043 17.7			
I 1842	0.0457	L T	88.1	48.8 46.5	55 49	152 153	60.3 58.6	0.41 0.41	12.7 1.20	1370 1370	44.4 44.4	0.0352 0.0352	967 21.3			
M 3378	0.0447	L T	90.3	40.0 45.5	60 49	155 153	59.6 61.8	0.35 0.35	12.4 1.13	1370 1370	41.6 41.6	0.0395 0.0395	1002 13.4			
I 2685	0.0456	L T	90.1	48.8 51.7	55 56	155 163	60.5 61.7	0.39 0.39	11.95 1.26	1371 1371	44.7 44.7	0.0399 0.0399	1057 13.7			
I 1823	0.0462	L T	90.3	47.6 48.0	49 45	153 154	62.5 64.4	0.46 0.46	12.9 1.21	1371 1371	42.0 42.0	0.0396 0.0396	985 11.8			
I 6922	0.0449	L T	90.6	49.6 44.3	58 48	154 154	60.7 63.4	0.39 0.39	12.6 1.24	1372 1372	45.6 45.6	0.0363 0.0363	973 19.7			
M 326C	0.0452	L T	90.6	44.7 49.5	49 53	150 158	61.6 66.1	0.21 0.21	12.45 1.19	1372 1372	42.4 42.4	0.0407 0.0407	1075 7.7			
I 1852	0.0441	L T	88.7	44.7 47.0	47 45	150 150	67.7 60.3									





TABLE A-11 (Continued)

Blanks															Helmets			
(1)	(2)	(3)	(4)	(5)	(6)	(7)	(8)	(9)			(10)	(11)	(12)	(13)	(14)			
Blank and Helmets Number	Average Thickness, inches	Tensile Specimen Orientation	As Received, R <sub>y</sub>	Hardness After Tensile Test, R <sub>c</sub>	0.2% Offset Yield Stress, 10 <sup>3</sup> psi	Maximum Stress, 10 <sup>3</sup> psi	Elongation in 2 Inches, percent	Chemical Analysis, percent			V <sub>50</sub> ft/sec	Average Hardness, H <sub>C</sub>	Average Thickness, inches	V <sub>50</sub> ft/sec	Average Reduction in Thickness, percent			
								Si	Mn	C								
I 2681	0.0466	L T	88.8	48.0 44.6	54 47	150 151	59.4 62.0	0.37	12.9	1.16	1393	44.2	0.0392	1016	15.9			
I 6993	0.0487	L T	91.2	47.5 47.5	52 50	165 165	69.0 69.0	0.39	12.6	1.21	1394	41.6	0.0402	1022	17.5			
I 1843	0.0450	L T	89.0	44.3 44.8	47 59	148 152.5	58.3 58.3	0.15	12.65	1.16	1397	42.8	0.0387	1086	14.0			
M 335A	0.0448	L T	90.6	46.8 45.5	48 43	152 151.5	62.5 64.5	0.40	12.25	1.29	1399	43.8	0.0367	998	18.1			
M 338D	0.0447	L T	89.3	50.0 47.0	63 52	160 157	64.1 63.4	0.45	13.0	1.21	1399	42.1	0.0387	1080	13.4			
I 4451	0.0443	L T	91.7	47.8	46 43	148.7 153	62.9 62.1	0.42	12.0	1.33	1399	43.2	0.0383	1041	13.5			
I 5636	0.0468	L T	91.2	48.2 49.0	56 52	156 158	61.5 63.4	0.42	12.9	1.16	1399	43.7	0.0395	1037	15.6			
I 6643	0.0465	L T	89.8	51.8 49.5	61 50	158 155	64.0 64.5	0.47	12.9	1.22	1399	45.7	0.0401	1062	13.8			
I 7582	0.0478	L T	91.9	47.5 47.5	48 47	149 149	67.8 64.0	0.40	12.2	1.18	1399	44.7	0.0399	1051	16.5			
I 1824	0.0462	L T	89.3	47.2 43.8	46 40	146 146	61.1 61.9	0.38	12.0	1.23	1400	45.0	0.0390	1053	15.5			
I 6325	0.0474	L T	91.7	48.0 46.2	54 50	155 170	67.5 69.2	0.45	12.9	1.22	1400	44.0	0.0408	982	14.8			
I 9112	0.0453	L T	92.6	48.5 46.0	48 46	155 155	70.8 65.3	0.53	12.5	1.25	1400	Not available	Not available	No Helmet Sent				

TABLE A-1. (Continued)

Blanks															Helmets			
(1)	(2)	(3)	(4)	(5)	(6)	(7)	(8)	(9)			(10)	(11)	(12)	(13)	(14)			
Blank and Helmets	Average Thickness, inches	Tensile Specimen Orientation	As Received, R <sub>p</sub>	Hardness After Tensile Test, R <sub>c</sub>	0.2% Offset Yield Stress, 10 <sup>3</sup> psi	Maximum Stress, 10 <sup>3</sup> psi	Elongation in 2 Inches, percent	Chemical Analysis, percent			V <sub>50</sub> ft/sec	Average Hardness, R <sub>c</sub>	Average Thickness, inches	V <sub>50</sub> , ft/sec	Average Reduction in Thickness, percent			
								Si	Mn	C								
I 1822	0.0459	L	89.1	42.3	48	142	62.2	0.36	12.05	1.21	1402	44.4	0.0390	1043	15.0			
		T		43.3	39	142	63.4											
I 6621	0.0452	L	89.8	44.5	46	147	62.5	0.50	12.15	1.23	1402	41.7	0.0384	934	15.0			
		T		45.0	44	145	59.2											
I 7572	0.0472	L	91.7	46.7	57	156	65	0.49	12.6	1.16	1402	43.1	0.0401	1052	15.0			
		T		48.5	57	153	60											
I 6662	0.0482	L	91.2	48.0	53	151	66.9	0.47	12.0	1.26	1403	42.4	0.0407	992	15.6			
		T		48.5	52	154	65.6											
M 3390	0.0446	L	90.8	49.0	57	162.5	67.1	0.46	13.2	1.27	1404	43.3	0.0393	1083	11.9			
		T		48.7	54	166	64.5											
I 1826	0.0448	L	90.6	46.3	62	161	62.8	0.44	13.3	1.25	1405	44.3	0.0422	1196	5.8			
		T		48.0	58	163	66.5											
I 6324	0.0476	L	92.0	44.8	53	151.5	61.5	0.44	11.2	1.18	1406	43.2	0.0426	1119	10.5			
		T		50.3	61	161	60.5											
I 9074	0.0487	L	90.9	48.8	62	161	67.2	0.42	13.12	1.17	1406	43.2	0.0417	1063	14.4			
		T		47.5	58	156.4	60.5											
I 5662	0.0476	L	89.9	49.5	58	152	60.4	0.47	12.65	1.19	1408	43.3	0.0410	1104	13.8			
		T		46.2	48	150	59.5											
I 6654	0.0471	L	92.4	51.1	68	164	65.5	0.42	12.25	1.25	1408	42.1	0.0438	1171	7.0			
		T		52.0	60	162	65.6											
I 6653	0.0480	L	91.7	48.3	50	153	62.9	0.38	13.05	1.18	1411	44.1	0.0395	949	17.7			
		T		47.8	51	154	60.5											
I 7005	0.0481	L	91.1	52.8	64	158	65.0	0.34	13.15	1.14	1411	43.9	0.0419	1116	12.9			
		T		46.3	58	158	65.0											

TABLE A-1. (Continued)

(1)	(2)	(3)	Blanks										Helmets							
			(4)		(5)	(6)	(7)	(8)	(9)			(10)	(11)	(12)	(13)	(14)				
			As Received, $R_p$	After Tensile Test, $R_p$	0.2% Offset Yield Stress, 10 psi	Maximum Stress, 10 psi	Elongation in 2 Inches, percent	Si	Mn	C	V 50 ft/sec	Average Hardness, $R_c$	Average Thickness, inches	V 50, ft/sec	Average Reduction in Thickness, percent					
Blank and Helmet Number	Average Thickness, inches	Tensile Specimen Orientation																		
I 9073	0.0489	L T	90.0	47.7		58 54	153 153.5		59.1 59.4	0.43	13.18	1.18	1.18	1411	42.5	0.0423	1096			13.5
M 336A	0.0464	L T	90.2	48.5 49.3		57 55	154 162			0.42	13.0	1.27	1.27	1412	45.9	0.0385	987			17.0
I 1812	0.0456	L T	91.8	50.2 51.8		61 62	158 170		64.6 65.2	0.44	13.0	1.31	1.31	1412	43.3	0.0387	1053			15.1
I 2684	0.0454	L T	89.3	48.3 44.7		55 39	153 144		59.4 60.5	0.35	12.45	1.17	1.17	1412	45.7	0.0369	999			18.8
I 2934	0.0452	L T	89.2	47.3 46.3		50 42	152 150		61.8 66.0	0.45	12.25	1.27	1.27	1413	44.8	0.0357	953			21.0
I 6651	0.0471	L T	91.7	47.8 47.6		57 54	158 156			0.41	13.2	1.20	1.20	1413	43.0	0.0421	1117			10.6
I 5661	0.0472	L T	89.8	48.0 43.5		56 51	148 150		58.4 60.0	0.47	12.8	1.21	1.21	1415	43.1	0.0390	1015			6.9
I 9075	0.0486	L T	89.5	49.2 47.5		63 59	157 160		60.0 63.4	0.43	13.3	1.22	1.22	1415	45.4	0.0384	1049			21.0
I 6991	0.0489	L T	90.4	47.0 46.8		56 51	145 150		58.0 63.0	0.40	12.0	1.17	1.17	1416	42.9	0.0418	1077			14.5
I 8261	0.0481	L T	91.4	44.8 50.0		57.5 60	160 163		65.1 61.5	0.53	13.25	1.28	1.28	1417	45.1	0.0415	1095			13.7
I 6242	0.0476	L T	89.5	46.7 49.2		56 55	157 158		59.5 61.5	0.43	12.6	1.29	1.29	1418	40.5	0.0405	1062			15.0
I 9925	0.0450	L T	89.8	49.3 45.8		52 43	154 148		64.0 65.0	0.39	11.9	1.26	1.26	1418	44.6	0.0381	972			15.3

TABLE A-1. (Continued)

Blanks										Helmetts						
(1) Blank and Helmet Number	(2) Average Thickness, inches	(3) Tensile Specimen Orientation	(4) Hardness		(5) As Received, Tensile Test, R <sub>g</sub>	(6) 0.2% Offset Yield Stress, 10 <sup>3</sup> psi		(7) Maximum Stress, 10 <sup>3</sup> psi	(8) Elongation in 2 inches, percent	(9) Chemical Analysis, percent		(10) V <sub>50</sub> ft/sec	(11) Average Hardness, R <sub>c</sub>	(12) Average Thickness, inches	(13) V <sub>50</sub> , ft/sec	(14) Average Reduction in Thickness, percent
			As Received, R <sub>g</sub>	After Tensile Test, R <sub>g</sub>		Si	Mn			C						
I 6253	0.0472	L T	89.8	50.0 47.7	55 47	55 47	154 151	63.9 65.0	0.38	12.55	1.31	1419	44.0	0.0395	1059	16.3
I 6254	0.0477	L T	89.5	49.7 44.2	53 49	53 49	155 154	65.1 60.2	0.39	12.6	1.38	1419	43.1	0.0419	1098	12.1
I 8233	0.0481	L T	91.5	49.8 49.8	58 56	58 56	160 158.5	60.1 62.8	0.45	13.2	1.18	1419	43.3	0.0413	1117	14.2
I 9062	0.0443	L T	89.2	50.0 50.7	68 62	68 62	157 160	59.8 63.2	0.48	13.45	1.16	1420	43.2	0.0414	1017	19.1
I 7001	0.0489	L T	91.1	48.7 48.8	62 58	62 58	154 155	61.5 62.1	0.33	12.7	1.22	1421	40.4	0.0451	1053	7.5
I 8263	0.0483	L T	91.7	51.5 44.7	68 53	68 53	165 162	63.6 67.9	0.54	13.11	1.24	1423	43.0	0.0417	1070	8.6
I 9111	0.0449	L T	91.8	51.1 48.8	56 50	56 50	157 156.5	67.5 63.6	0.49	11.8	1.28	1423	42.8	0.0366	976	18.5
I 7004	0.0487	L T	90.3	49.5 47.7	65 60	65 60	155 155	61.0 60.6	0.33	12.7	1.23	1424	44.4	0.0402	1022	17.5
I 7003	0.0478	L T	90.0	47.5 50.0	64 59	64 59	157 159	59.6 61.5	0.34	13.05	1.25	1425	42.8	0.0455	1205	4.8
I 6992	0.0487	L T	92.1	51.0 49.5	57 54	57 54	158 153	65.7 62.5	0.37	12.7	1.24	1427	48.4	0.0408	1031	16.2
I 8262	0.0483	L T	91.3	51.5	68	68	165	63.6	0.52	13.17	1.20	1432	43.9	0.0427	1140	11.6
I 6232	0.0475	L T	92.0	50.6 46.3	63 52	63 52	160 156	67.7 62.5	0.48	13.2	1.26	1433	44.7	0.0397	1037	16.4

TABLE A-1. (Continued)

(1) Blank and Helmet Number	(2) Average Thickness, inches	(3) Tensile Specimen Orientation	Blanks										Helmets				
			(4) Hardness		(5) R <sub>H</sub>	(6) Yield Stress, 10 <sup>3</sup> psi		(7) Maximum Stress, 10 <sup>3</sup> psi	(8) Elongation in 2 inches, percent	(9) Chemical Analysis, percent			(10) V <sub>50</sub> ft/sec	(11) Average Hardness, R <sub>C</sub>	(12) Average Thickness, inches	(13) V <sub>50</sub> , ft/sec	(14) Average Reduction in Thickness, percent
			As Received R <sub>H</sub>	After Tensile Test R <sub>H</sub>		0.2% Offset Yield Stress, 10 <sup>3</sup> psi	0.2% Offset Yield Stress, 10 <sup>3</sup> psi			Si	Mn	C					
I 7583	0.0476	L T	90.6	45.5 37.5		44 42.5	138 140	60.9 59.8		0.36	12.2	1.14	1436	45.3	0.0386	1004	19.0
I 1851	0.0449	L T	89.6	47.0 4.10		54 48	150 146	65.0 61.5		0.22	12.7	1.18	1438	43.6	0.0388	1056	13.6
I 8231	0.0494	L T	92.2	49.2 49.3		61 60	175 161	67.0 63.5		0.44	13.12	1.26	1438	44.5	0.0406	1048	17.8
I 5664	0.0474	L T	90.0	50.0 47.8		62 51	162 152	65.5 61.8		0.39	12.95	1.21	1440	43.0	0.0414	1098	12.7
I 6231	0.0468	L T	92.6	49.0 51.7		57 60	157 164	66.7 68.5		0.48	12.6	1.23	1440	43.7	0.0397	1064	15.2
I 6243	0.0473	L T	91.2	47.2 48.0		53 52	153 156	61.3 64.9		0.40	12.46	1.27	1440	43.9	0.0401	1064	15.2
I 8264	0.0472	L T	92.2	49.5 52.3		62 58	157 163	62.0 64.5		0.51	13.05	1.22	1440	45.5	0.0392	1029	17.0
I 9115	0.0460	L T	91.6	47.7 48.5		56 46	157 156	69.3 64.5		0.51	12.5	1.22	1444		Not available		No Helmet Sent
I 6641	0.0476	L T	90.6	49.8 52.1		56 59	159 164	65.6 64.0		0.47	12.6	1.25	1445		Not available		Not Returned
I 8234	0.0480	L T	91.8	49.2 49.7		61 58	162 171	64.0 66.6		0.42	13.1	1.21	1445	43.8	0.0404	1076	15.8
I 5637	0.0460	L T	92.2	52.0 53.0		68 67	166 171	63.5 65.5		0.53	12.6	1.34	1449	40.4	0.0397	1029	13.7
I 1811	0.0468	L T	90.4	51.5 48.8		63 60	167 169	67.0 63.5		0.42	13.05	1.33	1450	44.8	0.0396	1093	15.4





TABLE A2. HARDNESS, THICKNESS, AND  $V_p$  50's FOR THE UPPER AND LOWER SECTIONS OF 200 M1 HELMETS

Number	Lower Section (Rim)			Upper Section (Crown)		
	Average Hardness, Rc	Average Thickness, inch	$V_p$ 50, ft/sec	Average Hardness, Rc	Average Thickness, inch	$V_p$ 50, ft/sec
M 326B	48.3	0.0405	1079	46.6	0.0362	963
I 6214	42.0	0.0408	1002	42.9	0.0350	879
I 4462	40.4	0.0424	1147	40.4	0.0370	1021
I 7572	44.0	0.0416	1138	41.9	0.0380	996
I 9114	43.6	0.0400	1084	40.1	0.0369	1010
M 335B	45.5	0.0409	1066	43.6	0.0368	992
I 6665	47.5	0.0433	1114	46.3	0.0384	958
M 336B	47.1	0.0395	1033	45.2	0.0357	958
M 336A	46.8	0.0403	1046	45.1	0.0366	946
M 338B	47.2	0.0400	1028	45.0	0.0345	903
M 335D	45.5	0.0397	973	42.6	0.0361	914
I 6992	48.7	0.0427	1138	47.9	0.0383	940
M 322A	46.2	0.0392	1047	44.5	0.0353	907
M 337D	46.1	0.0396	1113	44.2	0.0360	933
M 326B	41.6	0.0418	1064	38.5	0.0375	963
I 5663	39.7	0.0439	1162	38.7	0.0392	995
I 6235	42.2	0.0426	1105	39.6	0.0382	964
I 6935	40.6	0.0422	1099	40.9	0.0352	922
I 5665	41.1	0.0438	1025	41.3	0.0388	1025
I 2503	41.6	0.0380	1055	40.1	0.0338	
I 9111	44.7	0.0380	1041	41.3	0.0356	958
I 1812	44.1	0.0410	1128	42.5	0.0362	984
I 6242	41.5	0.0430	1124	39.7	0.0382	1024
I 2501	40.0	0.0369	1047	38.5	0.0329	921
I 9113	44.6	0.0387	1038	42.8	0.0352	957
I 9125	42.1	0.0404	1101	41.0	0.0356	957
I 4463	41.3	0.0422	1145	40.7	0.0369	1017
I 6661	39.1	0.0444	1157	39.0	0.0390	988
I 2491	40.2	0.0372	1078	39.4	0.0323	864
I 2502	37.2	0.0391	1069	36.5	0.0350	971
I 6662	43.4	0.0424	1159	41.4	0.0390	997
I 6664	43.5	0.0422	1123	41.3	0.0383	1016
I 6921	39.1	0.0409	1114	38.3	0.0363	950
I 4452	40.0	0.0408	1113	40.6	0.0353	929
I 2931	40.0	0.0412	1095	41.3	0.0355	917
I 7001	41.2	0.0437	1136	39.7	0.0394	998
I 5637	40.8	0.0423	1098	40.0	0.0369	994
I 6995	44.5	0.0418	1141	42.9	0.0386	940
I 6231	44.9	0.0411	1168	42.1	0.0379	1033
I 6926	41.0	0.0435	1153	39.5	0.0385	1046
I 6924	40.7	0.0403	1103	40.2	0.0350	909
I 6991	43.5	0.0445	1149	42.3	0.0394	1013

TABLE A2 . (Continued)

Number	Lower Section (Rim)			Upper Section (Crown)		
	Average Hardness, RC	Average Thickness, inch	V <sub>p</sub> 50, ft/sec	Average Hardness, RC	Average Thickness, inch	V <sub>p</sub> 50, ft/sec
I 9925	45.1	0.0408	1068	44.1	0.0357	959
M 339B	45.3	0.0423	1188	44.7	0.0371	980
I 1813	48.5	0.0408	1134	47.1	0.0364	1026
I 6663	42.9	0.0436	1133	41.1	0.0393	935
M 339A	45.3	0.0401	1083	43.2	0.0364	1021
M 338A	43.5	0.0411	1075	42.0	0.0375	1018
M 336C	45.3	0.0386	1042	46.0	0.0343	922
M 324B	45.3	0.0394	1083	42.6	0.0356	970
I 9922	43.5	0.0417	1124	41.9	0.0365	941
M 322C	45.1	0.0390	1090	41.9	0.0361	947
M 324C	43.3	0.0406	1117	40.7	0.0366	997
M 341B	44.0	0.0396	1088	42.8	0.0357	969
M 335E	44.7	0.0399	1044	41.8	0.0360	944
M 337B	45.3	0.0361	1022	43.4	0.0342	861
M 333C	44.5	0.0376	1086	42.0	0.0342	928
M 337E	44.4	0.0393	1056	42.3	0.0358	970
I 2696	44.3	0.0414	1117	44.3	0.0362	899
M 335A	44.9	0.0388	1056	43.1	0.0352	956
M 321B	42.5	0.0397	1107	38.9	0.0359	1071
M 340A	44.2	0.0391	1116	42.8	0.0354	966
M 335C	44.3	0.0385	1029	42.0	0.0355	944
M 339D	43.9	0.0417	1146	42.7	0.0368	977
M 325E	49.8	0.0360	1066	46.7	0.0335	916
I 6233	44.7	0.0423	1124	42.1	0.0381	978
I 6923	42.5	0.0405	1098	41.3	0.0355	986
M 329A	44.5	0.0397	1208	42.4	0.0349	921
I 4454	42.7	0.0415	1144	43.2	0.0357	958
M 338D	42.8	0.0404	1108	41.8	0.0381	1093
I 8262	44.5	0.0449	1222	43.2	0.0399	1047
I 6251	45.6	0.0428	1152	43.8	0.0386	966
I 5661	43.7	0.0410	1098	42.3	0.0363	919
I 6232	45.6	0.0413	1102	43.3	0.0374	975
I 6244	44.5	0.0432	1190	42.7	0.0394	1046
I 6234	45.7	0.0425	1170	42.5	0.0390	1065
I 9121	44.5	0.0419	1192	42.7	0.0367	1022
I 1852	43.4	0.0428	1132	41.2	0.0383	1014
I 2915	42.4	0.0399	1131	41.6	0.0359	989
I 4422	44.9	0.0407	1084	42.1	0.0372	
I 6644	47.3	0.0413	1139	45.6	0.0371	968
I 6642	45.5	0.0426	1168	43.9	0.0388	1013
I 9124	48.9	0.0390	1122	45.9	0.0363	1022
I 6313	46.0	0.0409	1106	45.5	0.0355	924
I 9061	43.5	0.0431	1153	43.6	0.0373	976

TABLE A2. (Continued)

Number	Lower Section (Rim)			Upper Section (Crown)		
	Average Hardness, Rc	Average Thickness, inch	V <sub>p</sub> 50, ft/sec	Average Hardness, Rc	Average Thickness, inch	V <sub>p</sub> 50, ft/sec
I 5645	44.1	0.0413	1176	44.1	0.0364	1037
I 6325	44.6	0.0433	1060	43.5	0.0389	1043
I 1855	45.2	0.0390	1112	43.1	0.0351	934
I 6324	43.9	0.0451	1225	42.4	0.0399	1040
I 6637	44.3	0.0394	1085	43.3	0.0342	931
I 5662	43.9	0.0437	1198	42.7	0.0382	983
I 8244	45.3	0.0446	1187	44.1	0.0396	1015
I 7005	44.4	0.0446	1211	43.5	0.0396	1036
I 6245	44.5	0.0431	1162	42.6	0.0385	1031
I 6922	42.3	0.0418	1131	41.6	0.0370	992
I 9075	46.5	0.0403	1131	44.1	0.0361	944
I 9083	45.2	0.0430	1211	43.6	0.0385	1044
I 7582	45.6	0.0417	1130	43.7	0.0382	1034
I 6315	46.9	0.0387	1068	45.7	0.0355	951
I 7583	46.5	0.0396	1087	43.9	0.0373	988
I 9132	45.4	0.0401	1084	44.2	0.0353	934
I 2704	45.0	0.0413	1114	42.4	0.0380	997
I 2705	45.2	0.0394	1051	43.7	0.0364	938
I 6321	44.6	0.0434	1152	43.9	0.0391	1046
I 8263	43.7	0.0440	1131	42.2	0.0389	1040
I 7581	46.1	0.0424	1112	43.2	0.0387	998
I 1851	44.8	0.0403	1107	42.4	0.0371	1064
I 7584	45.0	0.0431	1185	43.6	0.0385	
I 2934	45.7	0.0382	1044	44.0	0.0333	872
I 2694	44.2	0.0421	1140	43.0	0.0365	972
I 8264	46.5	0.0406	1099	44.0	0.0372	984
I 1844	45.5	0.0403	1088	43.7	0.0357	986
I 2702	45.3	0.0396	1075	42.5	0.0403	1088
I 1841	44.9	0.0395	1121	43.9	0.0350	994
I 2695	46.5	0.0392	1046	45.0	0.0357	951
I 1822	45.5	0.0409	1137	43.2	0.0368	954
I 6651	44.5	0.0441	1178	41.9	0.0406	1053
I 2684	46.2	0.0392	1038	45.1	0.0348	946
I 1826	45.1	0.0441	1258	43.0	0.0392	1085
I 9913	44.3	0.0429	1148	41.2	0.0384	1026
I 1811	45.3	0.0416	1169	44.2	0.0375	1062
I 1843	44.5	0.0409	1137	41.5	0.0371	1015
I 182	46.4	0.0403	1087	43.3	0.0357	1003
I 2683	45.3	0.0395	1045	43.4	0.0350	903
I 8261	45.2	0.0436	1172	44.9	0.0386	1048
I 7573	46.0	0.0452	1169	43.6	0.0387	1045
I 2681	44.6	0.0419	1084	43.7	0.0358	974
I 6322	45.5	0.0428	1147	44.3	0.0376	962
I 8243	46.7	0.0440	1128	43.9	0.0390	994

TABLE A2. (Continued)

Number	Lower Section (Rim)			Upper Section (Crown)		
	Average Hardness, RC	Average Thickness, inch	V <sub>P</sub> 50, ft/sec	Average Hardness, RC	Average Thickness, inch	V <sub>P</sub> 50, ft/sec
I 7731	42.5	0.0435	1112	42.0	0.0373	954
I 6252	44.1	0.0445	1192	45.5	0.0378	995
I 6314	45.5	0.0419	1094	44.7	0.0376	959
I 6652	45.8	0.0419	1149	44.5	0.0376	1018
I 8242	45.3	0.0420	1139	42.6	0.0389	1053
I 1824	45.4	0.0411	1137	44.5	0.0364	1004
I 7585	45.3	0.0432	1153	42.8	0.0391	1073
I 6323	45.7	0.0408	1082	44.0	0.0367	955
I 1854	44.4	0.0423	1163	42.4	0.0378	1015
I 2706	46.1	0.0396	1071	43.8	0.0361	947
I 1823	45.4	0.0415	1123	43.6	0.0372	977
I 1825	47.4	0.0383	1036	44.8	0.0346	917
I 8241	45.1	0.0436	1125	42.4	0.0394	1077
I 1853	42.6	0.0405	1116	39.4	0.0363	1015
I 6421	41.3	0.0417	1111	42.3	0.0346	891
I 9131	42.7	0.0406	1062	40.8	0.0355	951
I 9923	41.4	0.0409	1046	41.0	0.0360	953
I 9134	42.6	0.0428	1095	41.9	0.0370	955
I 2703	42.7	0.0398	1029	40.1	0.0360	899
I 2685	41.8	0.0421	1065	41.5	0.0374	960
I 9911	44.3	0.0401	1012	41.0	0.0372	1009
I 6636	42.2	0.0411	1126	42.4	0.0354	940
I 6241	42.8	0.0432	1146	41.1	0.0393	1013
I 7002	43.7	0.0439	1137	42.2	0.0394	1011
I 7571	43.8	0.0390	1035	43.1	0.0364	992
I 2914	40.2	0.0408	1111	42.0	0.0347	926
I 6671	41.8	0.0408	1077	43.8	0.0342	873
I 6993	41.9	0.0434	1126	41.2	0.0391	965
I 7004	45.3	0.0421	1085	43.6	0.0386	983
I 7734	38.3	0.0424	1143	38.6	0.0373	982
I 9074	43.3	0.0444	1149	43.0	0.0387	972
I 5644	43.6	0.0425	1112	43.0	0.0367	971
I 9073	42.5	0.0449	1164	42.5	0.0391	981
I 6621	42.3	0.0400	1090	40.7	0.0358	916
I 4451	43.5	0.0413	1128	42.9	0.0351	927
I 6243	44.8	0.0421	1108	43.2	0.0384	1027
I 6654	42.5	0.0461	1263	41.6	0.0407	1057
I 6 11	45.8	0.0397	1033	43.5	0.0364	907
I 5611	43.0	0.0447	1191	43.1	0.0387	1003
I 6253	45.7	0.0413	1163	42.0	0.0376	1033
I 5643	44.2	0.0392	1037	42.9	0.0353	912
I 9081	44.0	0.0439	1188	42.8	0.0395	1066
I 6623	45.8	0.0425	1055	44.1	0.0366	911

TABLE A2. (Continued)

Number	Lower Section (Rim)			Upper Section (Crown)		
	Average Hardness, RC	Average Thickness, inch	V <sub>p</sub> 50, ft/sec	Average Hardness, RC	Average Thickness, inch	V <sub>p</sub> 50, ft/sec
I 5636	44.6	0.0419	1108	42.8	0.0373	1007
I 7732	41.7	0.0424	1093	39.9	0.0369	956
I 9082	43.2	0.0450	1209	39.0	0.0406	1121
I 6254	44.3	0.0441	1205	41.9	0.0395	1048
I 6643	46.5	0.0424	1134	44.8	0.0379	998
I 1845	47.5	0.0368	1039	45.0	0.0338	917
I 6312	45.3	0.0421	1144	43.8	0.0379	1020
I 9062	43.3	0.0445	1186	43.0	0.0387	997
I 2933	43.2	0.0423	1147	44.5	0.0360	996
I 9126	43.9	0.0420	1140	42.0	0.0372	1065
I 6631	43.0	0.0423	1154	43.0	0.0370	975
I 6246	42.7	0.0436	1151	39.3	0.0390	1063
I 9084	44.5	0.0418	1161	42.0	0.0383	1007
I 8231	45.2	0.0427	1108	43.8	0.0385	1016
I 8234	44.7	0.0425	1166	42.9	0.0385	998
I 6653	44.2	0.0422	1166	44.0	0.0368	937
I 7575	46.5	0.0397	1030	44.2	0.0370	972
I 7574	45.0	0.0425	1157	42.8	0.0393	1011
I 8233	43.8	0.0447	1197	43.0	0.0387	1014
I 2913	43.7	0.0387	1077	45.5	0.0330	916
M 321A	45.9	0.0384	1061	43.5	0.0342	983
I 4461	44.5	0.0420	1160	44.8	0.0362	1007
I 6673	43.9	0.0400	1080	42.3	0.0351	944
M 323A	45.1	0.0385	1061	41.2	0.0352	937
M 332A	44.5	0.0390	1097	42.2	0.0350	933
I 7733	43.5	0.0409	1169	42.4	0.0367	1034
I 7003	42.8	0.0459	1265	42.4	0.0433	
I 2932	40.0	0.0474	1047	40.4	0.0346	910

TABLE A3. HARDNESS, THICKNESS, AND  $V_p$  50 FOR  
96 ZONES IN 200 M1 HELMETS

Area Number*	Average Hardness, RC**	Average Thickness, inch**	$V_p$ 50, ft/sec
11	40.3	0.0374	1021
12	41.7	0.0382	1082
13	41.9	0.0378	984
21	Insufficient Data		
22	40.0	0.0379	1128
23	38.1	0.0385	1059
31	37.9	0.0384	1025
32	38.6	0.0390	1113
33	40.0	0.0383	1031
41	42.1	0.0381	1068
42	41.7	0.0378	1093
43	41.0	0.0378	992
51	44.0	0.0395	1001
52	44.1	0.0364	994
53	43.4	0.0358	990
61	42.6	0.0369	1026
62	40.7	0.0374	1072
63	40.5	0.0370	1042
71	41.0	0.0370	1030
72	40.8	0.0371	1059
73	41.4	0.0372	988
81	43.8	0.0372	993
82	43.0	0.0370	1046
83	42.6	0.0363	943
91	45.8	0.0351	908
92	44.0	0.0362	1065
93	45.2	0.0369	1053
101	47.3	0.0360	921
102	45.6	0.0364	1091
103	41.3	0.0382	997
111	42.8	0.0365	1016
112	43.4	0.0364	1078
113	43.0	0.0364	1041
121	43.4	0.0364	1000
122	44.8	0.0362	1042
123	43.5	0.0355	1012
131	43.5	0.0358	956
132	42.9	0.0365	1052
133	43.3	0.0353	976
141	43.3	0.0371	968
142	43.4	0.0370	1060
143	43.4	0.0368	968
151	44.2	0.0368	1008
152	44.6	0.0382	1084
153	42.3	0.0375	1025
161	45.8	0.0348	939
162	43.9	0.0363	1039
163	44.2	0.0363	985
171	42.8	0.0421	1162
172	44.2	0.0407	1327

TABLE A3. (Continued)

Area Number*	Average Hardness, RC**	Average Thickness, inch**	V <sub>p</sub> 50, ft/sec
173	44.7	0.0422	1138
181	44.5	0.0416	1122
182	44.6	0.0404	1169
183	41.9	0.0406	1128
191	42.3	0.0393	1083
192	43.5	0.0401	1215
193	44.3	0.0406	1162
201	43.7	0.0396	1080
202	43.5	0.0382	1149
203	43.1	0.0385	1059
211	44.6	0.0385	1057
212	43.1	0.0382	1120
213	43.8	0.0385	1081
221	41.9	0.0401	1157
222	41.1	0.0403	1184
223	41.5	0.0393	1098
231	41.1	0.0404	1125
232	44.9	0.0404	1168
233	43.9	0.0408	1150
241	43.3	0.0418	1183
242	46.1	0.0414	1233
243	42.1	0.0419	1120
251	43.8	0.0434	1130
252	46.8	0.0442	1226
253	48.4	0.0418	1118
261	44.7	0.0422	1170
262	45.6	0.0414	1185
263	42.7	0.0417	1147
271	43.9	0.0421	1158
272	44.3	0.0428	1258
273	44.6	0.0438	1191
281	43.6	0.0431	1163
282	44.4	0.0437	1293
283	45.7	0.0428	1185
291	43.5	0.0434	1163
292	45.0	0.0429	1228
293	44.6	0.0441	1223
301	44.0	0.0422	1205
302	44.5	0.0427	1217
303	44.5	0.0413	1136
311	44.0	0.0408	1106
312	47.6	0.0414	1174
313	46.5	0.0437	1155
321	45.7	0.0449	1160
322	45.4	0.0449	1267
323	44.0	0.0441	1141

\* See Figure 1 for location of zones.

(Example: Area 11 is Zone 1 right end.)

\*\*Averages from areas used in computation of V<sub>p</sub> 50.



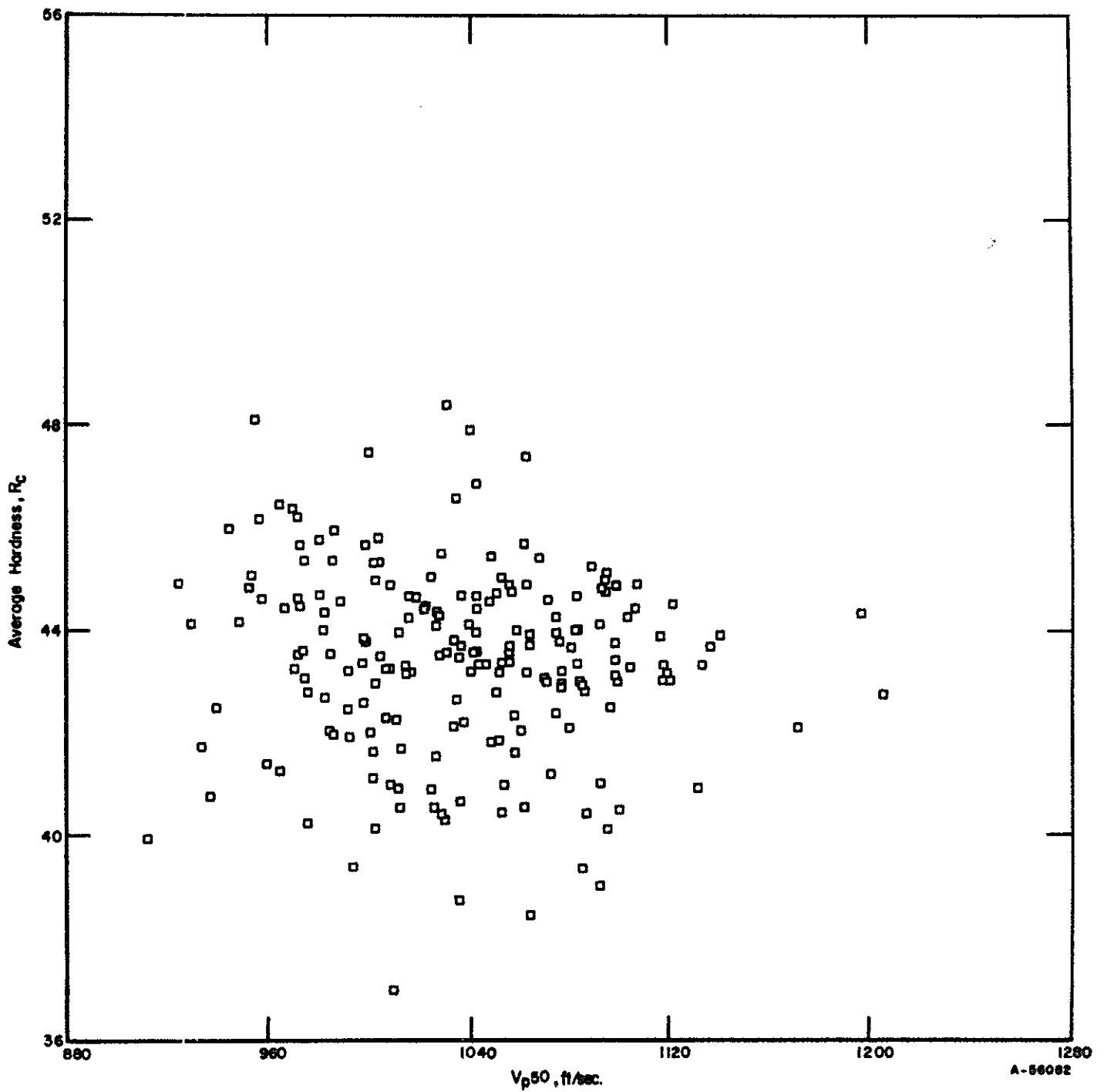


FIGURE A-1. EFFECT OF AVERAGE HARDNESS ON THE COMPOSITE  $V_{p50}$  OF M-1 HELMETS

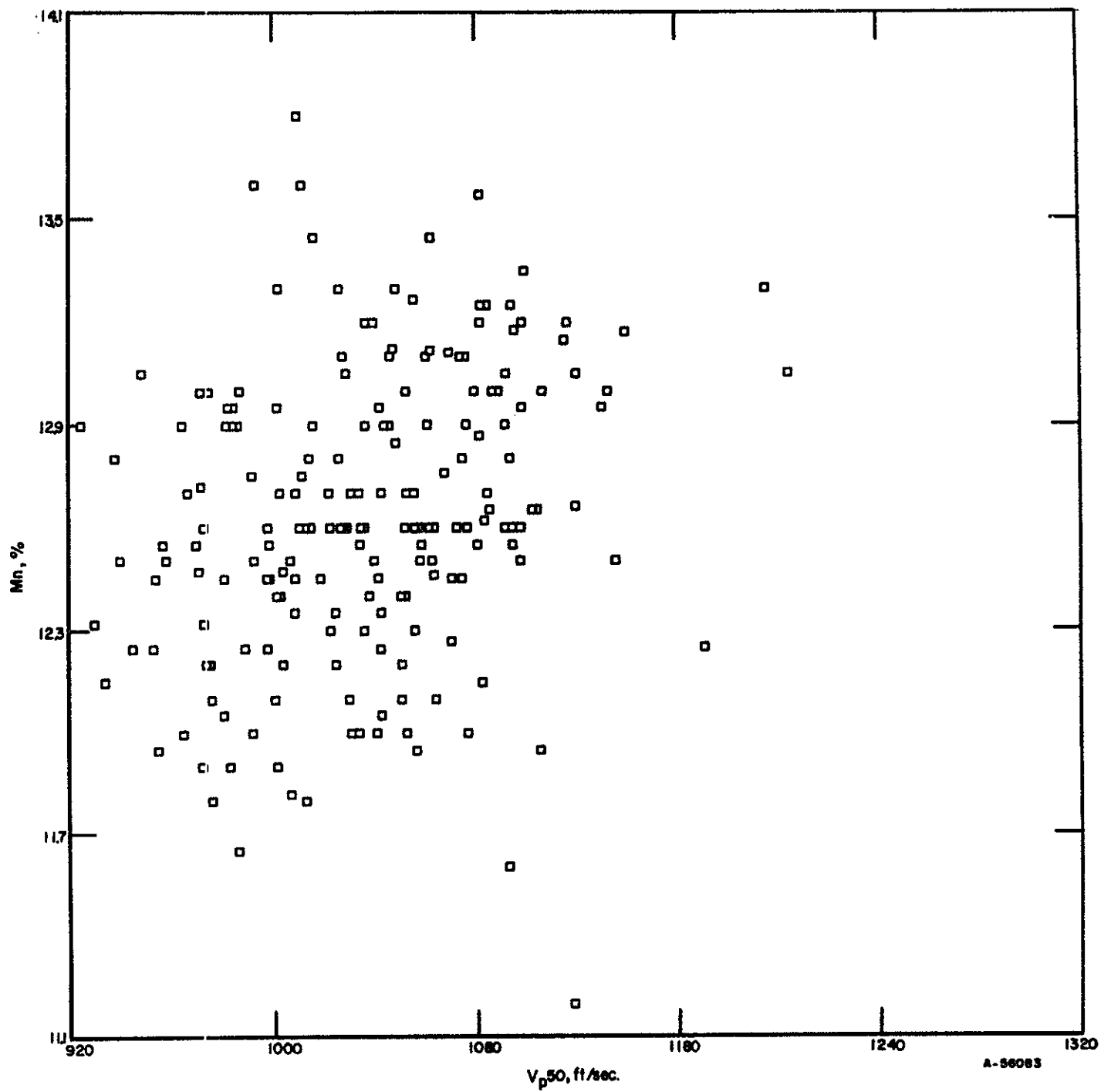


FIGURE A-2. THE EFFECT OF MANGANESE ON THE COMPOSITE Vp50 OF M-1 HELMETS

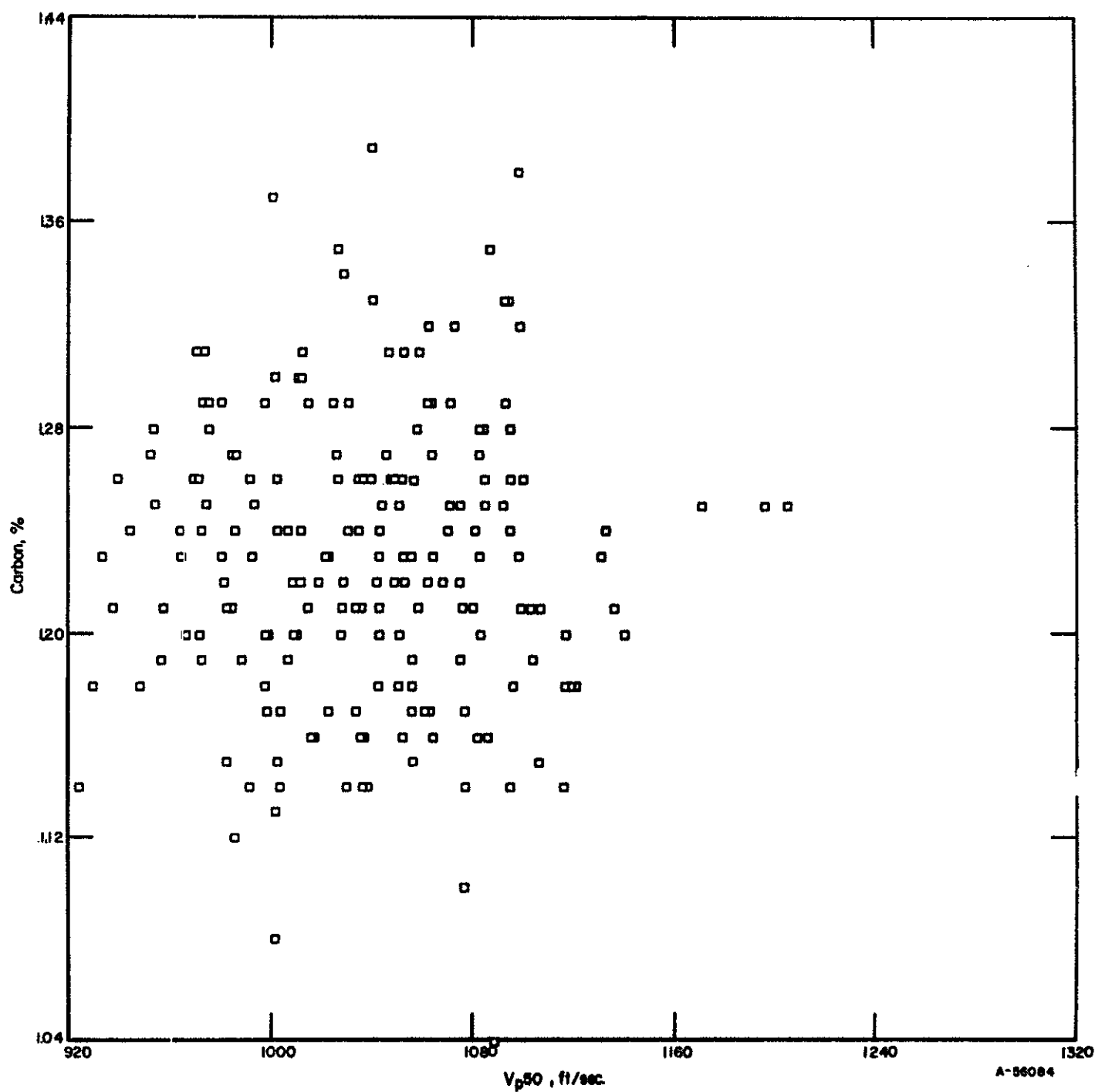


FIGURE A-3. EFFECT OF CARBON ON THE COMPOSITE Vp50 OF M-1 HELMETS

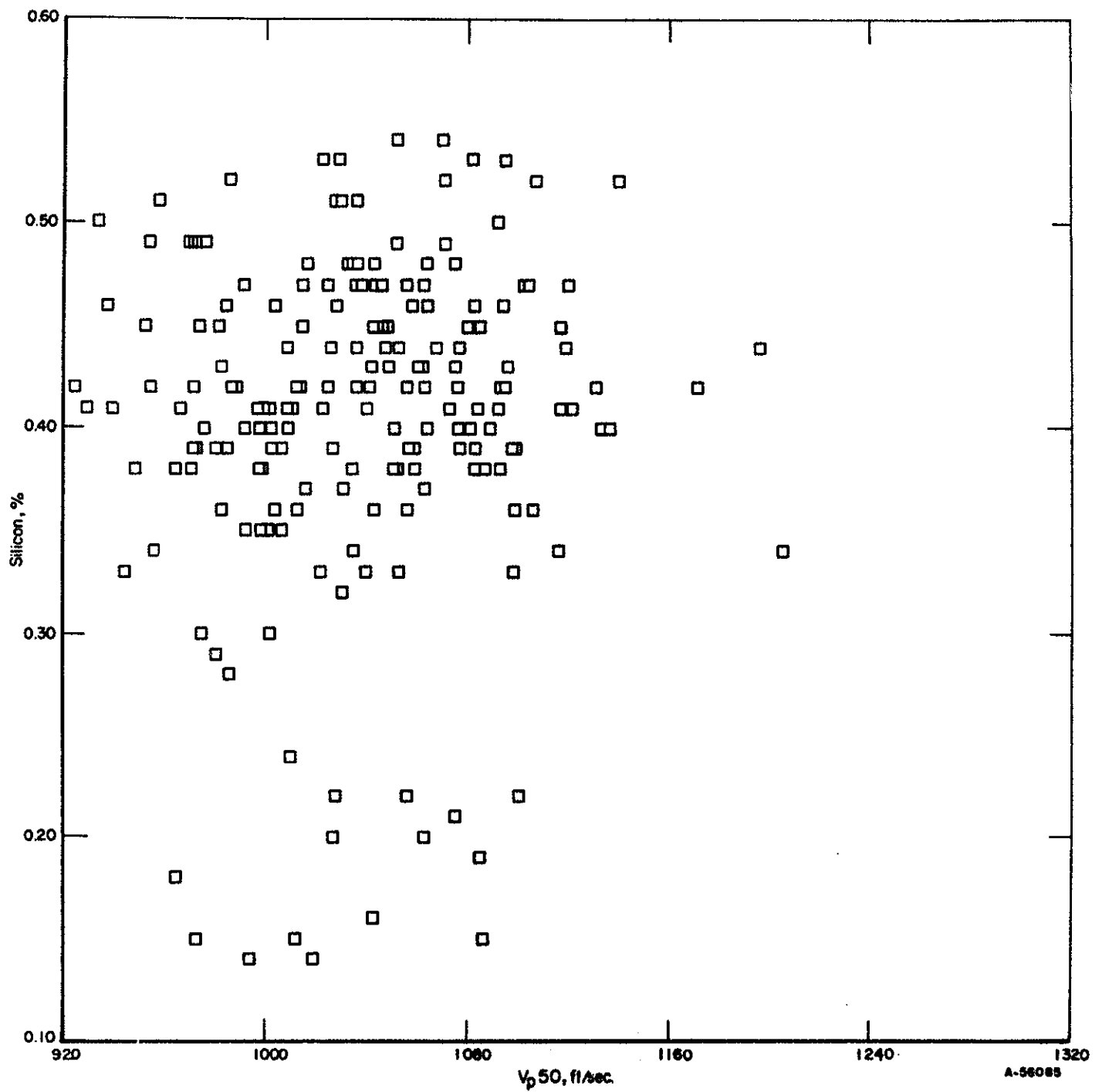


FIGURE A-4. EFFECT OF SILICON ON THE COMPOSITE Vp50 OF M-1 HELMETS